Very Nonlinear Quantum Optics

by

Juan Nicolás Quesada Mejía

A thesis submitted in conformity with the requirements
for the degree of Doctor of Philosophy
Graduate Department of Physics
University of Toronto

Abstract

Very Nonlinear Quantum Optics

Juan Nicolás Quesada Mejía
Doctor of Philosophy
Graduate Department of Physics
University of Toronto
2015

This thesis presents a study of photon generation and conversion processes in nonlinear optics. Our results extend beyond the first order perturbative regime, in which only pairs of photons are generated in spontaneous parametric down-conversion or four wave mixing. They also allow us to identify the limiting factors for achieving unit efficiency frequency conversion, and to correctly account for the propagation of bright nonclassical photon states generated in the nonlinear material. This is done using the Magnus expansion, which allows us to incorporate corrections due to time-ordering effects in the time evolution of the state, while also respecting the quantum statistics associated with squeezed states (in photon generation) and single photons or coherent states (in photon conversion). We show more generally that this expansion should be the preferred strategy when dealing with any type of time-dependent Hamiltonian that is a quadratic form in the creation and annihilation operators of the fields involved. Using the Magnus expansion, simple figures of merit to estimate the relevance of these time-ordering corrections are obtained. These quantities depend on the group velocities of the modes involved in the nonlinear process and provide a very simple physical picture of the interactions between the photons at different times. These time-ordering effects are shown to be important only when the photons and pump beam overlap within the nonlinear material for a significant amount of time. We also discuss the possibility of preparing Fock states with many photons using parametric down-conversion sources and realistic photon-number-resolving detectors. After discussing photon generation processes, we study photon conversion processes in which a nonlinear material and a classical strong

pump field are used modify the frequency of a second incoming low-intensity field. We show that time-ordering effects limit the efficiency of this conversion process, re-examine strategies to get around this problem, and show that it should be possible to have a clear observation of modified upconversion probabilities due to these effects, and thus have an experimental demonstration of time-ordering effects in nonlinear optics.

Acknowledgements

This is the first or second page to be read, but the last one written. I will try to thank all the people that made my five years in Toronto a fantastic experience, but I will forget something; so, in the best of Canadian manners, this is a preemptive "I am sorry".

First of all, I would like to thank the members of my supervisory committee, Prof. Daniel F.V. James, Prof. John. E. Sipe and Prof. Aephraim M. Steinberg. I learned a lot from you all regarding physics, but you also taught me about the tortuous ways of the English language, how to present my ideas coherently, and how to be a better scientist and person in general.

I would also like to thank Prof. Anna Sanpera and Prof. Andrew White for their kind hospitality during my visits to Barcelona and Brisbane respectively, and also extend my gratitude to Prof. Christine Silberhorn, Benjamin Brecht, Vahid Ansari and John Donohue for many valuable conversations over Skype and for sharing their experimental insight with this clueless theorist.

I would like to thank the people of Canada for the generous support they provide to basic scientific research. *J'aimerais remercier les gens du Canada pour leur généreux soutien envers la recherche scientifique fondamentale.*

Five years is a long time, during which I have learned a lot, in physics, English (I still have a lot to learn about these two), and cryogenics (~~thanks~~ Canadian winter). Even more importantly, I have made friends that are by now family. I will start this list chronologically, but I am bound to skip around sooner or later.

Juan Mi and Aleks, seeing you always makes me realize that the world out there is always full of possibilities for joy and happiness. I hope that never changes!

Sir Shreyas and Juan Matincito, you are two of the finest physicists I have ever met and also the best possible company for a pint after the daily grind of grad school.

Liebe Sigrid, not only did you introduce me to a certain *Canadienne*, but you also made a deep impression on me with your awesome Austrian hospitality. I can only look forward to my next visit to Graz. Also, I should thank your grandpa's company for furnishing great supplies for theoretical physics research ;).

Thanks to all the Toronto people: Mariu (and her friends and family in Madrid), Patrik, Robert, Juliette au chocolat...

Muchas gracias a mi familia navideña adoptiva Mexicana-Torontoniana: María de Avi, Emi, Pablo, Itzel, Alejandro y Lina, los extrañaremos mucho. Por ustedes sabemos que siempre tendremos que volver a Toronto (e ir a Bruselas o donde sea que andes María).

My deepest gratitude also goes to my lunch companions over the years: the muppets from the 10th floor (Praheen, Zanai, Zachary, Steve "T. Rex" Foster, Ciarán).

Thanks a lot MattheW: I will miss our conversations over lunch time and your careful debunking of my crazy ideas.

I would also like to thank the members of my group, the "senior" students, Asma, Omar and Kero, and especially the "junior" ones, Jas, Kevin, Mike and Dave; you taught me a lot, and I look forward to future encounters!

Thank you Aggie for being so generous with your ideas and friendship. I look forward to future collaborations :P.

Tanya and Matt, my favourite real and fake Ukrainians, I am grateful for all the great times. I can only wish you the best in your future with your loved ones!

Dr. Federico, Dra. Cata y Dr. Caja, muchas, muchas gracias por su amistad, siempre fue lindo encontrar gente en el departamento con quien ejercitar el español del terruño (o el parlache).

Muchas gracias mamá y papá, a pesar de la distancia su apoyo incondicional siempre lo sentí muy cerca. Los quiero mucho!

Ma Catou, sans toi, tout ceci aurait non seulement été extrêmement difficile mais ça n'aurait également eu aucun sens. Je t'aime.

Preface

This preface contains a list of the peer reviewed articles and conference proceedings that I have authored or coauthored during my Ph.D. studies.

List of publications in peer reviewed journals

- Nicolás Quesada and J.E. Sipe. Time-ordering effects in the generation of entangled photons using nonlinear optical processes. *Phys. Rev. Lett.*, 114(9):093903, 2015.
- Jaspreet Sahota and Nicolás Quesada. Quantum correlations in optical metrology: Heisenberg-limited phase estimation without mode entanglement. *Phys. Rev. A*, 91(1):013808, 2015.
- Nicolás Quesada and J.E. Sipe. Effects of time-ordering in quantum nonlinear optics. *Phys. Rev. A*, 90(6):063840, 2014.
- Nicolás Quesada and Anna Sanpera. Bound entanglement in the Jaynes–Cummings model. *J. Phys. B: At. Mol. Opt. Phys.*, 46(22):224002, 2013.
- Nicolás Quesada, Agata M. Brańczyk, and Daniel F.V. James. Self-calibrating tomography for multidimensional systems. *Phys. Rev. A*, 87(6):062118, 2013.
- Nicolás Quesada, Asma Al-Qasimi, and Daniel F.V. James. Quantum properties and dynamics of X states. *J. Mod. Opt.*, 59(15):1322–1329, 2012.
- Nicolás Quesada. Strong coupling of two quantum emitters to a single light mode: The dissipative Tavis-Cummings ladder. *Phys. Rev. A*, 86(1):013836, 2012.
- Paulo C. Cárdenas, Nicolás Quesada, Herbert Vinck-Posada, and Boris A. Rodríguez. Strong coupling of two interacting excitons confined in a nanocavity–quantum dot system. *J. Phys. Condens. Matter*, 23(26):265304, 2011.

List of publications in peer reviewed conference proceedings

- Nicolás Quesada and J.E. Sipe. Observing the effects of time-ordering in single photon frequency conversion. In *CLEO: Science and Innovations*, pages JTu5A–3. Optical Society of America, 2015.
- Nicolás Quesada and Jaspreet Sahota. Particle vs. mode entanglement in optical quantum metrology. In *CLEO: QELS_Fundamental Science*, pages FM1A–3. Optical Society of America, 2015.

- Nicolás Quesada, Agata M. Branczyk, and Daniel F.V. James. Holistic quantum state and process tomography. In *Frontiers in Optics*, pages FW1C–6. Optical Society of America, 2013.

- Nicolás Quesada. Quantum correlations in a mixed full rank qubit-qudit system: Discord and entanglement in the Jaynes-Cummings model. In *Quantum Information and Measurement*, pages W6–33. Optical Society of America, 2013.

- Nicolás Quesada, Daniel F.V. James, and Agata M. Branczyk. Self-calibrating tomography for non-unitary processes. In *Quantum Information and Measurement*, pages W6–38. Optical Society of America, 2013.

- Nicolás Quesada, Paulo C. Cárdenas, Boris A. Rodríguez, and Herbert Vinck-Posada. Strong coupling criterion for two interacting excitons in a nanocavity. In *Frontiers in Optics*, page JTuA22. Optical Society of America, 2011.

- Nicolás Quesada and Daniel F.V. James. An equation of motion for the concurrence of 2 qubit pure states. In *Frontiers in Optics*, page FThS3. Optical Society of America, 2011.

En el buen tiempo viejo, un señor trabajaba un año en un escritorio, haciendo cálculos, y luego enviaba un telegrama a un observatorio: "Dirijan el telescopio a la posición tal y verán un planeta desconocido". Los planetas eran muy corteses y tomaban lugar donde se les indicaba, como en un ballet bien organizado. Hoy, las partículas atómicas aparecen de súbito y como por escotillón, haciendo piruetas. La física de antaño tenía algo de fiesta de salón con música de Mozart, mientras que ahora parece una feria de diversiones, con salas de espejos, laberintos de sorpresas, tiro al blanco y hombres que pregonan fenómenos. Y a la astronomía, que era una recatada niña de su hogar, laboriosa y modesta, le ha salido ahora un hermano menor que ensucia la casa, convierte el altillo en polvorín, hace preguntas insoportables e inventa cuentos descabellados.

Ernesto Sábato, Física Escandalosa, Uno y el universo

Contents

List of Tables

List of Figures

List of Acronyms

BS: Beam splitter
FC: Frequency conversion
FWHM: Full width at half maximum
FWM: Four wave mixing
JCA: Joint conversion amplitude
JSA: Joint spectral amplitude
ME: Magnus expansion
PDC: Parametric down-conversion
PPLN: Periodically Poled Lithium Niobate
PVM: Projective-valued Measure
QIP: Quantum information processing
RA: Rotation in field a
RB: Rotation in field b
SFWM: Spontaneous four wave mixing
SPDC: Spontaneous parametric down-conversion
SQ: Squeezer/Squeezing
TMSV: Two-mode squeezed vacuum

Chapter 1

Introduction

> Etenim cognitio contemplatioque naturae manca quodam modo atque inchoata sit, si nulla actio rerum consequatur.
>
> Cicero, De Officiis, 1.153

Nonlinear photonic materials are some of the most versatile sources of nonclassical light. They allow the production of entangled states of light [1, 2, 3, 4] with very strong correlations beyond what any local realist theory could allow [5, 6]. Aided with high efficiency light detectors, they can be used to generate (to a very good approximation) states with a well defined number of light quanta; that is, states having no fluctuations in photon number [7, 8, 9, 10, 11, 12]. These photons can then be used as ultra-secure information carriers [13] or as information processors in their own right [14, 15, 16]. Moreover, the flexibility of these sources allows us to use them to teach experimental quantum physics to undergraduate students [17], yet also perform stringent tests of the strong non-classical correlations that entangled states can exhibit [4].

Besides being useful for generating quantum states of light, these materials have proven very useful for transforming and manipulating different degrees of freedom of light, in particular to change the central frequency and spectral profile [18, 19, 20]. For instance, nonlinear photonic materials can be used to double or halve the frequency of a single photon by borrowing or dumping the extra energy into a classical co-propagating electromagnetic field [21, 22, 23]; this process is known as frequency conversion (FC) [24, 25, 26]. FC is an important building block in several quantum information applications like deterministic implementations of controlled Z gates [27] and quantum pulse gates [20] between single photons. It is also useful in converting signals in regions of the electromagnetic spectrum where there are no good detectors, (for example around telecommunication wavelengths), to regions where there are good detectors (for example

the visible) [26, 28]. In the same way that frequency conversion can be thought as a fusion process, one can also understand the photon generation processes described in the previous paragraph as a photon fission process in which a high energy photon spontaneously "decays" into two low energy photons. This process is called Spontaneous Parametric Down-Conversion (SPDC). Because energy and linear momentum are preserved in the fission process, the two daughter photons have frequencies and wavevectors that add to the frequency and wavevector of the original photon. The two daughter photons are also born almost at the same time; this combination of constraints is precisely what gives these photons their non-classical correlations.

SPDC is not the only process that can give birth to very correlated photons. One can also consider the case of a pair of identical pump photons that transform into photons at different frequencies; this process is called Spontaneous Four Wave Mixing (SFWM). As we shall show later, SFWM has many similarities with SPDC; in particular, both involve destroying photons from a classical field and creating pairs of quantum-correlated light particles [29, 30].

The properties of the photons generated by SPDC and SFWM are extremely interesting, and one might wonder what allows these nonlinear materials to mediate interactions between photons, particles that hardly interact amongst themselves? The reason why this is possible is that the induced macroscopic polarization in these materials $\vec{P}(\vec{r})$ is a nonlinear function of the applied electric fields $\vec{E}(\vec{r})$ (or equivalently of the displacement field $\vec{D}(\vec{r})$). Thus, very generally one can write

$$P^i(\vec{r}) = \epsilon_0 \chi_1^{ij}(\vec{r}) E^j(\vec{r}) + \epsilon_0 \chi_2^{ijk}(\vec{r}) E^j(\vec{r}) E^k(\vec{r}) + \dots \tag{1.1}$$

$$\approx \Gamma_1^{ij}(\vec{r}) D^j(\vec{r}) + \Gamma_2^{ijk} D^j(\vec{r}) D^k(\vec{r}) + \dots \tag{1.2}$$

where ϵ_0 is the permittivity of free space, χ_2 is the 2^{nd} order electric susceptibility, and $E^i(\vec{r})$ is the i^{th} Cartesian component of the electric field. In the second line, we rewrote the polarization in terms of the displacement vector D, and introduced the Γ tensors relating the polarization and the different powers of the displacement field; in both equations we have used the Einstein summation convention. If we assume that there are two incident fields in the material at frequencies ω_a and ω_b, Eq. (1.1) tells us that the dipoles in the material can oscillate and radiate at frequencies $\omega_a \pm \omega_b$. This fact allows the matter degrees of freedom to generate harmonics, which were observed in the pioneering work of Franken *et al.* in 1961 [31]. Note that if there are only fields at one frequency ω, one can only expect to see radiation in multiples $n\omega$ in this classical picture. As we shall argue later, this will change once we consider the quantum mechanical picture and

include vacuum fluctuations.

Having the polarization written as in Eq. (1.1), we can write the nonlinear part of the Hamiltonian as[32]

$$H_{NL} = -\frac{1}{3\epsilon_0}\int d\vec{r}\Gamma_2^{ijk}D^i(\vec{r})D^j(\vec{r})D^k(\vec{r}). \tag{1.3}$$

After quantization, the displacement field in the structure can be written as a linear combination of creation and annihilation operators for photons at different frequencies. If we assume that the three displacement fields a, b, p in the crystal have the initial state $|0\rangle_a \otimes |0\rangle_b \otimes |\alpha\rangle_p$ (where $|0\rangle$ is the vacuum representing no photons in the field and $|\alpha\rangle$ is a coherent state representing the quantum analogue of a classical field), then it is not hard to show that to first order in perturbation theory, there will be a correction to the initial state due to the nonlinear Hamiltonian that will be given by

$$\hat{H}_{\mathrm{NL}} |0\rangle_a \otimes |0\rangle_b \otimes |\alpha\rangle_p \sim \left(\chi_2 \hat{a}^\dagger \otimes \hat{b}^\dagger \otimes \hat{c}\right)\left(|0\rangle_a \otimes |0\rangle_b \otimes |\alpha\rangle_p\right) = \chi_2\alpha\, |1\rangle_a \otimes |1\rangle_b \otimes |\alpha\rangle_p . \tag{1.4}$$

In the last equality we used the facts that the creation operators $\hat{a}^\dagger$ and $b^\dagger$ create one photon when acting on vacuum and, that coherent states are eigenstates of the destruction operator $\hat{c}$. These states and the action of the different operators on them will be introduced in the next chapter. Eq. (1.4) explicitly shows that to first order in perturbation theory a pair of photons in fields a and b will be created.

The use of this type of interaction as a source of pairs of photons was first theoretically proposed by Zel'dovich and Klyshko in 1969 [33] and experimentally demonstrated by Burnham and Weinberg [34] a year later. In the decade that followed these experiments, new sources of entangled photon pairs based on atomic transitions were used to perform experimental tests of local realism based on the ideas of John S. Bell [5] refined by John F. Clauser and coworkers [6]. In particular, Freedman and Clauser [35] used photons emitted from an atomic cascade in calcium to show violations of restrictions imposed by local realism on the correlations between polarization detectors in two distant locations. These violations were put on even stronger footing by the work of Alain Aspect and coworkers [36]. Two years after Aspect's experiments, Brassard and Bennett proposed using entangled pairs of photons to generate a secure secret key for the exchange of cryptographic messages [13] using pairs of polarization-entangled photons. Quantum cryptography is by now the most established quantum technology with commercial applications already

in the market. Interestingly, Acín *et al.* showed in 2006 that the security of quantum key distribution relies on the fact that the data used to construct the key also violates a Bell inequality [37].

Even though the original experiments on Bell's inequalities were performed using atomic sources of polarization-entangled photon pairs, nowadays the most advanced sources of such photons are provided by nonlinear crystal schemes developed by P. Kwiat and coworkers [2, 3, 4]. Finally, as mentioned at the beginning of this chapter, nonlinear photonic materials can also be aided with photon detectors to generate pure heralded single photons in a probabilistic manner as proposed and experimentally demonstrated by I. Walmsley and coworkers [7, 8, 9, 10].

In the previous paragraph, we described how nonlinear photonic materials can be used to generate single photons. Although these materials are by now one of the most mature sources of single photons they will likely be superseded by solid state sources [38, 39, 40]. The reason why this will probably happen is because the number purity of a single photon state generated in SPDC decreases with the probability of generating one in a heralded nondeterministic source. Even though nonlinear optical materials might not be the optimal source of single photons they might be an excellent source of bright non classical states of light. These states are typically squeezed states, which have been shown to be extremely useful in quantum metrology [41, 42, 43] and quantum computing [44, 45]. However, the theory describing the generation of bright states of light in a nonlinear material is less developed than its counterpart for single or pairs of photons. There are of course theoretical descriptions of the propagation of light in nonlinear materials beyond the perturbative regime necessary to describe pair generation or low efficiency frequency conversion. These treatments typically describe the evolution of the electric field operators in the Heisenberg picture and have been used by McGuiness *et al.* to treat frequency conversion [46, 47], by Lvovsky *et al.* for Type I degenerate SPDC [48, 49], by Gatti *et al.* for Type I and II SPDC [50, 51], and by Christ *et al.* [52] for Type II SPDC and FC. In the Heisenberg picture one will find equations of motion for the spatio-temporal field operators. For example, in the case of SPDC in the undepleted pump approximation and ignoring group velocity dispersion these equations are

$$\frac{\partial\hat{\psi}_a(z,t)}{\partial t}+v_a\frac{\partial\hat{\psi}_a(z,t)}{\partial z}+i\bar{\omega}_a\hat{\psi}_a(z,t)=i\zeta(z)\psi_p(z,t)\hat{\psi}_b^\dagger(z,t), \tag{1.5}$$

$$\frac{\partial\hat{\psi}_b(z,t)}{\partial t}+v_b\frac{\partial\hat{\psi}_b(z,t)}{\partial z}+i\bar{\omega}_b\hat{\psi}_b(z,t)=i\zeta(z)\psi_p(z,t)\hat{\psi}_a^\dagger(z,t) \tag{1.6}$$

where the field operators $\hat{\psi}^\dagger(z,t)_{a,b}$ create photons in the space time location (z,t), the

classical pump field $\psi_p(z,t) = \psi_p(z - v_p t, 0)$ evolves freely (this fact is equivalent to the undepleted pump approximation in this regime), $v_{a,b,p}(\bar{\omega}_{a,b,p})$ are the group velocities (central frequencies) of the different fields and $\zeta(z)$ describes the nonlinear interaction between the different fields. This last quantity is zero for space locations outside the length of the crystal. The important property of Eq. (1.5) is that the equations are linear in the quantum fields $\hat{\psi}^\dagger(z,t)_{a/b}, \hat{\psi}(z,t)_{a/b}$ and thus the quantum operators of the outgoing field operators must be linear combinations of the incoming operators. This linearity allows the authors to develop efficient numerical methods (or Green function techniques) to find the state generated in SPDC and this is precisely the property that is exploited in most of the studies just mentioned. These methods have the advantage that they are numerically exact. They have the disadvantage that one cannot separate the ideal operation of an SPDC device, given by the first order Magnus terms, from the time ordering corrections and thus it is hard to understand how to minimize them.

In this thesis we take a different route to study the generation of bright states of light and very high efficiency frequency conversion. Instead of propagating the equation of motion for the quantum operators, we calculate the unitary time evolution operator for the problem. Once we obtain this operator, we can reproduce the results obtained before by propagating the electric field operators or we can instead directly propagate the quantum *state* of the system. This approach has the added advantage of being much closer to the formalism of quantum information where one likes to think of multipartite states being modified by entangling and local operations [14]. Once having the state of the generated photons we can also investigate how using recently developed technology like photon-number resolving detectors [53] one can generate non-deterministically Fock states with *more* than one photon[54]. These states can be useful for implementing quantum enhanced metrology schemes [55] and also as bright non-Gaussian resource states in continuous variable quantum computation [56].

The main difficulty in obtaining the unitary evolution operator for the nonlinear processes we have considered is that the Hamiltonian describing this processes is typically time dependent and does commute with itself at different times. To understand this complication, let us consider the following interaction-picture Hamiltonian, which can be derived from the one in Eq. (1.3):

$$\hat{H}_I(t) = \tilde{\varepsilon} \int d\omega_a d\omega_b d\omega_p e^{i(\omega_a+\omega_b-\omega_c)t} \hat{c}(\omega_c)\hat{a}^\dagger(\omega_a)\hat{b}^\dagger(\omega_b)\Phi\left(\frac{\Delta k(\omega_a,\omega_b,\omega_c)L}{2}\right) + \text{H.c.}, \quad (1.7)$$

Here, field c is the field where the strong coherent pump is injected and fields a and b are the ones where photons will be generated. The quantity $\Phi\left(\Delta k(\omega_a,\omega_b,\omega_c)L/2\right) =$

$\Phi\left((k(\omega_a)+k(\omega_b)-k(\omega_c))L/2\right)$ is the phase matching function and is effectively the part of the Hamiltonian that will account for momentum conservation in the process. Finally, H.c. denotes Hermitian conjugate and $\tilde{\varepsilon}$ is a constant that characterizes the strength of the nonlinear interaction and is proportional to χ_2. Although it is not obvious at the moment, the Hamiltonian $\hat{H}_I(t)$ in Eq. (1.7) is directly related to the Hamiltonian in Eq. (1.3); their relation will be clarified in the chapter 3. The fact that there are three bosonic operators multiplied together in Eq. (1.7) is a direct consequence of the fact that the Hamiltonian in Eq. (1.3) contains three displacement fields multiplied together.
In most experimental situations, the pump field $\hat{c}(\omega_c)$ is prepared in a strong coherent state; thus it is legitimate to replace it by its expectation value over that coherent state, and we can write

$$H_I(t) = \tilde{\varepsilon}\int d\omega_a d\omega_b d\omega_p e^{i(\omega_a+\omega_b-\omega_c)t}\left\langle\hat{c}(\omega_c)\right\rangle\hat{a}^\dagger(\omega_a)\hat{b}^\dagger(\omega_b)\Phi\left(\frac{\Delta k(\omega_a,\omega_b,\omega_c)L}{2}\right)+\text{H.c.} \tag{1.8}$$

This is a time-dependent quadratic bosonic Hamiltonian that describes Parametric Down-Conversion (PDC) under the approximation that there are a large number of photons in the pump field, and that this number largely does not change during propagation in the nonlinear crystal. This approximation is the undepleted pump approximation. As it turns out, both SFWM and FC can also be described by time-dependent quadratic bosonic Hamiltonians under the undepleted pump approximation. Once we have a Hamiltonian like Eq. (1.8), we would like to know what is the time evolution it generates. To this end one would simply calculate the time evolution operator between an initial time t_0 and a final time t_1. This operator satisfies the time-dependent Schrödinger equation

$$i\hbar\frac{d}{dt}\hat{\mathcal{U}}(t,t_0) = \hat{H}_I(t)\hat{\mathcal{U}}(t,t_0), \tag{1.9}$$

and the boundary condition $\hat{\mathcal{U}}(t,t) = \hat{\mathbb{I}}$. Typically, one knows the state of the photons in fields a and b long before the interaction and would like to know their state long after the interaction thus one can set $t_0 \to -\infty$ and $t_1 \to \infty$. Naively [57, 58], one would find the unitary evolution operator connecting initial and final times to be simply

$$\hat{\mathcal{U}}(t,t_0) = \exp\left(-\frac{i}{\hbar}\int_{t_0}^{t} dt'\hat{H}_I(t')\right). \tag{1.10}$$

The last equation *is not correct*. This *would* be the exact solution of the problem *if* the

Hamiltonian commuted at different times

$$[\hat{H}_I(t), \hat{H}_I(t')] = 0. \tag{1.11}$$

It is straightforward to confirm that the Hamiltonian in Eq. (1.8) does not satisfy Eq. (1.11) and thus Eq. (1.10) is not the solution to the Schrödinger equation. The correct solution should precisely take into account the fact that Eq. (1.11) is not satisfied; thus, formally one writes

$$\hat{\mathcal{U}}(t, t_0) = \mathcal{T} \exp\left(-\frac{i}{\hbar}\int_{t_0}^{t} dt' \hat{H}_I(t')\right), \tag{1.12}$$

where $\mathcal{T}$ is the time-ordering operator.

Typically, the quantum optics community approximates the unitary evolution operator $\hat{\mathcal{U}}(t, t_0)$ using a power series of the Hamiltonian known as the Dyson series

$$\hat{\mathcal{U}}(t, t_0) \approx \hat{\mathbb{I}} - \frac{i}{\hbar}\int_{t_0}^{t} dt' \hat{H}_I(t') + \left(\frac{-i}{\hbar}\right)^2 \int_{t_0}^{t} dt' \int_{t_0}^{t'} dt'' \hat{H}_I(t')\hat{H}_I(t'') + \dots \tag{1.13}$$

If the interaction were very weak so that first order perturbation theory were sufficient to describe the output state, then the last equation would show directly that for very weak pump intensities the output state would indeed be a pair of photons in fields a and b (see Eq. (1.4)). One could hope that by including higher order terms in the series, one would get an increasingly better approximation of the exact solution of the problem [59, 60]. As we shall show in detail in chapter 4, the Magnus expansion provides a much better approximation strategy that is unitary at any truncation order and that respects the underlying physics of the exact solution. In the Magnus expansion, one writes a unitary approximation to $\hat{\mathcal{U}}(t, t_0)$ that explicitly separates the time-ordering contribution from the result that would be obtained if Eq. (1.11) held:

$$\hat{\mathcal{U}}(t, t_0) \approx \exp\left(-\frac{i}{\hbar}\int_{t_0}^{t} dt' \hat{H}_I(t') + \frac{(-i)^2}{2\hbar^2}\int_{t_0}^{t} dt' \int_{t_0}^{t'} dt'' \left[\hat{H}_I(t'), \hat{H}_I(t'')\right] + \dots\right). \tag{1.14}$$

The extra terms in the last equation relative to Eq. (1.10) are the time-ordering corrections. They are only relevant if one is considering the generation of bright states of light or when one is approaching unit conversion efficiency in frequency conversion. They also cause the generator (the operator inside the exponential) of the dynamics to be a nonlinear function of the pump electric field, and thus render the evolution of these quantum optical models *very* nonlinear. To the best of our knowledge this thesis is the first work

where the Magnus expansion is used to thoroughly examinate the dynamics of photon generation and conversion in nonlinear optics.

Using the Magnus expansion in the following chapters we explore how the time-ordering corrections manifest in the processes of photon generation in SPDC and SFWM and in photon frequency conversion. The results presented in this thesis allow us to understand what are the limitations imposed by the time-ordering corrections in the generation of pure bright squeezed states and in highly efficient frequency conversion. At the same time the methods developed in this work allows us to separate very cleanly the "ideal" operation of an SPDC/SFWM source/Frequency conversion device from the "undesirable" effects of time-ordering. Thus we will be able to explicitly write the operation of an SPDC/SFWM/FC gate, in a language very close to the one used in Quantum Information, as a unitary operation $\hat{\mathcal{U}}_{\text{SPDC/SFWM/FC}} = \exp(\hat{\Omega}_1 + \hat{\Omega}_2 + \hat{\Omega}_3 \ldots)$ that consists of a desired generator $\hat{\Omega}_1$ and time-ordering corrections $\hat{\Omega}_2, \hat{\Omega}_3, \ldots$ that modify the operation of the gate. Having this separation will help us understand when the time-ordering corrections are small and perhaps more interestingly, how to *make* them small. The understanding of this imperfections will give insights into how to generate bright squeezed light and bright Fock states and also how to perfectly upconvert single photons. As mentioned before, bright non classical light will lead to better metrology schemes and enhanced computational capabilities. Highly efficient frequency conversion will also have several applications. It can be used to move weak signals from a region of the spectrum where there are no efficient detectors to another where there are [28, 61]; it can modify in a controlled manner the properties of weak signals, a useful component of several quantum information processing protocols [20, 21, 22, 23, 27]; and it can be used to modify the spectral profile of single photons to make them more compatible with quantum memories [18, 19].

This thesis is organized as follows: In Chapter 2, we introduce some notions from quantum mechanics and basic operations and states from quantum optics (such as the coherent, squeezed and number states already mentioned) and a useful mathematical technique known as the Schmidt decomposition. In Chapter 3, as promised, we derive the nonlinear SPDC Hamiltonian Eq. (1.3) from the Maxwell equations and the constitutive relation Eq. (1.1), and we do the same for SFWM and FC. In Chapter 4 we introduce the Magnus expansion and derive some of its useful properties. We also compare it with the Dyson series and argue why it should be the preferred method for dealing with problems in nonlinear optics. We also apply the Magnus expansion to the problems that will be addressed in the next two chapters, namely photon generation and photon frequency conversion. These results have been published in N. Quesada and J.E.

Sipe, "Effects of time-ordering in quantum nonlinear optics", Phys. Rev. A **90** 063840 (2014). Then, in Chapter 5 we explore the effects of time-ordering in SPDC and SFWM. Using the Magnus expansion we obtain a simple intuitive picture of when time-ordering effects are important in photon generation. These effects are relevant only when the pump and the generated signal travel together for a significant amount of time in the nonlinear material. We also study how the photons generated in SPDC can be used to probabilistically generate Fock states using realistic photon-number-resolving detectors. These results correspond roughly to the material published in N. Quesada and J.E. Sipe, "Time-Ordering Effects in the Generation of Entangled Photons Using Nonlinear Optical Processes", Phys. Rev. Lett. **114** 093903 (2015) and N. Quesada, J.E. Sipe. and A.M. Brańczyk, "Optimized generation of bright squeezed and heralded-Fock states using parametric down-conversion" (in preparation). In Chapter 6 we look at frequency conversion and show how time-ordering effects limit the conversion efficiency of single photons. We also comment on how these effects can be attenuated and how they can be experimentally observed. This material corresponds to the results published in N. Quesada and J.E. Sipe, "Observing the effects of time-ordering in Single Photon Frequency Conversion", CLEO:2015 Conf. Proc. and "Limits in high efficiency frequency conversion" (submitted to Optics Letters, arXiv preprint 1508.03361). Finally, conclusions and future directions are presented in Chapter 7.

Chapter 2

Quantum Mechanics of the Harmonic Oscillator

> Two types of problems exist in quantum mechanics, those that you cannot solve and the harmonic oscillator. The trick is to push a problem from one category to the other.
>
> Marcos Moshinsky

In this chapter we discuss some basic notions of quantum mechanics applied to the simple harmonic oscillator. These ideas are later used to build some important states and operations in quantum optics such as squeezed and coherent states and squeezers and beam splitters. The discussion of quantum mechanics and quantum optics in this chapter is by no means exhaustive and the reader is referred to, for example, the books by Sakurai [62] and Gerry and Knight [63] respectively.

2.1 The Harmonic Oscillator

2.1.1 Classical Mechanics

The dynamics of a simple harmonic oscillator can be described by a classical Hamiltonian function in terms of its position q and canonical momentum p (which specify its state) as follows

$$H_0 = \frac{p^2}{2m} + \frac{m\omega^2 q^2}{2}, \tag{2.1}$$

where m is the mass of the oscillator and ω is the frequency of oscillation. The dynamics of this system is given by Hamilton's equations [64]

$$\frac{d}{dt}q = \{q, H\}_{q,p} = \frac{p}{m}, \quad \frac{d}{dt}p = \{p, H\}_{q,p} = -m\omega^2 q, \tag{2.2}$$

where $\{f, g\}_{q,p} \equiv \frac{\partial f}{\partial q}\frac{\partial g}{\partial p} - \frac{\partial f}{\partial p}\frac{\partial g}{\partial q}$ is the Poisson bracket of f and g. The variables q and p are said to be canonical because by definition they satisfy

$$\{q, p\}_{q,p} = 1. \tag{2.3}$$

There are infinitely many canonical variables. One particular handy set is the one defined by the amplitude a and its complex conjugate a^*

$$a = \frac{m\omega q + ip}{\sqrt{2m\omega}}, \quad a^* = \frac{m\omega q - ip}{\sqrt{2m\omega}}. \tag{2.4}$$

These variables are also canonical because they satisfy $\{a, ia^*\}_{p,q} = 1$. We then rewrite the Hamiltonian Eq. (2.1) as $H = \omega a^* a$. Because a and ia^* are canonical variables, we can easily find their equations of motion

$$\frac{d}{dt}a = \{a, H_0\}_{a,ia^*} = -i\omega a, \quad \frac{d}{dt}a^* = \{a^*, H_0\}_{a,ia^*} = i\omega a^*, \tag{2.5}$$

and integrate them immediately to get

$$a(t) = ae^{-i\omega t} \text{ and } a^*(t) = a^* e^{i\omega t}. \tag{2.6}$$

With these solutions, or by directly integrating Hamilton's Eqs. (2.2), we find the solution for the dynamics of q and p

$$q(t) = q\cos(\omega t) + \frac{p}{m\omega}\sin(\omega t), \quad p(t) = p\cos(\omega t) - m\omega q\sin(\omega t). \tag{2.7}$$

2.1.2 Quantum Mechanics

Upon quantization, the canonical variables q and p no longer specify the state of the system; instead they become Hermitian operators $\hat{q}$ and $\hat{p}$ acting on an infinite dimensional Hilbert space. These operators satisfy the canonical commutation relation

$$[\hat{q}, \hat{p}] \equiv \hat{q}\hat{p} - \hat{p}\hat{q} = i\hbar, \tag{2.8}$$

where $\hbar \approx 1.054571726 \times 10^{-34}$ Js is Planck's constant. Note the similarity between the canonical commutation relation and Eq. (2.3). One can heuristically make the correspondence [62]

$$\{,\}_{p,q} \to \frac{[,]}{i\hbar}. \tag{2.9}$$

The eigenfunctions of the operators $\hat{q}$ and $\hat{p}$ form continuous (as opposed to discrete), orthonormal, and complete sets of functions,

$$\hat{q}\,|q\rangle = q\,|q\rangle\,, \quad \hat{p}\,|p\rangle = p\,|p\rangle\,, \quad \langle q|p\rangle = \frac{1}{\sqrt{2\pi\hbar}} e^{iqp/\hbar}. \tag{2.10}$$

Because they form a continuous set, applications involving degrees of freedom that behave like harmonic oscillators are often termed "continuous variable" applications.

The state in quantum mechanics is specified by a vector $|\psi\rangle$ in a Hilbert space that evolves in time according to

$$|\psi(t)\rangle = \hat{\mathcal{U}}(t,t_0)\,|\psi(t_0)\rangle\,, \tag{2.11}$$

where $\hat{\mathcal{U}}(t,t_0)$ is the unitary time evolution operator satisfying the Schrödinger equation

$$i\hbar\frac{d}{dt}\hat{\mathcal{U}}(t,t_0) = \hat{H}(t)\hat{\mathcal{U}}(t,t_0) \tag{2.12}$$

and $\hat{H}(t)$ is the (in general time-dependent) Hamiltonian of the system. Expectation values of operators in a given quantum mechanical state are determined by the following rule

$$\langle\hat{O}(t)\rangle_\psi = \langle\psi(t)|\,\hat{O}(t_0)\,|\psi(t)\rangle = \langle\psi(t_0)|\,\hat{\mathcal{U}}(t,t_0)^\dagger\hat{O}(t_0)\hat{\mathcal{U}}(t,t_0)\,|\psi(t_0)\rangle\,. \tag{2.13}$$

Typically it is understood from the context which state is being used to calculate the expectation value, and thus from now we will drop the subindex indicating the state. This rule suggests that instead of using $\hat{\mathcal{U}}(t,t_0)$ to propagate the initial state $|\psi(t_0)\rangle$ we can use it to propagate the operators in the following manner

$$\hat{O}(t) = \hat{\mathcal{U}}(t,t_0)^\dagger\hat{O}(t_0)\hat{\mathcal{U}}(t,t_0), \tag{2.14}$$

while leaving the initial state fixed. These two ideas — propagating states versus propagating operators — are called the Schrödinger and Heisenberg pictures of quantum

mechanics, respectively. In either picture the expectation values of quantities will clearly be the same. If we take the time derivative of Eq. (2.14) and use Eq. (2.12), we obtain

$$\frac{d}{dt}\hat{O}(t) = \frac{[\hat{O}(t), \hat{H}(t)]}{i\hbar}, \tag{2.15}$$

which is precisely what one would have guessed by combining Hamilton's equations with the heuristic Eq. (2.9). Besides being able to define expectation values, we can also introduce the variance of an operator in a given state $|\psi\rangle$. It is defined as

$$\Delta^2\hat{O} \equiv \langle\hat{O}^2\rangle - \langle\hat{O}\rangle^2. \tag{2.16}$$

An important property of two non-commuting observables is that the product of their variances is bounded from below; this bound is known as the Heisenberg uncertainty relation [62]

$$\Delta^2\hat{A}\Delta^2\hat{B} \geq \frac{1}{4}|\langle[\hat{A}, \hat{B}]\rangle|^2, \tag{2.17}$$

and in particular $\Delta\hat{q}\Delta\hat{p} \geq \hbar/2$ where $\Delta x = \sqrt{\Delta^2 x}$.

The quantized version of the Hamiltonian of the harmonic oscillator can be obtained by replacing the canonical variables with operators in Eq. (2.1)

$$\hat{H} = \frac{\hat{p}^2}{2m} + \frac{m\omega^2\hat{q}^2}{2}. \tag{2.18}$$

Given the operator $\hat{H}$ one would like to find its eigenvalues E_n and eigenfunctions $|n\rangle$ satisfying $\hat{H}|n\rangle = E_n|n\rangle$. The simplest way to obtain such quantities is to introduce operators analogous to the amplitudes introduced in Eq. (2.4),

$$\hat{a} = \frac{m\omega\hat{q} + i\hat{p}}{\sqrt{2m\omega\hbar}}, \quad \hat{a}^\dagger = \frac{m\omega\hat{q} - i\hat{p}}{\sqrt{2m\omega\hbar}}. \tag{2.19}$$

These operators are called annihilation and creation operators, and satisfy

$$[\hat{a}, \hat{a}^\dagger] = 1. \tag{2.20}$$

We can now write the Hamiltonian Eq. (2.18) as

$$\hat{H} = \hbar\omega\left(\hat{n} + \frac{1}{2}\right) = \hbar\omega\left(\hat{a}^\dagger\hat{a} + \frac{1}{2}\right). \tag{2.21}$$

In the last line, we introduced the Hermitian positive semidefinite number operator $\hat{n} = \hat{a}^\dagger \hat{a}$. With the Hamiltonian in this form, it is easy to show that there is an eigenstate of lowest energy $|0\rangle$ with eigenenergy $\hbar\omega/2$ and eigennumber 0, and that all the eigenstates of $\hat{H}$ are given by $|n\rangle = \frac{\left(\hat{a}^\dagger\right)^n}{\sqrt{n!}}|0\rangle$ with n a positive integer. The eigenvalues are given by $\hbar\omega(n+1/2)$ for $\hat{H}$ and n for $\hat{n}$. The states $|n\rangle$ are called number states. These states are analogous to states of the electromagnetic field containing a well defined number of photons. They are sometimes called Fock states, and the state $|0\rangle$ containing no photons is called the vacuum. Number states $|n\rangle$ satisfy $\Delta\hat{q}\Delta\hat{p} = (n+1/2)\hbar$, hence the only number state that saturates the uncertainty relation Eq. (2.17) is $|0\rangle$, for which $\Delta\hat{q}\Delta\hat{p} = \hbar/2$. Having the eigenstates and eigenvalues of the Hamiltonian, we can immediately solve the Schrödinger equation. Since in this case the Hamiltonian is time independent, the time evolution operator is simply

$$\begin{aligned}\hat{\mathcal{U}}_0(t,t_0) &= \exp\left(-\frac{i}{\hbar}\int_{t_0}^{t} dt' \hat{H}_0\right) = \exp\left(-i\omega(t-t_0)(\hat{n}+1/2)\right) \\ &= \sum_{n=0}^{\infty} e^{-i\omega(t-t_0)(n+1/2)} |n\rangle\langle n| . \end{aligned} \tag{2.22}$$

It is now straightforward to show that the operators $\hat{a}$ and $\hat{a}^\dagger$ evolve in the Heisenberg picture exactly like their classical counterparts a and a^* in Eq. (2.6)

$$\hat{\mathcal{U}}_0^\dagger(t,0)\hat{a}\hat{\mathcal{U}}_0(t,0) = \hat{a}e^{-i\omega t} \text{ and } \hat{\mathcal{U}}_0^\dagger(t,0)\hat{a}^\dagger\hat{\mathcal{U}}_0(t,0) = \hat{a}^\dagger e^{i\omega t}. \tag{2.23}$$

It was mentioned before that the vacuum state for the harmonic oscillator $|0\rangle$ saturated the uncertainty relation. Another set of states that saturates this relation for all times under the evolution given by Eq. (2.22) are the set of coherent states. They are parametrized by a complex number α and are defined as follows

$$|\alpha\rangle = \hat{D}(\alpha)|0\rangle = \exp(\alpha\hat{a}^\dagger - \alpha^*\hat{a})|0\rangle = e^{-|\alpha|^2/2}e^{\alpha\hat{a}^\dagger}e^{-\alpha^*\hat{a}}|0\rangle = e^{-|\alpha|^2/2}\sum_{n=0}^{\infty}\frac{\alpha^n}{\sqrt{n!}}|n\rangle . \tag{2.24}$$

In the last line we introduced the displacement operator $\hat{D}(\alpha)$ and decomposed the coherent state in the number basis. To obtain this decomposition we used the well known Baker-Campbell-Hausdorff formula [65]

$$e^{\hat{A}+\hat{B}} = e^{\hat{A}}e^{\hat{B}}e^{-[\hat{A},\hat{B}]/2}, \tag{2.25}$$

which is valid if $[\hat{A}, \hat{B}]$ commutes with $\hat{A}$ and $\hat{B}$. The displacement operator transforms the creation and annihilation operators as follows

$$\hat{D}^\dagger(\alpha)\hat{a}\hat{D}(\alpha) = \hat{a} + \alpha, \quad \hat{D}^\dagger(\alpha)\hat{a}^\dagger\hat{D}(\alpha) = \hat{a}^\dagger + \alpha^*. \tag{2.26}$$

Coherent states are right eigenstates of $\hat{a}$ and left eigenstates of $\hat{a}^\dagger$

$$\hat{a}\,|\alpha\rangle = \alpha\,|\alpha\rangle\,, \quad \langle\alpha|\,a^\dagger = \alpha^*\,\langle\alpha|\,. \tag{2.27}$$

These states provide the closest analogue to the classical dynamics of the variables a and a^* because the expectation value of the operators $\hat{a}$ and $\hat{a}^\dagger$ evolves exactly like the classical variables $a = \alpha$ and $a^* = \alpha^*$. If we evaluate their expectation values with number states instead, we would get 0.

2.1.3 The Forced Harmonic Oscillator: Time-Ordering Effects

Let us study now how the coherent states introduced at the end of the last subsection can be generated. This study will also lead naturally to encounter time-ordering effects in a very simple context where we can study both the exact solution and an approximated solution ignoring time-ordering corrections.

Let us assume that our harmonic oscillator is being driven by some external force $-F(t)$. To account for this new force we write the Hamiltonian as

$$\hat{H}(t) = \frac{\hat{p}^2}{2m} + \frac{m\omega^2\hat{q}^2}{2} + \hat{q}F(t) = \underbrace{\hbar\omega\left(\hat{a}^\dagger\hat{a} + \frac{1}{2}\right)}_{\equiv\hat{H}_0} + \underbrace{\sqrt{\frac{\hbar}{2m\omega}}\left(\hat{a} + \hat{a}^\dagger\right)F(t)}_{\equiv\hat{V}(t)}. \tag{2.28}$$

To study the dynamics of the problem let us consider what is the equation of motion obeyed by a modified time evolution operator $\hat{\mathcal{U}}_I$ related to the original time evolution operator $\hat{\mathcal{U}}$ via

$$\hat{\mathcal{U}}_I(t, t_0) \equiv e^{i\hat{H}_0(t-t_0)/\hbar}\hat{\mathcal{U}}(t, t_0). \tag{2.29}$$

Using the Schrödinger equation for $\hat{\mathcal{U}}$ in Eq. (2.12) we find that

$$i\hbar\frac{d}{dt}\hat{\mathcal{U}}_I(t, t_0) = \left(e^{i\hat{H}_0(t-t_0)/\hbar}\hat{V}(t)e^{-i\hat{H}_0(t-t_0)/\hbar}\right)\hat{\mathcal{U}}_I(t, t_0) = \hat{V}_I(t)\hat{\mathcal{U}}_I(t, t_0). \tag{2.30}$$

In the last line we introduced the interaction picture Hamiltonian $\hat{V}_I(t)$. If we apply this

procedure to the forced Harmonic oscillator we find

$$\hat{V}_I(t) = \sqrt{\frac{\hbar}{2m\omega}} \left(\hat{a}e^{-i\omega t} + \hat{a}^\dagger e^{i\omega t}\right) F(t). \tag{2.31}$$

Now, we would like to solve the Schrödinger Eq. (2.30) for $\hat{\mathcal{U}}_I(t, t_0)$ with $\hat{V}_I(t)$ in Eq. (2.31). Our first guess would be to put

$$\hat{\mathcal{U}}_I(t, t_0) = \exp\left(-i \int_{t_0}^{t} dt' \hat{V}_I(t')/\hbar\right). \tag{2.32}$$

This is incorrect because

$$[\hat{V}_I(t), \hat{V}_I(t')] = i\frac{\hbar}{m\omega} F(t)F(t') \sin(\omega(t - t')) \neq 0. \tag{2.33}$$

The correct formal solution is given by the time-ordered version of Eq. (2.32) [62]

$$\hat{\mathcal{U}}_I(t, t_0) = \mathcal{T} \exp\left(-i \int_{t_0}^{t} dt' \hat{V}_I(t')/\hbar\right), \tag{2.34}$$

where $\mathcal{T}$ is the time-ordering operator. In Chapter 4 we will show using the Magnus expansion that the exact solution to Eq. (2.30) for the Forced Harmonic oscillator is

$$\begin{aligned}
\hat{\mathcal{U}}_I(t, t_0) &= \exp\left(-\frac{i}{\hbar}\int_{t_0}^{t} dt' \hat{V}_I(t') + \frac{(-i)^2}{2\hbar^2}\int_{t_0}^{t} dt' \int_{t_0}^{t'} dt'' \left[\hat{V}_I(t'), \hat{V}_I(t'')\right]\right) \qquad (2.35)\\
&= \exp\left(\underbrace{\left[-\frac{i}{\sqrt{2m\omega\hbar}}\int_{t_0}^{t} dt' e^{i\omega t'} F(t')\right]}_{\equiv\alpha(t)} \hat{a}^\dagger - \text{H.c.}\right) \times \\
&\quad \exp\left(\underbrace{-\frac{i}{2\hbar m\omega}\int_{t_0}^{t} dt' \int_{t_0}^{t'} dt'' F(t')F(t'') \sin(\omega(t'' - t'))}_{\equiv\phi(t)}\right) = \hat{D}(\alpha(t))e^{i\phi(t)}.
\end{aligned}$$

In the last line, we used the definition of the displacement operator in Eq. (2.24).
Now we see that if at time $t_0 = 0$ the Harmonic oscillator is prepared in the ground state $|0\rangle$ it will evolve at later times to

$$\begin{aligned}
|\psi(t)\rangle &= \hat{\mathcal{U}}(t, 0)|0\rangle = e^{-i\hat{H}_0 t/\hbar}\hat{\mathcal{U}}_I(t, 0)|0\rangle = e^{-i\hat{H}_0 t/\hbar}\hat{\mathcal{U}}_I(t, 0)e^{i\hat{H}_0 t/\hbar}e^{-i\hat{H}_0 t/\hbar}|0\rangle \qquad (2.36)\\
&= e^{i\phi(t)}e^{-i\omega t/2}e^{-i\hat{H}_0 t/\hbar}\hat{D}(\alpha(t))e^{i\hat{H}_0 t/\hbar}|0\rangle = e^{i(\phi(t)-\omega t/2)}\hat{D}\left(\alpha(t)e^{i\omega t}\right)|0\rangle, \qquad (2.37)
\end{aligned}$$

generating a coherent state with amplitude $\alpha(t)e^{i\omega t}$. In the last equality, we resolved the identity as $\hat{\mathbb{I}} = e^{i\hat{H}_0 t/\hbar}e^{-i\hat{H}_0 t/\hbar}$ and used the fact that $\hat{\mathcal{U}}e^{\hat{A}}\hat{\mathcal{U}}^\dagger = e^{\hat{\mathcal{U}}\hat{A}\hat{\mathcal{U}}^\dagger}$ holds for any unitary operator $\hat{\mathcal{U}}$. Finally, let us study a rather simple case for the external force: $F(t) = F_0(e^{i\omega_0 t} + e^{-i\omega_0 t})$. We can write

$$\alpha(t) = -\frac{iF_0}{\sqrt{2m\omega\hbar}}\int_{t_0}^{t} dt' e^{i\omega t'}(e^{i\omega_0 t'} + e^{-i\omega_0 t'}) \tag{2.38}$$

$$= -\frac{F_0}{\sqrt{2m\omega\hbar}}\left(\frac{e^{it(\omega-\omega_0)} - e^{it_0(\omega-\omega_0)}}{\omega-\omega_0} + \frac{e^{it(\omega+\omega_0)} - e^{it_0(\omega+\omega_0)}}{\omega+\omega_0}\right). \tag{2.39}$$

Under near resonant excitation $\omega \approx \omega_0$ we can neglect the last term in the last equation, because the dynamics is dominated by the resonant term oscillating at $e^{i(\omega-\omega_0)t}$. This approximation is known as the rotating wave approximation (RWA), it will be used several times in the following chapters.

2.2 Two Harmonic Oscillators: Squeezing and Beam Splitters

The Hamiltonian of two oscillators (assuming for the moment that they are non-interacting) is

$$\hat{H}_0 = \hbar\omega_a(\hat{a}^\dagger\hat{a} + 1/2) + \hbar\omega_b(\hat{b}^\dagger\hat{b} + 1/2) = \sum_{f=\{a,b\}} \hbar\omega_f(\hat{f}^\dagger\hat{f} + 1/2). \tag{2.40}$$

where the $\hat{a}$ and $\hat{b}$ satisfy $[\hat{a}, \hat{a}^\dagger] = [\hat{b}, \hat{b}^\dagger] = 1$ and all other commutators are zero. A natural basis for states is the one parametrized by the occupation numbers of the two oscillators

$$|n, m\rangle \equiv \frac{(\hat{a}^\dagger)^n(\hat{b}^\dagger)^m}{\sqrt{n!m!}}|0, 0\rangle \tag{2.41}$$

where $|0, 0\rangle$ is the ground state of the Hamiltonian Eq. (2.40).

2.2.1 Beam-splitter transformations

Assume now that there is coupling between the oscillators of the form

$$\hat{V}(t) = -\hbar g\left(e^{i\omega_c t}\hat{a}^\dagger\hat{b} + e^{-i\omega_c t}\hat{a}\hat{b}^\dagger\right). \tag{2.42}$$

The interaction picture version of this Hamiltonian with respect to $\hat{H}_0$ is

$$\hat{V}_I(t) = -\hbar g \left(e^{i(\omega_c+\omega_a-\omega_b)t} \hat{a}^\dagger \hat{b} + e^{-i(\omega_c+\omega_a-\omega_b)t} \hat{a} \hat{b}^\dagger \right) \tag{2.43}$$

If we take $\omega_c = \omega_b - \omega_a$ then $\hat{V}_I(t)$ is time independent. Under this condition the time evolution operator is

$$\hat{\mathcal{U}}_I = \exp(ir(\hat{a}^\dagger \hat{b} + \hat{b}\hat{a}^\dagger) \tag{2.44}$$

with $r = g(t - t_0)$. This last operator induces a beam-splitter (BS) transformation. It can be shown that it transforms the canonical operators $\hat{a}$ and $\hat{b}$ according to [63]

$$e^{-ir(\hat{a}^\dagger \hat{b} + \text{H.c.})} \hat{a} e^{ir(\hat{a}^\dagger \hat{b} + \text{H.c.})} = \cos(r)\hat{a} + i \sin(r)\hat{b}, \tag{2.45}$$

$$e^{-ir(\hat{a}^\dagger \hat{b} + \text{H.c.})} \hat{b} e^{ir(\hat{a}^\dagger \hat{b} + \text{H.c.})} = i \sin(r)\hat{a} + \cos(r)\hat{b}. \tag{2.46}$$

In the Schrödinger picture a state with one excitation (a single photon) in harmonic oscillator a and zero in harmonic oscillator b will evolve to

$$\begin{aligned} |\psi\rangle &= \hat{\mathcal{U}}_0 \hat{\mathcal{U}}_I |1,0\rangle = \hat{\mathcal{U}}_0 \hat{\mathcal{U}}_I \hat{a}^\dagger |0,0\rangle = \hat{\mathcal{U}}_0 \left(\cos(r)\hat{a}^\dagger + i \sin(r)\hat{b}^\dagger \right) |0,0\rangle \\ &= \hat{\mathcal{U}}_0 (\cos(r) |1,0\rangle + i \sin(r) |0,1\rangle) = \cos(r) e^{-i(3\omega_a t)/2} |1,0\rangle + i \sin(r) e^{-i(3\omega_b t)/2} |0,1\rangle . \end{aligned} \tag{2.47}$$

This last state is entangled unless $r = n\pi/2$ with $n \in \mathbb{Z}$. It is entangled because we cannot write it as $|\psi(t)\rangle = |\mu^a\rangle |\nu^b\rangle$, a separable state . Note that if a state is separable (not entangled) we can assign a state vector to each subsystem, for instance $|\mu^a\rangle$ for a and $|\nu^b\rangle$ for b in the last example. Even though we cannot assign state vectors to the subsystems of an entangled system, we *can* assign density matrices to them . These are constructed by tracing out the subsystems that are not of interest; for example,

$$\hat{\rho}_a = \text{tr}_b (|\psi\rangle \langle\psi|) = \sum_{m=0}^{\infty} \langle m^b | \psi \rangle \langle \psi | m^b \rangle = \cos^2(r) |1^a\rangle \langle 1^a| + \sin^2(r) |0^a\rangle \langle 0^a| . \tag{2.48}$$

Once we have a density matrix for a subsystem, we can calculate expectation values with a slightly modified rule. Instead of using Eq. (2.13), the expectation values for an operator in system a are obtained according to $\langle \hat{O}_a \rangle = \text{tr}(\hat{\rho}_a \hat{O}_a)$. In the case where the composite system is separable $|\psi\rangle = |\mu^a\rangle |\nu^b\rangle$, the density matrix is simply a projector into the corresponding subsystem vector, $\hat{\rho}_a = |\mu^a\rangle \langle \mu^a|$ and $\hat{\rho}_b = |\nu^b\rangle \langle \nu^b|$.

2.2.2 Squeezing transformations

Another interesting coupling Hamiltonian that we will find later on is

$$\hat{V}(t) = -\hbar g \left(e^{-i\omega_c t} \hat{a}^\dagger \hat{b}^\dagger + e^{i\omega_c t} \hat{a}\hat{b} \right). \tag{2.49}$$

In the interaction picture with respect to $\hat{H}_0$, this Hamiltonian becomes

$$\hat{V}_I(t) = -\hbar g \left(e^{i(-\omega_c+\omega_a+\omega_b)t} \hat{a}^\dagger \hat{b}^\dagger + e^{-i(\omega_c-\omega_a-\omega_b)t} \hat{a}\hat{b} \right). \tag{2.50}$$

We will now assume that $\omega_c = \omega_a + \omega_b$, and then we again get a time independent interaction Hamiltonian with evolution operator

$$\hat{\mathcal{U}}_I = \exp(is(\hat{a}^\dagger \hat{b}^\dagger + \hat{a}\hat{b})), \tag{2.51}$$

with $s = g(t - t_0)$. This operator is known as a two-mode squeezing (SQ) operator and transforms the canonical operators according to

$$e^{-is(\hat{a}^\dagger \hat{b}^\dagger + \text{H.c.})} \hat{a} e^{is(\hat{a}^\dagger \hat{b}^\dagger + \text{H.c.})} = \cosh(s)\hat{a} + i \sinh(s)\hat{b}^\dagger, \tag{2.52}$$

$$e^{-is(\hat{a}^\dagger \hat{b}^\dagger + \text{H.c.})} \hat{b} e^{is(\hat{a}^\dagger \hat{b}^\dagger + \text{H.c.})} = i \sinh(s)\hat{a}^\dagger + \cosh(s)\hat{b}. \tag{2.53}$$

When this operator acts on vacuum, one obtains a two-mode squeezed vacuum (TMSV) state

$$|s\rangle = \exp(is(\hat{a}^\dagger \hat{b}^\dagger + \hat{a}\hat{b})) |0,0\rangle = \sum_{n=0}^{\infty} \frac{i^n \tanh^n s}{\cosh s} |n,n\rangle . \tag{2.54}$$

One direct way of obtaining the last decomposition in terms of number states is by using the following identity (see Appendix 5 of [65])

$$\exp\left(is \left(\hat{a}^\dagger \hat{b}^\dagger + \hat{a}\hat{b} \right) \right) = e^{i\hat{a}^\dagger \hat{b}^\dagger \tanh s} e^{-\left(\hat{a}^\dagger \hat{a} + \hat{b}^\dagger \hat{b} + 1\right) \log\cosh s} e^{i\hat{a}\hat{b} \tanh s}. \tag{2.55}$$

The two-mode squeezed vacuum is also entangled. The reduced density matrix of system a is

$$\hat{\rho}_a = \sum_{n=0}^{\infty} \frac{\tanh^{2n}(s)}{\cosh^2(s)} |n^a\rangle \langle n^a| . \tag{2.56}$$

Density matrices of the form Eq. (2.56) that are diagonal in the number basis and that have coefficients that follow a geometric distribution in n are called thermal states.

We can use this density operator to calculate for example the expectation value of the number operator $\hat{n}_a$. If the states $|n\rangle$ label different Fock states this is the mean number of photons and is given by

$$\langle \hat{n}_a \rangle = \mathrm{tr}(\hat{\rho}_a \hat{n}_a) = \sinh^2(s). \tag{2.57}$$

2.2.3 Generating functions and Gaussian states

In quantum mechanics the states, represented by a vector $|\psi\rangle$ or a density matrix $\hat{\rho}$, contain all the information necessary to make predictions about the outcome of an experiment. In classical mechanics a probability density function over the canonical variables will play an analogous role to the state in quantum mechanics. In the same way that one can completely describe a probability distribution by its moments, encoded in their moment generating function, a continuous variable (CV) quantum state can be described by its moment generating function (also called characteristic function). The normal ordered generating function is defined as

$$\chi(\alpha, \alpha^*, \beta, \beta^*) = \mathrm{tr}\left(\hat{\rho} e^{\alpha \hat{a}^\dagger + \beta \hat{b}^\dagger} e^{\alpha^* \hat{a} + \beta^* \hat{b}}\right), \tag{2.58}$$

where $\hat{\rho} = |\psi\rangle\langle\psi|$ is the density matrix of the system. There is a special category of quantum states called Gaussian states. They are characterized by the fact that their generating function (any one of them) is gaussian in $(\alpha, \alpha^*, \beta, \beta^*)$ [66]. In this thesis we will be mostly interested in Gaussian states with zero mean, for which $\langle \hat{a} \rangle = \langle \hat{b} \rangle = 0$ and we can write the normal ordered generating function as (See Chapter 3 of Ref. [65])

$$\chi(\alpha, \alpha^*, \beta, \beta^*) = \chi(z) = \exp(S) = \exp\left(-\frac{1}{2} z^\dagger V z\right), \tag{2.59}$$

$$z = (\alpha^*, \alpha, \beta^*, \beta)^T, \tag{2.60}$$

$$V = \begin{pmatrix} \langle \hat{a}^\dagger \hat{a} \rangle & -\langle (\hat{a}^\dagger)^2 \rangle & \langle \hat{a}^\dagger \hat{b} \rangle & -\langle \hat{a}^\dagger \hat{b}^\dagger \rangle \\ -\langle \hat{a}^2 \rangle & \langle \hat{a}^\dagger \hat{a} \rangle & -\langle \hat{a} \hat{b} \rangle & \langle \hat{b}^\dagger \hat{a} \rangle \\ \langle \hat{b}^\dagger \hat{a} \rangle & -\langle \hat{a}^\dagger \hat{b}^\dagger \rangle & \langle \hat{b}^\dagger \hat{b} \rangle & -\langle (\hat{b}^\dagger)^2 \rangle \\ -\langle \hat{a} \hat{b} \rangle & \langle \hat{a}^\dagger \hat{b} \rangle & -\langle \hat{b}^2 \rangle & \langle \hat{b}^\dagger \hat{b} \rangle \end{pmatrix}. \tag{2.61}$$

V is called the covariance matrix of the state, and it contains all the information necessary to characterize a Gaussian state with zero mean. Examples of Gaussian states with zero mean are $|0, 0\rangle$, the thermal state and the two-mode squeezed vacuum state. The second

Transformation	Action on the annihilation operators
Beam Splitter	$e^{-ir(\hat{a}^\dagger\hat{b}+\text{H.c.})}\hat{a}e^{ir(\hat{a}^\dagger\hat{b}+\text{H.c.})} = \cos(r)\hat{a} + i\sin(r)\hat{b}$,
	$e^{-ir(\hat{a}^\dagger b+\text{H.c.})}\hat{b}e^{ir(\hat{a}^\dagger\hat{b}+\text{H.c.})} = i\sin(r)\hat{a} + \cos(r)\hat{b}$,
Two-mode squeezing	$e^{-is(\hat{a}^\dagger\hat{b}^\dagger+\text{H.c.})}ae^{is(\hat{a}^\dagger\hat{b}^\dagger+\text{H.c.})} = \cosh(s)\hat{a} + i\sinh(s)\hat{b}^\dagger$
	$e^{-is(\hat{a}^\dagger\hat{b}^\dagger+\text{H.c.})}\hat{b}e^{is(\hat{a}^\dagger\hat{b}^\dagger+\text{H.c.})} = i\sinh(s)\hat{a}^\dagger + \cosh(s)\hat{b}$
Rotations	$e^{-iu\hat{a}^\dagger a}\hat{a}e^{iu\hat{a}^\dagger\hat{a}} = \hat{a}e^{iu}$
	$e^{-iv\hat{b}^\dagger\hat{b}}be^{iv\hat{b}^\dagger\hat{b}} = \hat{b}e^{iv}$

Table 2.1: In this table we summarize how the annihilation operators transform under different Gaussian operations. In all cases the operators are mapped to linear combinations of creation and annihilation operators of the modes.

moments of the TMSV are

$$\langle(\hat{a}^\dagger)^2\rangle = \langle\hat{a}^2\rangle = \langle\hat{b}^2\rangle = \langle(\hat{b}^\dagger)^2\rangle = \langle\hat{a}^\dagger\hat{b}\rangle = \langle\hat{a}\hat{b}^\dagger\rangle = 0 \tag{2.62}$$

$$\langle\hat{a}^\dagger\hat{a}\rangle = \langle\hat{b}^\dagger\hat{b}\rangle = \sinh^2(s), \quad \langle\hat{a}\hat{b}\rangle = (\langle\hat{a}^\dagger\hat{b}^\dagger\rangle)^* = i\sinh(s)\cosh(s), \tag{2.63}$$

and the same moments for vacuum are all 0. Besides Gaussian states there are also Gaussian transformations sometimes also called linear Bogoliubov transformations. These are transformations that map Gaussian states to Gaussian states. An alternative characterization of these transformations is that they map the canonical operators $\hat{a}, \hat{a}^\dagger, \hat{b}, \hat{b}^\dagger$ to linear combinations of those operators. The two-mode squeezing operator and the beam-splitter operators generate Gaussian transformations of the states. In Table 2.1 we summarize the action of different Gaussian transformations over the annihilation operators.

2.2.4 Lossy two-mode squeezed vacuum states

As an application of the relations we derived in the last sections, let us consider what happens to a TMSV state that undergoes losses. Losses are typically modeled by a beam splitter in which one of the inputs is the system that will undergo loss and the other input is vacuum. We can model losses in mode a (b) by sending it through a BS operation where the other arm c (d) is in vacuum. Thus we need to consider

$$e^{ir'(\hat{b}^\dagger\hat{d}+\text{H.c.})}e^{ir(\hat{a}^\dagger\hat{c}+\text{H.c.})}e^{is(\hat{a}^\dagger\hat{b}^\dagger+\text{H.c.})}\left|0,0,0,0\right\rangle, \tag{2.64}$$

where $\hat{c}$ and $\hat{d}$ are annihilation operators satisfying the usual commutation relations and $|0,0,0,0\rangle \equiv |0\rangle_a|0\rangle_b|0\rangle_c|0\rangle_d$. We are now interested in the density matrix of systems

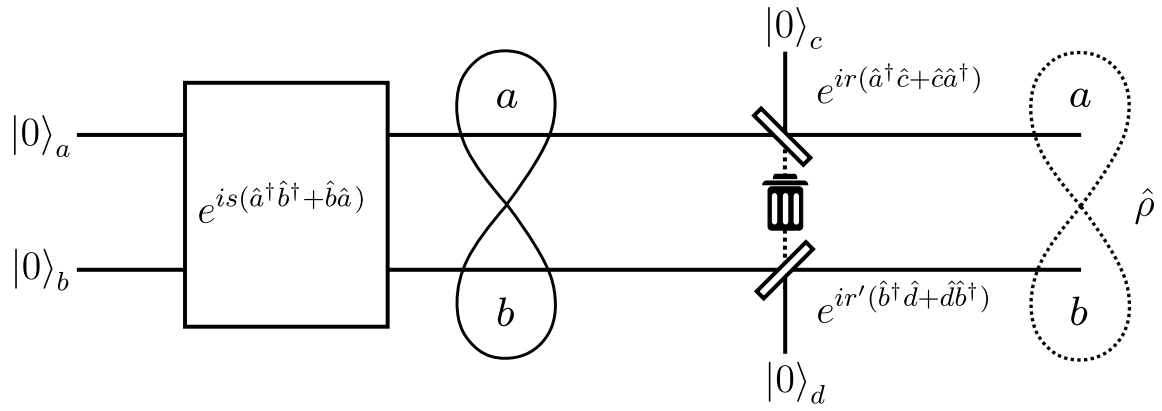

Figure 2.1: This diagram illustrates how to model losses for a two-mode squeezed vacuum state. First the TMSV state is prepared, generating entanglement (symbolized by the loop). Then each mode is sent to a beam splitter where the other input is vacuum. We then trace out the extra harmonic oscillators (symbolized by the trash bin) and look at the resultant state in modes a and b which is in general less entangled and represented by a mixed density matrix $\hat{\rho}$.

a and b. To obtain this quantity we need to trace out modes c and d. Note nevertheless that the operations and initial state in Eq. (2.64) are Gaussian thus a complete characterization of such a state is contained in the second moments that determine the covariance matrix

$$\begin{aligned}&\langle(\hat{a}^\dagger)^2\rangle = \langle\hat{a}^2\rangle = \langle\hat{b}^2\rangle = \langle(\hat{b}^\dagger)^2\rangle = \langle\hat{a}^\dagger\hat{b}\rangle = \langle\hat{a}\hat{b}^\dagger\rangle = 0, \\ &\langle\hat{a}^\dagger\hat{a}\rangle = T\sinh^2(s), \quad \langle\hat{b}^\dagger\hat{b}\rangle = T'\sinh^2(s), \quad \langle\hat{a}\hat{b}\rangle = (\langle\hat{a}^\dagger\hat{b}^\dagger\rangle)^* = \sqrt{TT'}i\sinh(s)\cosh(s),\end{aligned} \tag{2.65}$$

where $\sqrt{T} = |\cos(r)|$ and $\sqrt{T'} = |\cos(r')|$. These moments contain all the information necessary to write the covariance matrix and thus the state. It can be shown [54] that the following density matrix for systems a and b

$$\hat{\rho} = e^{is'(\hat{a}^\dagger\hat{b}^\dagger+\text{H.c.})}\left(\frac{1}{1+\bar{n}}\frac{1}{1+\bar{m}}\sum_{n,m=0}^{\infty}\left(\frac{\bar{n}}{1+\bar{n}}\right)^n\left(\frac{\bar{m}}{1+\bar{m}}\right)^m|n,m\rangle\langle n,m|\right)e^{-is'(\hat{a}^\dagger\hat{b}^\dagger+\text{H.c.})} \tag{2.66}$$

is Gaussian and has the same second moments Eq. (2.65) provided that

$$\tanh(2s') = \frac{2\sqrt{TT'}\sinh(s)\cosh(s)}{\sinh^2(s)(T+T')+1}, \tag{2.67}$$

$$\bar{n}+\bar{m} = \sqrt{\left(\sinh^2(s)(T+T')+1\right)^2 - 4TT'\sinh^2(s)\cosh^2(s)} - 1, \tag{2.68}$$

$$\bar{n}-\bar{m} = (T-T')\sinh^2(s). \tag{2.69}$$

Since covariance matrices specify a Gaussian state (or density matrix) uniquely we conclude that the density matrix in Eq. (2.66) is the one corresponding to systems a and b when systems c and d are traced out in Eq. (2.64). Eq. (2.66) is useful because it allows one to express a TMSV state after loss as a product of thermal states that undergoes squeezing. An interesting special case of Eqs. (2.67) is when only one of the modes undergoes losses, that is one of T and T' is equal to one. In that case $\bar{n} = 0$ if $T' = 1$ and $\bar{m} = 0$ if $T = 1$.

2.3 Continuous variable Gaussian transformations and states

In this section we generalize some of the results from the previous section to a continuum of harmonic oscillators (a continuum of continuous variable systems). To this end, we introduce creation and annihilation operators labeled by a continuous index ω. They will now satisfy the commutation relations

$$[\hat{a}(\omega), \hat{a}^\dagger(\omega')] = \delta(\omega-\omega'), \quad [\hat{a}(\omega), \hat{a}(\omega')] = 0. \tag{2.70}$$

and will create photons at a single sharply defined frequency ω. In this thesis we will assume that the states of a photon can be specified by its frequency. This is a simplification that is only valid in a quasi 1-D situation. More generally states will be specified by wavevectors $\vec{k}$ in 3-D space.

The noninteracting Hamiltonian of these oscillators is given by $H_0 = \int d\omega \hbar\omega \hat{a}^\dagger(\omega)\hat{a}(\omega)$, where we have omitted the factor of $1/2$ that corresponds to the zero point energy of the state with no photons. At this point we will start to refer to the collection of oscillators as a field. The first state of the field that we will care about is the vacuum $|\text{vac}\rangle$. This state satisfies

$$\hat{a}(\omega)\,|\text{vac}\rangle = 0 \quad \forall\omega. \tag{2.71}$$

We can now introduce normalized broadband states containing a single excitation,

$$|1_{g(\omega)}\rangle = \int d\omega g(\omega)\hat{a}^\dagger(\omega)\,|\text{vac}\rangle\,, \quad \int d\omega |g(\omega)| = 1, \tag{2.72}$$

analogous to the state studied in Eq. (2.47). Broadband coherent states are defined as

$$|g(\omega)\rangle = \exp\left(\sqrt{N}\int d\omega g(\omega)\hat{a}^\dagger(\omega) - \text{H.c.}\right)|\text{vac}\rangle\,. \tag{2.73}$$

where $N = \int d\omega_a \langle \hat{a}^\dagger(\omega_a)\hat{a}(\omega_a)\rangle$ is the mean number of photons in $|g(\omega)\rangle$.

2.3.1 Multimode Beam Splitters and Squeezers

Next we would like to construct operations analogous to the BS and SQ operations for the fields. To this end another field $\hat{b}(\omega)$ is introduced

$$[\hat{b}(\omega), \hat{b}^\dagger(\omega')] = \delta(\omega - \omega'), \quad [\hat{b}(\omega), \hat{b}(\omega')] = 0. \tag{2.74}$$

The field operators $\hat{b}(\omega_b), \hat{b}^\dagger(\omega_b)$ commute with all the $\hat{a}(\omega)$ and $\hat{a}^\dagger(\omega)$. With these two sets, the beam-splitter and squeezing operators are generalized to

$$\hat{\mathcal{U}}_{\text{SQ}} = \exp\left(i\int d\omega_a d\omega_b K(\omega_a,\omega_b)\hat{a}^\dagger(\omega_a)\hat{b}(\omega_b) + \text{H.c.}\right), \tag{2.75}$$

$$\hat{\mathcal{U}}_{\text{BS}} = \exp\left(i\int d\omega_a d\omega_b F(\omega_a,\omega_b)\hat{a}^\dagger(\omega_a)\hat{b}^\dagger(\omega_b) + \text{H.c.}\right). \tag{2.76}$$

For future convenience we will also study the following operators

$$\hat{\mathcal{U}}_{\text{RA}} = \exp\left(i\int d\omega_a d\omega_a' G(\omega_a,\omega_a')\hat{a}^\dagger(\omega_a)\hat{a}(\omega_a')\right), \tag{2.77}$$

$$\hat{\mathcal{U}}_{\text{RB}} = \exp\left(i\int d\omega_b d\omega_b' H(\omega_b,\omega_b')\hat{b}^\dagger(\omega_b)\hat{b}(\omega_b')\right). \tag{2.78}$$

Here, the subindices RA and RB stand for rotation operation in the a and b modes, and the functions G and H are assumed to be hermitian, $G(\omega,\omega') = G^*(\omega',\omega)$ and $H(\omega,\omega') = H^*(\omega',\omega)$.

As we shall show in the next chapters, operations like the ones just mentioned can be performed over the electromagnetic field using nonlinear optical materials. For the moment we would like to know how operations like BS, RA, RB and SQ transform different states. To learn how to apply these transformations, the Schmidt decompositions

of F and K are introduced

$$F(\omega_a, \omega_b) = \sum_\lambda s_\lambda f_\lambda(\omega_a) j_\lambda(\omega_b), \quad K(\omega_a, \omega_b) = \sum_\theta r_\theta k_\theta(\omega_a) l^*_\theta(\omega_b). \tag{2.79}$$

The quantities s_λ and r_θ are positive and the functions f, j, k, l satisfy the following orthonormality and completeness relations:

$$\int_{-\infty}^{\infty} d\omega_a f_\lambda(\omega_a) f^*_{\lambda'}(\omega_a) = \int_{-\infty}^{\infty} d\omega_a k_\lambda(\omega_a) k^*_{\lambda'}(\omega_a) = \delta_{\lambda\lambda'}, \tag{2.80}$$

$$\sum_\lambda f_\lambda(\omega_a) f^*_\lambda(\omega'_a) = \sum_\lambda k_\lambda(\omega_a) k^*_\lambda(\omega'_a) = \delta(\omega_a - \omega'_a), \tag{2.81}$$

$$\int_{-\infty}^{\infty} d\omega_b j_\lambda(\omega_b) j^*_{\lambda'}(\omega_b) = \int_{-\infty}^{\infty} d\omega_b l_\lambda(\omega_b) l^*_{\lambda'}(\omega_b) = \delta_{\lambda\lambda'}, \tag{2.82}$$

$$\sum_\lambda j_\lambda(\omega_b) j^*_\lambda(\omega'_b) = \sum_\lambda l_\lambda(\omega_b) l^*_\lambda(\omega'_b) = \delta(\omega_b - \omega'_b). \tag{2.83}$$

Likewise for the functions F and H, one introduces their eigendecompositions

$$G(\omega_a, \omega'_a) = \sum_\alpha u_\alpha g_\alpha(\omega_a) g^*_\alpha(\omega'_a), \quad H(\omega_b, \omega'_b) = \sum_\beta v_\beta h_\beta(\omega_b) h^*_\beta(\omega'_b), \tag{2.84}$$

where the numbers u_α and v_β are real numbers and the functions g and h satisfy

$$\int_{-\infty}^{\infty} d\omega_a g^*_\alpha(\omega_a) g_{\alpha'}(\omega_a) = \int_{-\infty}^{\infty} d\omega_b h^*_\alpha(\omega_b) h_{\alpha'}(\omega_b) = \delta_{\alpha\alpha'}, \tag{2.85}$$

$$\sum_\alpha g^*_\alpha(\omega) g_\alpha(\omega') = \sum_\beta h^*_\beta(\omega) h_\beta(\omega') = \delta(\omega - \omega'). \tag{2.86}$$

These decompositions exist if the functions are square integrable. In Appendix B we show how one can numerically approximate the Schmidt decomposition using the singular value decomposition (SVD) of matrices. With these definitions one introduces broadband creation and annihilation operators

$$\hat{A}_\lambda = \int d\omega_a f^*_\lambda(\omega_a) \hat{a}(\omega_a), \quad \hat{\mathcal{A}}_\lambda = \int d\omega_a k^*_\lambda(\omega_a) \hat{a}(\omega_a), \quad \hat{\mathfrak{A}}_\lambda = \int d\omega_a g^*_\lambda(\omega_a) \hat{a}(\omega_a), \tag{2.87}$$

$$\hat{B}_\lambda = \int d\omega_b j^*_\lambda(\omega_b) \hat{b}(\omega_b), \quad \hat{\mathcal{B}}_\lambda = \int d\omega_b l^*_\lambda(\omega_b) \hat{b}(\omega_b), \quad \hat{\mathfrak{B}}_\lambda = \int d\omega_b h^*_\lambda(\omega_b) \hat{b}(\omega_b). \tag{2.88}$$

One can then easily rewrite

$$\hat{\mathcal{U}}_{\rm SQ} = \exp\left(i\sum_{\lambda} s_\lambda \hat{A}^\dagger_\lambda \hat{B}^\dagger_\lambda + \text{H.c.}\right) = \bigotimes_{\lambda} \exp\left(is_\lambda \hat{A}^\dagger_\lambda \hat{B}^\dagger_\lambda + \text{H.c.}\right), \tag{2.89}$$

$$\hat{\mathcal{U}}_{\rm BS} = \exp\left(i\sum_{\theta} r_\theta \hat{\mathcal{A}}^\dagger_\theta \hat{\mathcal{B}}_\theta + \text{H.c.}\right) = \bigotimes_{\theta} \exp\left(ir_\theta \hat{\mathcal{A}}^\dagger_\theta \hat{\mathcal{B}}_\theta + \text{H.c.}\right), \tag{2.90}$$

$$\hat{\mathcal{U}}_{\rm RA} = \exp\left(i\sum_{\alpha} u_\alpha \hat{\mathfrak{A}}^\dagger_\alpha \hat{\mathfrak{A}}_\alpha\right) = \bigotimes_{\alpha} \exp\left(iu_\alpha \hat{\mathfrak{A}}^\dagger_\alpha \hat{\mathfrak{A}}_\alpha\right), \tag{2.91}$$

$$\hat{\mathcal{U}}_{\rm RB} = \exp\left(i\sum_{\beta} v_\beta \hat{\mathfrak{B}}^\dagger_\beta \hat{\mathfrak{B}}_\beta\right) = \bigotimes_{\beta} \exp\left(iv_\beta \hat{\mathfrak{B}}^\dagger_\beta \hat{\mathfrak{B}}_\beta\right). \tag{2.92}$$

where we have used the completeness and orthogonality relations.

The Schmidt decompositions just introduced will play an important role in the following chapters. By using the completeness and orthogonality of the Schmidt functions we can study what is the effect of the multimode field operators on arbitrary field states. The Schmidt coefficients will play the role of the squeezing parameters s or rotation angles r introduced in Sec. 2.2. For example, using the Schmidt decomposition we can investigate how an annihilation operator for a photon of frequency ω, $\hat{a}(\omega)$ transforms under a BS transformation

$$\begin{aligned}
\hat{\mathcal{U}}^\dagger_{\rm BS}\hat{a}(\omega_a)\hat{\mathcal{U}}_{\rm BS} &= \hat{\mathcal{U}}^\dagger_{\rm BS}\int d\omega'_a \delta(\omega_a-\omega'_a)\hat{a}(\omega'_a)\hat{\mathcal{U}}_{\rm BS} = \hat{\mathcal{U}}^\dagger_{\rm BS}\int d\omega'_a \sum_\theta f^*_\theta(\omega'_a)k_\theta(\omega_a)\hat{a}(\omega'_a)\hat{\mathcal{U}}_{\rm BS} \\
&= \sum_\theta k_\theta(\omega_a)\hat{\mathcal{U}}^\dagger_{\rm BS}\hat{\mathcal{A}}_\theta\hat{\mathcal{U}}_{\rm BS} = \sum_\theta k_\theta(\omega_a)\left(\hat{\mathcal{A}}_\theta\cos(r_\theta) + i\sin(r_\theta)\hat{\mathcal{B}}_\theta\right) \\
&= \sum_\theta k_\theta(\omega_a)\left(\int d\omega'_a f^*_\theta(\omega'_a)\hat{a}(\omega'_a)\cos(r_\theta) + i\int d\omega'_b \sin(r_\theta) l_\theta(\omega'_b)\hat{b}(\omega'_b)\right) \\
&= \int d\omega'_a\left(\sum_\theta k_\theta(\omega_a)f^*_\theta(\omega'_a)\cos(r_\theta)\right)\hat{a}(\omega'_a) \\
&\quad + i\int d\omega'_b\left(\sum_\theta k_\theta(\omega_a)l_\theta(\omega'_b)\sin(r_\theta)\right)\hat{b}(\omega'_b)
\end{aligned} \tag{2.93}$$

In Table 2.2 we summarize the transformations of the annihilation operators for the different transformations. With these decompositions, we can investigate how multimode

states transform. For instance, let us look at

$$\hat{\mathcal{U}}_{\rm BS}\left|1_{\alpha(\omega)}\right\rangle = \hat{\mathcal{U}}_{\rm BS}\int d\omega\alpha(\omega)\hat{a}^\dagger(\omega)\left|{\rm vac}\right\rangle = \int d\omega\alpha(\omega)\hat{\mathcal{U}}_{\rm BS}\hat{a}^\dagger(\omega)\hat{\mathcal{U}}_{\rm BS}^\dagger\left|{\rm vac}\right\rangle \tag{2.94}$$

$$= \sum_\theta\left(\int d\omega k_\theta^*(\omega)\alpha(\omega)\right)\left(\cos(r_\theta)\hat{\mathcal{A}}_\theta^\dagger + i\sin(r_\theta)\hat{\mathcal{B}}_\theta^\dagger\right)\left|{\rm vac}\right\rangle. \tag{2.95}$$

This is almost like the result in Eq. (2.47). These equations can in fact be made completely identical if we take $\alpha(\omega) = k_{\theta'}(\omega)$ since in that case the last equation becomes

$$\hat{\mathcal{U}}_{\rm BS}\left|1_{k_{\theta'}(\omega)}\right\rangle = \left(\cos(r_{\theta'})\hat{\mathcal{A}}_{\theta'}^\dagger + i\sin(r_{\theta'})\hat{\mathcal{B}}_{\theta'}^\dagger\right)\left|{\rm vac}\right\rangle \tag{2.96}$$

The results in Table 2.2 are also useful because they allow us to calculate moments of the operators, for instance the following expectation values of interest:

$$N_a(\omega_a) = \langle{\rm vac}|\hat{\mathcal{U}}_{\rm SQ}^\dagger\hat{a}^\dagger(\omega_a)\hat{a}(\omega_a)\hat{\mathcal{U}}_{\rm SQ}\left|{\rm vac}\right\rangle = \sum_\lambda \sinh^2(s_\lambda)|f_\lambda(\omega_a)|^2 \tag{2.97}$$

$$N_b(\omega_b) = \langle{\rm vac}|\hat{\mathcal{U}}_{\rm SQ}^\dagger\hat{b}^\dagger(\omega_b)\hat{b}(\omega_b)\hat{\mathcal{U}}_{\rm SQ}\left|{\rm vac}\right\rangle = \sum_\lambda \sinh^2(s_\lambda)|j_\lambda(\omega_b)|^2. \tag{2.98}$$

These results are again very similar to the ones obtained for discrete modes in Eq. (2.57). In the limit of $\sinh(s_\lambda) \approx s_\lambda \ll 1$ this allows us to confirm that, for example,

$$\int d\omega_b|F(\omega_a,\omega_b)|^2 = \sum_\lambda s_\lambda^2|f_\lambda(\omega_a)|^2 \approx \langle{\rm vac}|\hat{\mathcal{U}}_{\rm SQ}\hat{a}^\dagger(\omega_a)\hat{a}(\omega_a)\hat{\mathcal{U}}_{\rm SQ}\left|{\rm vac}\right\rangle. \tag{2.99}$$

Finally, let us introduce a useful quantity called the Schmidt number [67]. If we write the Schmidt decomposition of the function F as in Eq. (2.79) then the Schmidt number of the function F is

$$S = \frac{\left(\sum_\lambda s_\lambda^2\right)^2}{\sum_\lambda s_\lambda^4}. \tag{2.100}$$

Note that if the function F is normalized $\int d\omega_a d\omega_b|F(\omega_a,\omega_b)|^2 = \sum_\lambda s_\lambda^2 = 1$ then the numerator of the last equation is simply 1. The Schmidt number of a separable function $F(\omega_a,\omega_b) = sf(\omega_a)j(\omega_b)$ is 1. Functions that are not separable have a Schmidt number greater than 1 and the bigger it is the more terms its Schmidt decomposition has.

$$\hat{\mathcal{U}}_{\rm SQ}^{\dagger}\hat{a}(\omega_a)\hat{\mathcal{U}}_{\rm SQ} = \int d\omega_a' \left(\sum_{\lambda} f_{\lambda}(\omega_a) f_{\lambda}^{*}(\omega_a') \cosh(s_{\lambda})\right) \hat{a}(\omega_a') + i \int d\omega_b' \left(\sum_{\lambda} f_{\lambda}(\omega_a) j_{\lambda}(\omega_b') \sinh(s_{\lambda})\right) \hat{b}^{\dagger}(\omega_b')$$

$$\hat{\mathcal{U}}_{\rm SQ}^{\dagger}\hat{b}(\omega_b)\hat{\mathcal{U}}_{\rm SQ} = i \int d\omega_a' \left(\sum_{\lambda} f_{\lambda}(\omega_a') j_{\lambda}(\omega_b) \sinh(s_{\lambda})\right) \hat{a}^{\dagger}(\omega_a') + \int d\omega_b' \left(\sum_{\lambda} \cosh(s_{\lambda}) j_{\lambda}(\omega_b) j_{\lambda}^{*}(\omega_b')\right) \hat{b}(\omega_b'),$$

$$\hat{\mathcal{U}}_{\rm BS}^{\dagger}\hat{a}(\omega_a)\hat{\mathcal{U}}_{\rm BS} = \int d\omega_a' \left(\sum_{\theta} k_{\theta}(\omega_a) k_{\theta}^{*}(\omega_a') \cos(r_{\theta})\right) \hat{a}(\omega_a') + i \int d\omega_b' \left(\sum_{\theta} k_{\theta}(\omega_a) l_{\theta}^{*}(\omega_b') \sin(r_{\theta})\right) \hat{b}(\omega_b'),$$

$$\hat{\mathcal{U}}_{\rm BS}^{\dagger}\hat{b}(\omega_b)\hat{\mathcal{U}}_{\rm BS} = i \int d\omega_a' \left(\sum_{\theta} \sin(r_{\theta}) l_{\theta}(\omega_b) k_{\theta}^{*}(\omega_a')\right) \hat{a}(\omega_a') + \int d\omega_b' \left(\sum_{\theta} l_{\theta}(\omega_b) l_{\theta}^{*}(\omega_b') \cos(r_{\theta})\right) \hat{b}(\omega_b'),$$

$$\hat{\mathcal{U}}_{\rm RA}^{\dagger}\hat{a}(\omega_a)\hat{\mathcal{U}}_{\rm RA} = \int d\omega_a' \left(\sum_{\alpha} g_{\alpha}(\omega_a) g_{\alpha}^{*}(\omega_a') e^{iu_{\alpha}}\right) \hat{a}(\omega_a'),$$

$$\hat{\mathcal{U}}_{\rm RB}^{\dagger}\hat{b}(\omega_b)\hat{\mathcal{U}}_{\rm RB} = \int d\omega_b' \left(\sum_{\beta} h_{\beta}(\omega_b) h_{\beta}^{*}(\omega_b') e^{iv_{\beta}}\right) \hat{b}(\omega_b').$$

Table 2.2: Transformation of the annihilation operators for the different multimode operations considered in Eq. (2.75) and Eq. (2.77). Note the similarities with Table 2.1 and the fact that annihilation operators are mapped to linear combinations of creation and annihilation operators.

Chapter 3

Nonlinear optics

In this chapter we will quantize the electromagnetic field in a medium and will write the interaction picture Hamiltonians for the nonlinear processes that will be studied in the thesis. It will be shown that the mathematical structure used to describe the quantized electromagnetic field is completely analogous to the one corresponding to a collection of quantum harmonic oscillators. For the derivation of the nonlinear Hamiltonian we will essentially follow the approach of Sipe *et al.* [68, 69, 32].

3.1 Classical Fields

Before studying the nonlinear Hamiltonian we will quantize the electromagnetic field. To this end we will write Maxwell's equations for the Displacement $\vec{D}(\vec{r})$ and Magnetic $\vec{B}(\vec{r})$ fields in a non-magnetic medium as follows

$$\vec{\nabla}\cdot\vec{D}\left(\vec{r}\right)=0, \qquad \vec{\nabla}\cdot\vec{B}\left(\vec{r}\right)=0, \tag{3.1}$$

$$-i\omega\vec{B}\left(\vec{r}\right)=-\vec{\nabla}\times\left(\frac{\vec{D}(\vec{r})}{\epsilon_0 n^2(x,y;\omega)}\right), \qquad -i\omega\vec{D}(\vec{r})=\vec{\nabla}\times\left(\frac{\vec{B}(\vec{r})}{\mu_0}\right).$$

In the last equation we assumed that fields vary harmonically and thus we used

$$f(\vec{r},t) = f(\vec{r})e^{-i\omega t} + \text{c.c.} \tag{3.2}$$

where f is any scalar or vector function. The electric and magnetizing fields are related to the displacement and magnetic fields via

$$\vec{E}(\vec{r}) = \frac{\vec{D}(\vec{r})}{\epsilon_0 n^2(x,y;\omega)}, \qquad \vec{H}(\vec{r}) = \frac{\vec{B}(\vec{r})}{\mu_0}, \tag{3.3}$$

where we assumed the refractive index $n(x,y;\omega)$ to be frequency dependent and space dependent in the directions x, y orthogonal to the direction of propagation z. We are interested in solving Eqs. (3.1) for a set of spatial modes that behave like $\exp(ikz)$ and that can be labeled by their wavevector k and another index (or set of indices) J. The solutions to Eqs. (3.1) can be found by solving the "Master-equation" commonly used in photonic crystal studies [70, 69, 32],

$$\vec{\nabla}\times\left(\frac{\vec{\nabla}\times\vec{B}_{Jk}(\vec{r})}{n^2(x,y;\omega_{Jk})}\right) = \frac{\omega_{Jk}^2}{c^2}\vec{B}_{Jk}(\vec{r}). \tag{3.4}$$

Once the solutions to the Master equation have been found one can directly obtain the displacement field from the last of Eqs. (3.1). Because of the form we assumed for $\vec{B}_{Jk}(\vec{r})$ we can automatically write for the other fields

$$\vec{B}_{Jk}(\vec{r}) = \vec{b}_{Jk}(x,y)\frac{e^{ikz}}{\sqrt{2\pi}}, \qquad \vec{D}_{Jk}(\vec{r}) = \vec{d}_{Jk}(x,y)\frac{e^{ikz}}{\sqrt{2\pi}}, \tag{3.5}$$

$$\vec{H}_{Jk}(\vec{r}) = \vec{h}_{Jk}(x,y)\frac{e^{ikz}}{\sqrt{2\pi}}, \qquad \vec{E}_{Jk}(\vec{r}) = \vec{e}_{Jk}(x,y)\frac{e^{ikz}}{\sqrt{2\pi}}. \tag{3.6}$$

Having the modes we can now write the classical fields as

$$\vec{B}(\vec{r},t) = \sum_J \int dk\ A_{Jk}\vec{B}_{Jk}(\vec{r})e^{-i\omega_{Jk}t} + \text{c.c.}, \tag{3.7}$$

$$\vec{D}(\vec{r},t) = \sum_J \int dk\ A_{Jk}\vec{D}_{Jk}(\vec{r})e^{-i\omega_{Jk}t} + \text{c.c.},$$

$$\vec{H}(\vec{r},t) = \sum_J \int dk\ A_{Jk}\vec{H}_{Jk}(\vec{r})e^{-i\omega_{Jk}t} + \text{c.c.},$$

$$\vec{E}(\vec{r},t) = \sum_J \int dk\ A_{Jk}\vec{E}_{Jk}(\vec{r})e^{-i\omega_{Jk}t} + \text{c.c.}$$

We can in principle choose any normalization for the transverse part of the fields. One that turns out to be convenient when dealing with dispersive media [69] is

$$\int dxdy \frac{\vec{d}^*_{Jk}(x,y)\cdot\vec{d}_{Jk}(x,y)}{\epsilon_0 n^2(x,y;\omega_{Jk})}\frac{v_p(x,y;\omega_{Jk})}{v_g(x,y;\omega_{Jk})} = 1. \tag{3.8}$$

where v_p and v_g are the local phase and group velocities in the medium.

3.2 Quantization

To quantize the fields we turn the amplitudes A_{Jk} into operators $\hat{a}_{Jk}$ modulo some prefactors (these appear because of the normalization used in Eq. (3.8)). This is analogous to how we turned the amplitudes a and a^* into the operators $\hat{a}$ and $\hat{a}^\dagger$ in the last chapter. Now the Schrödinger operators are

$$\begin{aligned}
\vec{B}(\vec{r}) &= \sum_J \int dk\ \sqrt{\frac{\hbar\omega_{Jk}}{2}}\hat{a}_{Jk}\vec{B}_{Jk}(\vec{r}) + \text{H.c.}, \\
\vec{D}(\vec{r}) &= \sum_J \int dk\ \sqrt{\frac{\hbar\omega_{Jk}}{2}}\hat{a}_{Jk}\vec{D}_{Jk}(\vec{r}) + \text{H.c.}, \\
\vec{H}(\vec{r}) &= \sum_J \int dk\ \sqrt{\frac{\hbar\omega_{Jk}}{2}}\hat{a}_{Jk}\vec{H}_{Jk}(\vec{r}) + \text{H.c.}, \\
\vec{E}(\vec{r}) &= \sum_J \int dk\ \sqrt{\frac{\hbar\omega_{Jk}}{2}}\hat{a}_{Jk}\vec{E}_{Jk}(\vec{r}) + \text{H.c.}
\end{aligned} \tag{3.9}$$

The annihilation operators $\hat{a}_{Jk}$ and their adjoints $\hat{a}^\dagger_{Jk}$ satisfy

$$[\hat{a}_{Ik}, \hat{a}_{I'k'}] = 0, \qquad \left[\hat{a}_{Ik}, \hat{a}^\dagger_{I'k'}\right] = \delta_{II'}\delta(k-k') \tag{3.10}$$

and their dynamics is dictated by the linear Hamiltonian

$$\hat{H}_L = \sum_J \int dk\ \hbar\omega_{Jk}\hat{a}^\dagger_{Jk}\hat{a}_{Jk}. \tag{3.11}$$

3.3 The nonlinear interaction

Writing the polarization in the material like we did in the introduction Eq. (1.1)

$$P^i(\vec{r},t) = \Gamma^{ij}_{(1)}(\vec{r})D^j(\vec{r},t) + \Gamma^{ijk}_{(2)}(\vec{r})\,D^j(\vec{r},t)D^k(\vec{r},t) + \ldots \tag{3.12}$$

we can write the nonlinear part of the Hamiltonian as

$$H_{NL} = -\frac{1}{3\epsilon_0}\int d\vec{r}\,\Gamma^{ijk}_{(2)}(\vec{r})D^i(\vec{r})D^j(\vec{r})D^k(\vec{r}) + \ldots \tag{3.13}$$

It can be shown that the $\Gamma_{(2)}$ tensor is related to the more commonly used nonlinear tensor $\chi_{(2)}$ via [32]

$$\Gamma^{ijk}_{(2)}(\vec{r}) \rightarrow \frac{\chi^{ijk}_{(2)}(\vec{r})}{\epsilon_0 n^2(\vec{r}\omega_{Pk_P})n^2(\vec{r},\omega_{Sk_S})n^2(\vec{r},\omega_{Ik_I})} \tag{3.14}$$

and assuming there are only three modes of interest labeled S, I, P and doing the rotating wave approximation we obtain the following Hamiltonian

$$\begin{aligned}\hat{H}_{NL} = &-2\epsilon_0\int dk_P dk_S dk_I \sqrt{\frac{\hbar\omega_{Pk}}{4\pi}\frac{\hbar\omega_{Sk}}{4\pi}\frac{\hbar\omega_{Ik}}{4\pi}}\hat{a}^\dagger_{Sk_S}\hat{a}^\dagger_{Ik_I}\hat{a}_{Pk_P}\int dz e^{i(k_P-k_S-k_I)z}\times \\ &\int dxdy\;\chi^{ijk}_{(2)}(x,y)\frac{\left(d^i_{Sk_S}(x,y)\right)^*\left(d^j_{Ik_I}(x,y)\right)^* d^k_{Pk_P}(x,y)}{\epsilon_0^3 n^2(x,y;\omega_{Sk_S})n^2(x,y;\omega_{Ik_I})n^2(x,y;\omega_{Pk_P})} + \text{H.c.} + \ldots\end{aligned} \tag{3.15}$$

Up to this point we have developed a very general theory of the interaction of photons mediated by a nonlinear structure. In what follows we will specialize this theory to the case of an effective one dimensional structure where the states of the photons can be specified by their frequency ω.

3.4 The interaction Hamiltonian for a χ_2 process

The nonlinear Hamiltonian in the Schrödinger picture Eq. (3.15) can be rewritten as

$$\hat{H}_{NL} = -\int_k dk_a dk_b dk_c S_I(k_c,k_a,k_b)\hat{c}(k_c)\hat{a}^\dagger(k_a)\hat{b}^\dagger(k_b) + \text{H.c.}, \tag{3.16}$$

where we have relabeled $\hat{a}_{Pk_P} \rightarrow \hat{c}(k), \hat{a}_{Ik_I} \rightarrow \hat{b}(k), \hat{a}_{Sk_S} \rightarrow \hat{a}(k)$ and these operators satisfy $[\hat{c}(k),\hat{c}^\dagger(k')] = [\hat{b}(k),\hat{b}^\dagger(k')] = [\hat{a}(k),\hat{a}^\dagger(k')] = \delta(k-k')$ and any other commutator between operators equal to zero. We assume that the wavenumber ranges and/or the polarizations of the pump photons (destruction operator $\hat{c}(k_c)$) and the down-converted photons (destruction operators $\hat{a}(k_a)$ and $\hat{b}(k_b)$) are distinct. Letting the frequency associated with k_l be ω_l, where $l = a, b$, or c, the coupling coefficient $S_I(k_c,k_a,k_b)$ is given

by

$$S_I(k_c,k_a,k_b) = \frac{2}{\epsilon_0}\sqrt{\frac{\hbar\omega_c\hbar\omega_a\hbar\omega_b}{(4\pi)^3}}\frac{\chi_2}{\epsilon_0 n_c^2\,(\omega_c)\,n_a^2(\omega_a)n_b^2(\omega_b)}$$
$$\int_A dxdy\; d_c(x,y)d^*{}_a(x,y)d^*{}_b(x,y)\int_{-L/2}^{L/2} dz\; e^{i(k_c-k_a-k_b)z}, \tag{3.17}$$

where we have put $n_l(\omega_l)$ for $n(\vec{r},\omega_{Kk})$ as the effective index of the indicated mode type. Here we have simplified the expression from the last section for the nonlinear Hamiltonian Eq. (3.15) by neglecting the tensor nature of χ_2 and the vector nature of the $d_l(x,y)$, which characterize the mode profiles of the displacement field; in our expression Eq. (3.17) for $S_I(k_c,k_a,k_b)$ the parameter χ_2 can be taken to characterize the strength of the nonlinearity, which we assume to be present only from $-L/2$ to $L/2$, and we take the $d_l(x,y)$ to be uniform over an area A. The vectors $\vec{d_l}(x,y)$ are normalized according to Eq. (3.8) which can be simplified to

$$\int dxdy\frac{\vec{d_l^*}(x,y)\cdot\vec{d_l}(x,y)}{\epsilon_0 n_l^2(\omega_l)}\frac{v_p(l)}{v_g(l)} = 1, \tag{3.18}$$

where $v_p(l) = c/n_l(\omega_l)$ and $v_g(l) = d\omega_l/dk_l$ are the phase and group velocities (assumed to be constant in the area A), this leads to

$$d_l = \sqrt{\frac{v_g(l)n_l^2(\omega_l)\epsilon_0}{v_p(l)A}}, \tag{3.19}$$

and using this in Eq. (3.17) we have

$$S_I(k_c,k_a,k_b) = 2L\chi_2\sqrt{\frac{\hbar\omega_c\hbar\omega_a\hbar\omega_b v_g(a)v_g(b)v_g(c)}{(4\pi)^3\epsilon_0 A v_p(a)v_p(b)v_p(c)n_a^2n_b^2n_c^2}}\;\mathrm{sinc}\left(\frac{L}{2}(k_c-k_a-k_b)\right). \tag{3.20}$$

In the last equation $\mathrm{sinc}\left(\frac{L}{2}(k_c-k_a-k_b)\right)$ is the so called phase matching function.
For fields propagating in a single direction it is conventional to work with frequency rather than wavenumber labels; hence we take, for example, $\hat{c}(k_c)\to\sqrt{d\omega_c/dk_c}\hat{c}(\omega_c)$, such that

$\left[\hat{c}(\omega_a), \hat{c}^\dagger(\omega_a')\right] = \delta(\omega_a - \omega_a')$. Then changing to frequency variables in Eq. (3.17) we have

$$\hat{H}_I(t) = -2\int_0^\infty d\omega_a d\omega_b d\omega_c L\chi_2 \hat{c}(\omega_c)\hat{a}^\dagger(\omega_a)\hat{b}^\dagger(\omega_b)e^{i\Delta t}\sqrt{\frac{\hbar\omega_c\hbar\omega_a\hbar\omega_b}{(4\pi)^3\epsilon_0 A c^3 n_a(\omega_a)n_b(\omega_b)n_c(\omega_c)}} \times \operatorname{sinc}\left(\frac{L}{2}(k(\omega_c) - k(\omega_a) - k_b(\omega_b))\right) + \text{H.c.}, \tag{3.21}$$

where we have also moved to the interaction picture defined by linear evolution, $\hat{H}_{NL} \to \hat{H}_I(t)$, with $\hat{c}(\omega_c)\hat{a}^\dagger(\omega_a)\hat{b}^\dagger(\omega_b)$ picking up the phase factor $\exp(i\Delta t)$, where $\Delta = \omega_a + \omega_b - \omega_c$. Eq. (3.21) shows explicitly that there will be a significant interaction between fields a, b and c only if the central frequencies $\bar{\omega}$ and central wavevectors satisfy

$$\bar{\omega}_a + \bar{\omega}_b - \bar{\omega}_c \approx 0, \tag{3.22}$$

$$k(\bar{\omega}_a) + k(\bar{\omega}_b) - k(\bar{\omega}_c) \approx 0. \tag{3.23}$$

These two constraints give precisely the energy and momentum conservation rules mentioned in Chapter 1. Note that one can modify the momentum conservation rule if the nonlinearity in the material is also modulated at some spatial periodicity Λ. In that case the $\chi^{ijk}_{(2)}(x,y)$ in Eq. (3.15) should be changed to $\chi^{ijk}_{(2)}(x,y)e^{\pm i2\pi z/\Lambda}$ consequently the argument of the sinc function in Eq. (3.21) is $\frac{L}{2}(k(\omega_c) - k(\omega_a) - k_b(\omega_b) \pm 2\pi/\Lambda)$ and the momentum conservation rule is $k(\bar{\omega}_a) + k(\bar{\omega}_b) - k(\bar{\omega}_c) \approx \pm 2\pi/\Lambda$ [71, 72].

In the same interaction picture mentioned before the electric field operator can be related to the displacement field operator in the usual way Eq. (3.3); using this expression and our expression for the transverse displacement vector Eq. (3.19) we find

$$\vec{E}(\vec{r},t) = \sum_l \int_0^\infty \frac{d\omega_l}{n_l}\sqrt{\frac{\hbar\omega_l}{4\pi\epsilon_0 v_p(l)A}}\hat{q}_l(\omega_l)e^{ik(\omega_l)z - i\omega_l t} + \text{H.c.} \tag{3.24}$$

where l is summed over a, b, and c, $q_l(\omega_l)$ ranges over the destruction operators $\hat{a}(\omega_a)$, $\hat{b}(\omega_b)$, and $\hat{c}(\omega_c)$. Taking the expectation value of the above operator with respect to a coherent state for the pump field (and vacuum for the down-converted photon frequencies) turns $\hat{c}(\omega_c)$ into a c-number $\beta(\omega)$, where we drop the subscript c. Now we can compare this with a classical pulse with energy U_0, centered at $\bar{\omega}_l$ and frequency variance σ^2 (See

Eq. A.11)

$$\begin{aligned}\vec{E}(\vec{r},t) &= E_0 \int_0^\infty d\omega e^{i(k(\omega)z-\omega t)} \frac{1}{\sqrt{2\pi}\sigma} e^{-(\omega-\bar{\omega}_l)^2/2\sigma^2} \\ &= \int_0^\infty d\omega \sqrt{\frac{(U_0/\sqrt{\pi})\sigma}{2\epsilon_0 n(\omega) c A}} e^{i(k(\omega)z-\omega t)} \frac{1}{\sqrt{2\pi}\sigma} e^{-(\omega-\bar{\omega}_l)^2/2\sigma^2},\end{aligned} \tag{3.25}$$

and identify

$$\beta(\omega) = \sqrt{\frac{U_0/\sqrt{\pi}}{\hbar\omega\sigma}} e^{-(\omega-\bar{\omega})^2/2\sigma^2}. \tag{3.26}$$

It is convenient to replace σ by the inverse standard deviation of the time-dependent pump intensity, $\tau = 1/\sqrt{2}\sigma = 2\sqrt{2\ln 2}$ FWHM,(where FWHM is the full width at half maximum of a Gaussian distribution) and write

$$\beta(\omega) = \sqrt{\frac{U_0/\sqrt{\pi/2}}{\hbar\tau\omega}} \tau e^{-\tau^2(\omega-\bar{\omega})^2}. \tag{3.27}$$

With this in hand we can return to the nonlinear Hamiltonian Eq. (3.21) and write

$$\begin{aligned}\hat{H}_I(t) = -\hbar\varepsilon \int_0^\infty d\omega_a d\omega_b d\omega_c \mathrm{sinc}\left(\frac{L}{2}(k(\omega_c) - k_a(\omega_a) - k_b(\omega_b))\right) e^{i\Delta t} \alpha(\omega_c) \hat{a}^\dagger(\omega_a) \hat{b}^\dagger(\omega_b) \\ + \text{H.c.},\end{aligned} \tag{3.28}$$

for an PDC process with a classically described undepleted pump field c, where we introduced the dimensionless perturbation parameter ε

$$\varepsilon = 2L\chi_2 \sqrt{\frac{\sqrt{2}U_0\pi\bar{\omega}_b\bar{\omega}_a}{\sqrt{\pi}(4\pi)^3\epsilon_0 A c^3 n_a(\bar{\omega}_a) n_b(\bar{\omega}_b) n_c(\bar{\omega}_c)\tau}} \tag{3.29}$$

and in benign frequency factors (like the refractive indices and the nonlinear coefficient $\chi_{(2)}$) we have evaluated $\omega_a, \omega_b, \omega_c$ at the central frequencies $\bar{\omega}_a, \bar{\omega}_b, \bar{\omega}_c$. These are the frequencies where the phase-matching condition is assumed to be satisfied exactly. We also introduced

$$\alpha(\omega_c) = \frac{\tau}{\sqrt{\pi}} e^{-\tau^2(\omega_c-\bar{\omega}_c)^2}, \tag{3.30}$$

which is essentially the *shape* of the pulse used to pump the crystal and which has units of time. Eq. (3.28) is the final form of the Hamiltonian we will use in the rest of the

thesis for χ_2 processes.

3.5 The interaction Hamiltonian for a χ_3 process

For a third order process, the straightforward extension of the nonlinear Hamiltonian Eq. (3.16) [32] in the Schrödinger picture is given by

$$\hat{H}_{NL} = -\frac{1}{4\epsilon_0}\int_V d\vec{r}\Gamma_3^{ijkl}\hat{D}^i(\vec{r})\hat{D}^j(\vec{r})\hat{D}^k(\vec{r})\hat{D}^l(\vec{r}), \tag{3.31}$$

where indices refer to Cartesian components and are to be summed over when repeated; Γ_3^{ijkl} can be written in terms of the more usual third order optical susceptibility χ_3^{ijkl} and the linear indices at the appropriate frequency components involved [73]; as in the subsection above we use the symbol χ_3 (without tensor indices) to indicate the size of the component(s) that are important when the relevant fields are used in the different $D^i(\vec{r})$. For Four Wave Mixing (FWM) we require destruction operators for the pump fields ($c(\omega_c)$ and $c(\omega_c')$) and creation operators for the photons generated described by $a\,(\omega_a)$ and $b(\omega_b)$, and in analogy with the result of the last chapter we find

$$\begin{aligned}\hat{H}_I(t) = -\int_{-L/2}^{L/2}dz\int_0^\infty d\omega_c d\omega_c' d\omega_b d\omega_a \frac{3\chi_3}{\epsilon_0^3 n_c^2(\omega_c)n_c^2(\omega_c')n_b^2(\omega_b)n_a^2(\omega_a)}\sqrt{\frac{\hbar\omega_c}{4\pi}\frac{\hbar\omega_c'}{4\pi}\frac{\hbar\omega_a}{4\pi}\frac{\hbar\omega_b}{4\pi}}\\ \frac{An_a(\omega_a)n_b(\omega_b)n_c(\omega_c)n_c(\omega_c')}{\sqrt{v_g(a)v_g(b)v_g(c)v_g(c')}}\sqrt{\frac{v_g(c')\epsilon_0}{v_p(c')A}\frac{v_g(c)\epsilon_0}{v_p(c)A}}\sqrt{\frac{v_g(a)\epsilon_0}{v_p(a)A}\frac{v_g(b)\epsilon_0}{v_p(b)A}}\\ \hat{a}^\dagger(\omega_a)\hat{b}^\dagger(\omega_b)\hat{c}(\omega_c)\hat{c}(\omega_c')e^{-i(\omega_c+\omega_c'-\omega_a-\omega_b)t}e^{i(k_c(\omega_c)+k_c(\omega_c')-k_a(\omega_a)-k_b(\omega_b))z} + \text{H.c.}\end{aligned} \tag{3.32}$$

The factor of 3 in the fraction containing χ_3 is $(4!/2!)/4$, with $(4!/2!)$ the number of permutations involving the ordering of the creation and annihilation operators; note that this is twice the corresponding factor appearing in [73] because here we assume that the creation operators $a^\dagger(\omega_a)$ and $b^\dagger(\omega_b)$ involve different ranges of frequency and/or polarization. The refractive index factors in the denominator, and the appearance of ϵ_0^3, arise because of the conversion from Γ^{ijkl} to χ_3^{ijkl} and the prefactor of ϵ_0^{-1} in Eq. (3.31); compare with the corresponding terms in Eq. (3.17). The terms of the form $\sqrt{\hbar\omega_l/4\pi}$ arise from the expansion of the displacement field in terms of raising and lowering operators, and again find their correspondence in terms in Eq. (3.17). The factor of A comes from integrating over the area in our "toy model" for our waveguide and its modes; the factor $(v_g(a)v_g(b)v_g(c)v_g(c'))^{-1/2}$ arises from the change of variables from wave numbers to frequencies; and the next terms are the expressions for the mode

profiles Eq. (3.19). Supposing that all the frequency prefactors vary slowly relative to the harmonic dependence in space and time due to the phase factors, in those prefactors we set ω_c and ω_c' at the center frequency $\bar{\omega}_c$ of the pump, and evaluate ω_a and ω_b at the frequencies $\bar{\omega}_a$ and $\bar{\omega}_b$ where the phase-matching is optimum; Eq. (3.32) then reduces to

$$\hat{H}_I(t) = -\frac{3\chi_3\hbar^2}{\epsilon_0 A(4\pi)^2c^2}\sqrt{\left(\frac{\bar{\omega}_c}{n_c(\bar{\omega}_c)}\right)^2\frac{\bar{\omega}_a}{n_a(\bar{\omega}_a)}\frac{\bar{\omega}_b}{n_b(\bar{\omega}_b)}}\int_{-L/2}^{L/2}dz\int_0^\infty d\omega_c d\omega_c' d\omega_b d\omega_a \qquad (3.33)$$
$$\times\,\hat{a}^\dagger(\omega_a)\hat{b}^\dagger(\omega_b)\hat{c}(\omega_c)\hat{c}(\omega_c')e^{-i(\omega_c+\omega_c'-\omega_a-\omega_b)t}e^{i(k_c(\omega_c)+k_c(\omega_c')-k_a(\omega_a)-k_b(\omega_b))z} + \text{H.c.}$$

As in the last subsection we replace the c operators by classical functions (see Eq. (3.27)) and assume that $\sigma \ll \bar{\omega}_c$, which allows us to extend the range of the ω_c and ω_c' integrals to $-\infty$ to ∞, and we find

$$\hat{H}_I(t) = -\frac{3\chi_3\hbar^2}{\epsilon_0 A(4\pi)^2c^2}\sqrt{\left(\frac{\bar{\omega}_c}{n_c(\bar{\omega}_c)}\right)^2\frac{\bar{\omega}_a}{n_a(\bar{\omega}_a)}\frac{\bar{\omega}_b}{n_b(\bar{\omega}_b)}}\frac{U_0/\sqrt{\pi/2}}{\hbar\bar{\omega}_c\sigma}\int_{-L/2}^{L/2}dz\int d\omega_c d\omega_c' d\omega_b d\omega_a$$
$$e^{-(\omega_c-\bar{\omega}_c)^2/2\sigma^2}e^{-(\omega_c'-\bar{\omega}_c)^2/2\sigma^2}e^{i(k_c(\omega_c)+k_c(\omega_c')-k_a(\omega_a)-k_b(\omega_b))z}e^{-i(\omega_c+\omega_c'-\omega_a-\omega_b)t}$$
$$\hat{a}^\dagger(\omega_a)\hat{b}^\dagger(\omega_b) + \text{H.c.} \qquad (3.34)$$

To simplify this further we look at the integrals over ω_c and ω_c',

$$I = \int d\omega_c d\omega_c' e^{i(k_c(\omega_c)+k_c(\omega_c'))z - i(\omega_c+\omega_c')t}e^{-(\omega_c-\bar{\omega}_c)^2/2\sigma^2}e^{-(\omega_c'-\bar{\omega}_c)^2/2\sigma^2}. \qquad (3.35)$$

Expanding $k_c(\omega_c)$ and $k_c(\omega_c')$ as

$$k(\omega) = k(\bar{\omega}) + (\omega-\bar{\omega})/v_g + \frac{1}{2}\kappa_{\bar{\omega}}(\omega-\bar{\omega})^2, \qquad (3.36)$$

with $\kappa_{\bar{\omega}} = (d^2k/d\omega^2)_{\omega=\bar{\omega}}$, v_g being the group velocity and introducing $\omega_\pm = \omega_c \pm \omega_c'$, we find that Eq. (3.35) equals

$$I = \int d\omega_+ e^{ik_+(\omega_+)z}e^{-i\omega_+ t}e^{-(\omega_+-2\bar{\omega}_c)^2/4\sigma^2}\int\frac{d\omega_-}{2}e^{-\frac{\omega_-^2}{4}\left(\frac{1}{\sigma^2}-i\kappa_{\bar{\omega}_c}z\right)}, \qquad (3.37)$$

where

$$k_+(\omega_+) = 2k_c(\bar{\omega}_c) + (\omega_+-2\bar{\omega}_c)/v_c + \frac{\kappa_{\bar{\omega}_c}}{4}(\omega_+-2\bar{\omega}_c)^2. \qquad (3.38)$$

We can formally perform the integral over ω_- to get

$$\int \frac{d\omega_-}{2} e^{-\frac{\omega_-^2}{4}\left(\frac{1}{\sigma^2} - i\kappa_{\bar{\omega}_c} z\right)} = \sqrt{\pi}\sigma g(z), \tag{3.39}$$

where

$$g(z) \equiv \frac{1}{\sqrt{1 - i\kappa_{\bar{\omega}_c} z\sigma^2}}. \tag{3.40}$$

Although the square root in the last equation produces two different complex numbers one can always go back to the defining integral Eq. (3.39) which is completely unambiguous. We can then finally write the Hamiltonian as

$$\hat{H}_I(t) = -\hbar\tilde{\varepsilon} \int d\omega_+ \int d\omega_b \int d\omega_a \tilde{\Phi}(\Delta k) e^{i\tilde{\Delta}t} \hat{a}^\dagger(\omega_a) \hat{b}^\dagger(\omega_b) \tilde{\alpha}(\omega_+) + \text{H.c.},$$

where

$$\tilde{\alpha}(\omega_+) \equiv \frac{\tilde{\tau} e^{-\tilde{\tau}^2(\omega_+ - 2\bar{\omega}_c)^2}}{\sqrt{\pi}}, \tag{3.41}$$

(with units of time) characterizes the bandwidth of the pump, and we have introduced $\tilde{\tau} = 1/(2\sigma)$ and $\tilde{\Delta} \equiv \omega_a + \omega_b - \omega_+$, (note the difference between these quantities and the corresponding α, τ, and Δ from the last subsection); the dimensionless perturbation parameter

$$\tilde{\varepsilon} = \frac{6\sqrt{2\pi}\chi_3 U_0 L\sigma}{\epsilon_0 A(4\pi)^2 n_c c^2} \sqrt{\frac{\bar{\omega}_a}{n_a}\frac{\bar{\omega}_b}{n_b}}, \tag{3.42}$$

which characterizes the strength of the nonlinear interaction, and the modified phase matching function is

$$\tilde{\Phi}(\Delta k) \equiv \int_{-L/2}^{L/2} \frac{dz}{L} e^{i(k_a(\omega_a) + k_b(\omega_b) - k_+(\omega_+))z} g(z). \tag{3.43}$$

If the effect of group velocity dispersion on the pump pulse is negligible over the length L of the nonlinear region, for all relevant z we have $|\kappa_{\bar{\omega}_c} z\sigma^2| \ll 1$, we can set $g(z) \to 1$, $k_+(\omega_+) = 2k_c(\omega_+/2)$ and $\tilde{\Phi}(\Delta k) = \text{sinc}(\Delta k L/2)$. Finally, note that we can rewrite expression Eq. (3.41) in a slightly more suggestive manner,

$$\hat{H}_I(t) = -\hbar\tilde{\varepsilon} \int d\omega_+ \int d\omega_b \int d\omega_a \tilde{\Phi}(\Delta k) e^{i\tilde{\Delta}t} \hat{a}^\dagger(\omega_a) \hat{b}^\dagger(\omega_b) \frac{\zeta(\omega_+/2 - \bar{\omega}_c)^2}{2\sigma} + \text{H.c.} \tag{3.44}$$

where $\zeta(\omega) = \exp(-\omega^2/(2\sigma^2))$ is proportional to the electric field amplitude, explicitly displaying the dependence of $\hat{H}_I(t)$ on the square of that amplitude. Of course, the details of the argument given here rely on the assumed Gaussian nature of the pump. But we can expect that the general form Eq. (3.41) will survive even for more general pump pulses, as long as the effect of group velocity dispersion on the pump pulse is negligible.

In the following chapters we will treat the evolution generated by the Hamiltonians Eq. (3.28) and Eq. (3.41) in a non-perturbative way. For the case of SPDC, this implies that we will consider higher powers of the nonlinear susceptibility χ_2, which naturally leads to the question of whether higher order susceptibilities like χ_3 need to be considered. To address this question one should remember that to have a significant nonlinear interaction requires not only intense fields, but also satisfying energy and momentum conservation. Thus if energy and linear momentum are conserved for photon generation via SPDC (see Eq. (3.22)), it is easy to see that one cannot have photon generation via a χ_3 process since this process will not be phase matched and will not preserve energy. The same argument allows us to rule out photon generation through higher order susceptibilities for phase-matched χ_2 and χ_3 processes.

The argument just presented allows us to ignore the photon generation component of a χ_3 process if we design a structure for SPDC. Nevertheless there are other χ_3 processes that are automatically phase-matched and preserve energy. Two such processes are self-phase modulation of the pump pulse and cross-phase modulation of the pump on the down-converted photons [74]. The interplay of the time ordering effects to be discussed in the following chapters and the self- and cross- phase modulation just mentioned is under active study [75].

Chapter 4

The Magnus expansion

> Wigner also describes Pauli as giving the label *die Gruppenpest* ("the group pestilence") to the increasing use of group theory in quantum mechanics
>
> Peter Wolt in Not even Wrong.

4.1 Introduction

Spontaneous parametric down-conversion (SPDC), spontaneous four-wave mixing (SFWM), and frequency conversion (FC) are three of the most common nonlinear processes used in quantum optics. In the first two a nonlinear medium is used to convert photons from a pump laser into pairs of quantum correlated photons [12]. In the third, the frequency of a photon is increased or decreased after it interacts with a strong pump field inside a nonlinear medium. Pair generation is often modeled in a straightforward manner using the first order of a Dyson series, or the first term in a Taylor-like series that results if consequences of time ordering are ignored [57]. But when the nonlinear interaction becomes sufficiently strong a more involved theoretical treatment is required. In particular, the Taylor-like series is suspect beyond a few orders because the interaction Hamiltonian does not commute with itself at different times.

In previous work [59, 60] the Dyson series has been used to investigate parametric down-conversion (PDC), and it was shown that when the initial state of the down-converted fields is vacuum (SPDC), the Taylor-like and Dyson series give identical results up to second order. In a subsequent study, Christ *et al.* [52] used the Heisenberg picture to investigate time-ordering issues in both SPDC and FC. They noticed that when the pump is approximated as undepleted and treated classically, the Hamiltonian is quadratic in the bosonic operators of the down-converted fields, and thus the equations of motion of the operators are necessarily *linear*. This implies that the outgoing fields are related to the

incoming fields by a linear Bogoliubov transformation [76]. They used this observation to build an *ansatz* solution, and develop a numerical algorithm that permits the calculation of the linear transformation relating output to input. Another consequence of the linear Bogoliubov relation between output and input is that the state of the down-converted photons in SPDC cannot be more complicated than a two-mode squeezed vacuum. This is at odds with a result of Brańczyk *et al.* [60], who found that the third order correction to the SPDC state contains a six photon energy correlated state. As we shall show, this discrepancy is related to the fact that the Dyson series does not retain the Gaussian preserving nature of the quadratic Hamiltonian, or equivalently the linear Bogoliubov nature of the transformation relating input and output fields.

In this chapter we employ the Magnus Expansion (ME), which is able to deal properly with time ordering at each level, and thus is unitary to all orders. Yet, unlike the Dyson series, it respects the Gaussian preserving nature of the process for the class of Hamiltonians that are quadratic in bosonic operators, giving rise to a linear Bogoliubov transformation to whatever order it is taken. Thus we feel it should be the preferred strategy for the description of photon generation and conversion in nonlinear quantum optics.

In section 4.2 we introduce the ME and mention some of its important properties, deriving a useful simplification of its terms when dealing with a broad class of Hamiltonians used in quantum optics; we also show why the ME automatically respects the Gaussian nature of usual nonlinear quantum optical processes. In section 4.3 we apply the ME to the PDC and FWM Hamiltonians. While the ME has been used in the past in quantum nonlinear optics (see e.g. Yang *et al.* [32] and references cited therein), usually only the first term in the expansion has been kept. We calculate the second and third order terms, and also introduce diagrams akin to Feynman diagrams that allow for a simple tabulation of the higher order processes in the ME. Using these diagrams we easily demonstrate why it is necessary to go to third order in the expansion to see a correction to the SPDC and SFWM states. In section 4.4 we extend these ideas to FC processes. We show that the expansion formulas derived for FC are completely analogous to those derived for PDC and FWM. In section 4.5 we show how the ME can be taken to a form more amenable to direct calculation and develop a expansion for the joint spectral amplitude (JSA) of the down converted photons in SPDC and SFWM. In section 4.6 we show that for perfect phase matching the second and third order Magnus terms vanish.

4.2 Properties of the Magnus expansion

In quantum mechanics it is often necessary to solve the time-dependent Schrödinger equation for the time evolution operator $\hat{\mathcal{U}}(t,t_0)$,

$$i\hbar\frac{d}{dt}\hat{\mathcal{U}}(t,t_0)=\hat{H}_I(t)\hat{\mathcal{U}}(t,t_0), \tag{4.1}$$

where $\hat{H}_I(t)$ is the interaction picture Hamiltonian. One common way to approximate the solution of Eq. (4.1) is to use the Dyson series in which the evolution operator is expanded as a power series

$$\begin{aligned}\hat{\mathcal{U}}(t_1,t_0)&=\hat{\mathbb{I}}+\hat{T}_1(t_1,t_0)+\hat{T}_2(t_1,t_0)+\dots \\ &=\mathbb{I}+(-i)\int_{t_0}^{t_1}dt'\frac{\hat{H}_I(t')}{\hbar}+(-i)^2\int_{t_0}^{t_1}dt'\int_{t_0}^{t'}dt''\frac{\hat{H}_I(t')\hat{H}_I(t'')}{\hbar^2}+\dots\end{aligned} \tag{4.2}$$

Often after time ordering some of the terms appearing, depicted as Feynman diagrams, can be grouped into classes and summed. Here instead we use the Magnus expansion [77, 78] in which a series expansion is developed as the argument of an exponential,

$$\hat{\mathcal{U}}(t_1,t_0)=\exp\left(\hat{\Omega}_1(t_1,t_0)+\hat{\Omega}_2(t_1,t_0)+\hat{\Omega}_3(t_1,t_0)+\dots\right), \tag{4.3a}$$

$$\hat{\Omega}_1(t_1,t_0)=-\frac{i}{\hbar}\int_{t_0}^{t_1}dt\hat{H}_I(t), \tag{4.3b}$$

$$\hat{\Omega}_2(t_1,t_0)=\frac{(-i)^2}{2\hbar^2}\int_{t_0}^{t_1}dt\int_{t_0}^{t}dt'\left[\hat{H}_I(t),\hat{H}_I(t')\right], \tag{4.3c}$$

$$\begin{aligned}\hat{\Omega}_3(t_1,t_0)=\frac{(-i)^3}{6\hbar^3}\int_{t_0}^{t_1}dt\int_{t_0}^{t}dt'\int_{t_0}^{t'}dt''\Big(&\left[\hat{H}_I(t),\left[\hat{H}_I(t'),\hat{H}_I(t'')\right]\right]\\ &+\left[\left[\hat{H}_I(t),\hat{H}_I(t')\right],\hat{H}_I(t'')\right]\Big).\end{aligned} \tag{4.3d}$$

in general all the terms of the Magnus series are time-ordered integrals of *commutators* of the Hamiltonian at different times [78]. This series will terminate at the second order for the case of the forced harmonic oscillator considered in section 2.1.3 because the commutator of the Hamiltonian at two different times for that problem is a number (see Eq. (2.33)). Thus Eq. (2.35) is indeed the exact propagator for this problem.

In the rest of the thesis we will take unless otherwise indicated $t_0\to-\infty$ and $t_1\to\infty$. In the following we calculate the terms in such a series for a rather broad class of Hamiltonians relevant to nonlinear quantum optics. We write the time dependence of

the interaction Hamiltonian as

$$\hat{H}_I(t) = \hbar \int d\boldsymbol{\omega} \left(\hat{h}(\boldsymbol{\omega}) e^{i\Delta t} + \hat{h}^\dagger(\boldsymbol{\omega}) e^{-i\Delta t} \right), \tag{4.4}$$

where we use the shorthand notation

$$\begin{aligned} \hat{h}(\boldsymbol{\omega}) &= \hat{h}(\omega_1, \omega_2, \ldots, \omega_n), \\ d\boldsymbol{\omega} &= d\omega_1 d\omega_2 \ldots d\omega_n, \\ \Delta &= \Delta(\omega_1, \omega_2, \ldots, \omega_n). \end{aligned} \tag{4.5}$$

For the moment we leave the integration limits of the frequencies $\boldsymbol{\omega}$ unspecified; in the next sections we will specify them for particular cases. For the first order Magnus term one simply finds

$$\hat{\Omega}_1 = -\frac{i}{\hbar} \int dt \hat{H}_I(t) = -2\pi i \int d\boldsymbol{\omega} \left(\hat{h}(\boldsymbol{\omega}) + \text{H.c.} \right) \delta(\Delta). \tag{4.6}$$

In the last equation we have adopted the convention that whenever the lower (or upper) limit of an integral over time is not specified it is meant to be understood as $-\infty$ (or $+\infty$). The term in Eq. (4.6), exponentiated, corresponds to the sum of the Taylor-like series for $\hat{\mathcal{U}}$ that could be constructed by time ordering the series Eq. (4.2) and ignoring the fact that the Hamiltonians $\hat{H}_I(t)$ at different times t need not commute. In fact, if $[\hat{H}_I(t), \hat{H}_I(t')] = 0$ for all t and t', then $\exp \hat{\Omega}_1$ constitutes the *exact* solution of the problem, since all the higher order Magnus terms vanish. Hence we refer to terms in the Magnus expansion beyond $\hat{\Omega}_1$ as "time-ordering corrections".

In general no simplifications can be made to the higher order Magnus terms if no further assumptions are made about $\hat{H}_I(t)$. We make the following assumption:

$$[\hat{h}(\boldsymbol{\omega}), \hat{h}(\boldsymbol{\omega}')] = [\hat{h}^\dagger(\boldsymbol{\omega}), \hat{h}^\dagger(\boldsymbol{\omega}')] = 0, \tag{4.7}$$

which is indeed valid for the Hamiltonians usually employed to describe both type I and II parametric down-conversion, four wave mixing, and frequency conversion, either if the pump is treated classically or if it is treated quantum mechanically. Using property Eq. (4.7) and the fact that

$$\int dt \int^t dt' e^{i\Delta t - i\Delta' t'} = 2\pi^2 \delta(\Delta)\delta(\Delta') + 2\pi i \delta(\Delta - \Delta') \frac{\mathcal{P}}{\Delta}, \tag{4.8}$$

with $\mathcal{P}$ indicating a principal value, the second order Magnus term, generally given by

Eq. (4.3c) can be simplified to

$$\hat{\Omega}_2 = -2\pi i \fint d\boldsymbol{\omega} d\boldsymbol{\omega}' \left[\hat{h}(\boldsymbol{\omega}), \hat{h}^\dagger(\boldsymbol{\omega}')\right] \frac{\delta(\Delta - \Delta')}{\Delta}. \tag{4.9}$$

In the last equation we have used the principal value integral symbol $\fint$. This is necessary because the result Eq. (4.8) is only valid under a principal value integration sign. Only the second term of Eq. (4.8) contributes to the second order term. This is to be expected since the first term is just

$$2\pi^2 \delta(\Delta)\delta(\Delta') = \frac{1}{2}\int dt \int dt' e^{i\Delta t - i\Delta' t'}, \tag{4.10}$$

which is the expression that would be obtained from Eq. (4.8) ignoring the time ordering; note the difference in limits between Eq. (4.10) and Eq. (4.8).

Now let us look at the third order Magnus term Eq. (4.3d). Here the relevant time integrals take the form

$$\begin{aligned}\int dt \int^t dt' \int^{t'} dt'' e^{i\mu t + i\nu t' + i\xi t''} = 2\pi^3 \delta(\mu)\,\delta(\nu)\,\delta(\xi) - 2\pi^2 i \delta(\nu+\xi)\,\delta(\mu+\nu+\xi)\,\frac{\mathcal{P}}{\xi} \\ + 2\pi^2 i \delta(\mu+\nu)\,\delta(\mu+\nu+\xi)\,\frac{\mathcal{P}}{\mu} - 2\pi \delta(\mu+\nu+\xi)\,\frac{\mathcal{P}}{\mu+\nu}\frac{\mathcal{P}}{\mu}.\end{aligned} \tag{4.11}$$

Because of the condition Eq. (4.7) the only term that contributes to $\hat{\Omega}_3$ in Eq. (4.11) is the last one, and then upon relabeling one obtains:

$$\begin{aligned}\hat{\Omega}_3 = -2\pi i \fint d\boldsymbol{\omega} d\boldsymbol{\omega}' d\boldsymbol{\omega}'' \left([\hat{h}(\boldsymbol{\omega}), [\hat{h}(\boldsymbol{\omega}'), \hat{h}^\dagger(\boldsymbol{\omega}'')]] + \text{H.c.}\right) \\ \times \frac{\delta(\Delta + \Delta' - \Delta'')}{3}\left(\frac{1}{\Delta\Delta''} + \frac{1}{\Delta\Delta'}\right).\end{aligned} \tag{4.12}$$

We emphasize that the simple form obtained for $\hat{\Omega}_3$ critically depends on assumption Eq. (4.7). If this did not hold, then the second and third terms in Eq. (4.11) would also contribute, leading to a much more complicated expression. However, even if Eq. (4.7) were not to hold the first term of Eq. (4.11) would never contribute to $\hat{\Omega}_3$, which is related to the fact that it is proportional to terms that would arise if time order were ignored, and their effects have all been included in $\hat{\Omega}_1$.

Finally, let us note that the Magnus expansion is more robust in preserving qualitative features of the exact solution for $\hat{\mathcal{U}}$ than the Dyson expansion, particularly for problems in nonlinear quantum optics. Generally, of course, the Magnus expansion truncated at any

level will always give rise to a unitary evolution operator if the Hamiltonian is Hermitian, as is assumed when writing Eq. (4.4), while a truncated Dyson expansion will not. More specifically, the Magnus expansion truncated at any level will always give rise, in the Heisenberg picture, to a linear Bogoliubov transformation of the bosonic operators if the Hamiltonian is quadratic in them. Since such quadratic bosonic Hamiltonians (QBH) often appear in nonlinear quantum optics, and since for such a Hamiltonian the exact solution for the Heisenberg picture evolution of the bosonic operators indeed takes the form of a linear Bogoliubov transformation [76], this is a very desirable feature of the Magnus approximation. Here is the proof that any Magnus approximation displays this feature: From the general commutator identity

$$[\hat{A}\hat{B},\hat{C}\hat{D}] = [\hat{A},\hat{C}]\hat{B}\hat{D} + \hat{A}[\hat{B},\hat{C}]\hat{D} + \hat{C}[\hat{A},\hat{D}]\hat{B} + \hat{C}\hat{A}[\hat{B},\hat{D}]. \tag{4.13}$$

we see that if $\hat{A},\hat{B},\hat{C},\hat{D}$ are all bosonic operators then the commutators on the right hand side are all $c-$numbers, and in fact if they do not vanish they are delta functions, either Kronecker or Dirac. Since all the terms $\hat{\Omega}_1,\hat{\Omega}_2$ etc., in the Magnus series involve commutators, it is clear that for a QBH all the terms $\hat{\Omega}_i$ will be quadratic functions of the bosonic operators, and the M^{th} order approximation to the Magnus expansion

$$\hat{\mathcal{U}}_M(t_f,t_0) = \exp(\hat{\Omega}_1(t_f,t_0) + \hat{\Omega}_2(t_f,t_0) + \ldots + \hat{\Omega}_M(t_f,t_0)) = \exp(\hat{\mathcal{O}}_M(t_f,t_0)), \tag{4.14}$$

where we reinstate general initial and final times, t_0 and t_f respectively, is characterized by an operator $\hat{\mathcal{O}}(t_f,t_0)$ that is anti-Hermitian and a quadratic function of the boson operators. Now in the Heisenberg picture and initial operator $\hat{A}(t_0)$ evolves to a later operator $\hat{A}(t_f)$ according to

$$\hat{A}(t_f) = \hat{\mathcal{U}}^\dagger(t_f,t_0)\hat{A}(t_0)\hat{\mathcal{U}}(t_f,t_0). \tag{4.15}$$

Using the approximation given by Eq. (4.14) and the Baker-Campbell-Hausdorff (BCH) lemma

$$e^{\hat{X}}\hat{Y}e^{-\hat{X}} = \hat{Y} + \left[\hat{X},\hat{Y}\right] + \frac{1}{2!}\left[\hat{X},\left[\hat{X},\hat{Y}\right]\right] + \cdots, \tag{4.16}$$

we find

$$\hat{A}(t_f) = \hat{A}(t_0) + [\hat{A}(t_0),\hat{\mathcal{O}}_M(t_f,t_0)] + \frac{1}{2!}[[\hat{A}(t_0),\hat{\mathcal{O}}_M(t_f,t_0)],\hat{\mathcal{O}}_M(t_f,t_0)] + \ldots \tag{4.17}$$

Using the general commutator identity

$$[\hat{A}, \hat{B}\hat{C}] = [\hat{A}, \hat{B}]\hat{C} + \hat{B}[\hat{A}, \hat{C}], \tag{4.18}$$

we see that if $\hat{A}(t_0)$ is a bosonic operator the commutators on the right hand side of Eq. (4.17) will all be bosonic operators, and thus the Heisenberg bosonic operators at t_f are indeed linear functions of the Heisenberg bosonic operators at t_0. This completes the proof. In the Schrödinger picture, the result implies that any Magnus approximation for evolution under a QBH will share the property of the exact solution that the general Gaussian nature of an initial state will be preserved; that is, the exact evolution constitutes a unitary Gaussian channel, and any Magnus approximation for the evolution constitutes a unitary Gaussian channel as well [66].

4.3 Time ordering in Parametric Down-Conversion and Four Wave Mixing

In type II SPDC an incoming photon at frequency ω_p is transformed into two photons of different polarizations at frequencies ω_a and ω_b which are roughly half the frequency of the incoming photon. Within the usual rotating wave and undepleted pump approximations, the interaction Hamiltonian governing this process in an effectively one-dimensional structure with all relevant fields propagating in the same direction, such as a channel or ridge waveguide, is (see section 3.5)

$$\hat{H}_I(t) = -\hbar\varepsilon \int d\omega_a d\omega_b d\omega_p e^{i\Delta t} \Phi(\omega_a, \omega_b, \omega_p) \alpha(\omega_p) \hat{a}^\dagger(\omega_a) \hat{b}^\dagger(\omega_b) + \text{H.c.}, \tag{4.19}$$

$$\Delta = \omega_a + \omega_b - \omega_p. \tag{4.20}$$

where $\hat{a}(\omega_a)$ and $\hat{b}(\omega_b)$ are photon destruction operators associated with the wavevectors $k_a(\omega_a)$ and $k_b(\omega_b)$, constructed to satisfy the commutation relations

$$[\hat{a}(\omega), \hat{a}^\dagger(\omega')] = [\hat{b}(\omega), \hat{b}^\dagger(\omega')] = \delta(\omega - \omega'), \tag{4.21}$$

and all other commutators between destruction and creation operators vanishing; $\alpha(\omega_p)$ is a classical function proportional to the electric field amplitude of the undepleted pump field with wavevector $k(\omega_p)$. The assumption Eq. (4.21) is well justified because for

type II SPDC the down converted photons appear in orthogonal polarizations, and their frequency support is far away from the frequency support of the pump field characterized by $\alpha(\omega_p)$. Because of this the limits of integration for the frequencies of the fields will range from 0 to ∞. Nevertheless, since the bandwidth of the photons is much smaller than their central frequencies these integrals can be safely extended in their lower limit to $-\infty$.

The phase matching function Φ incorporates the spatial dependence of the fields and the nonlinearity profile; It takes the form

$$\Phi(\omega_a, \omega_b, \omega_p) = \mathrm{sinc}\left(\frac{\Delta k L}{2}\right), \quad \Delta k = k_a(\omega_a) + k_b(\omega_b) - k_p(\omega_p), \tag{4.22}$$

when the nonlinearity is assumed to be uniform in a region of space from $-L/2$ to $L/2$, and in Eq. (4.19) ε is a dimensionless constant incorporating parameters such as the strength of the nonlinearity profile and the effective cross sectional area of the crystal. There will be corrections to the integrand of Eq. (4.19) depending in a benign way on the frequencies (see Eq. (3.29)), and for simplicity we neglect them here.

In SFWM a pair of photons from a pump field at frequencies ω_p and ω_p' are converted into a pair of photons of different frequencies $\omega_p \pm \Delta\omega_p$. The description of this process is inherently more complicated than that of SPDC, but we show in Sec. 3.5 that if the pump field is treated classically and undepleted, then the Hamiltonian governing the process is formally identical to Eq. (4.19) if the effects of group velocity dispersion on the propagation of the pump pulse can be neglected. In that limit we find

$$\hat{H}_I(t) = -\hbar\tilde{\varepsilon} \int d\omega_a d\omega_b d\omega_+ e^{i\tilde{\Delta}t} \tilde{\Phi}(\omega_a, \omega_b, \omega_+) \tilde{\alpha}(\omega_+) \hat{a}^\dagger(\omega_a) \hat{b}^\dagger(\omega_b) + \mathrm{H.c.}, \tag{4.23}$$

where here $\tilde{\Delta} = \omega_a + \omega_b - \omega_+$, $\omega_p + \omega_p' = \omega_+$ and

$$\tilde{\Phi}(\omega_a, \omega_b, \omega_+) = \mathrm{sinc}\left(\frac{\Delta k L}{2}\right), \quad \Delta k = k_a(\omega_a) + k_b(\omega_b) - 2k_p\left(\frac{\omega_+}{2}\right), \tag{4.24}$$

and now $\tilde{\alpha}(\omega_+)$ is proportional to the square of the amplitude of the electric field of the pump. Again we have assumed that the generated photons at ω_a and ω_b are characterized by distinct polarizations and/or frequency ranges – the latter, for example, might arise due to phase matching constraints [79] – and thus the only nonvanishing commutation relations are given by Eq. (4.21).

While the approach introduced in this chapter can be applied to more complicated scenarios for SFWM, we restrict ourselves here to situations where Eq. (4.23) is appli-

cable; then the analysis of SPDC and SFWM is essentially the same. The interaction Hamiltonian $H_I(t)$ takes the form Eq. (4.4) with

$$\hat{h}(\omega_a, \omega_b, \omega_p) = F(\omega_a, \omega_b, \omega_p)\hat{a}^\dagger(\omega_a)\hat{b}^\dagger(\omega_b), \tag{4.25}$$

$$F(\omega_a, \omega_b, \omega_p) = -\varepsilon\alpha(\omega_p)\Phi(\omega_a, \omega_b, \omega_p), \tag{4.26}$$

for SPDC; for SFWM we simply replace ω_p by ω_+, $\alpha(\omega_p)$ by $\tilde{\alpha}(\omega_+)$, ε by $\tilde{\varepsilon}$ and $\Phi(\omega_a, \omega_b, \omega_c)$ by $\tilde{\Phi}(\omega_a, \omega_b, \omega_+)$. So although in the calculations below we explicitly use the notation for SPDC, the generalization to SFWM is trivial.

With the notation introduced in the paragraphs above, the first order Magnus term is

$$\hat{\Omega}_1 = -2\pi i \int d\omega_a d\omega_b \big(J_1(\omega_a, \omega_b)\hat{a}^\dagger(\omega_a)\hat{b}^\dagger(\omega_b) + \text{H.c.}\big), \tag{4.27}$$

with

$$J_1(\omega_a, \omega_b) = F(\omega_a, \omega_b, \omega_a + \omega_b). \tag{4.28}$$

This process can be represented by the diagram (a) in Fig. 4.1 in which a photon of frequency of ω_p (or two photons of frequency ω_p for SFWM) is converted to two photons of frequency ω_a and ω_b; we associate it with the term $J_1(\omega_a, \omega_b)\, a^\dagger(\omega_a)b^\dagger(\omega_b)$. To have a Hermitian Hamiltonian, the reverse process needs to be possible and this is associated with $J_1^*(\omega_a, \omega_b)\, a(\omega_a)b(\omega_b)$ where x^* is the complex conjugate of x. We note that with the approximation of keeping only the first term in the Magnus expansion, as well as the assumption that its effect is small, we have

$$|\psi(\infty)\rangle = \hat{\mathcal{U}}\,|\psi(-\infty)\rangle \approx e^{\hat{\Omega}_1}\,|\psi(-\infty)\rangle \approx (\mathbb{I} + \hat{\Omega}_1)\,|\psi(-\infty)\rangle = (\hat{\mathbb{I}} + \hat{T}_1)\,|\psi(-\infty)\rangle\,, \tag{4.29}$$

where T_1 is the first term of the Dyson series Eq. (4.2), this is, as shown in the last equation, identical to the first order Magnus term $\hat{\Omega}_1$.
For the second order Magnus term we need the following:

$$\begin{aligned}\Big[\hat{h}(\boldsymbol{\omega}), \hat{h}^\dagger(\boldsymbol{\omega'})\Big] = &-\delta(\omega_b' - \omega_b)F(\omega_a, \omega_b, \omega_p)\, F^*\left(\omega_a', \omega_b', \omega_p'\right)\hat{a}^\dagger(\omega_a)\hat{a}(\omega_a') \\ &-\delta(\omega_a' - \omega_a)F(\omega_a, \omega_b, \omega_p)\, F^*\left(\omega_a', \omega_b', \omega_p'\right)\hat{b}^\dagger(\omega_b)\hat{b}(\omega_b').\end{aligned} \tag{4.30}$$

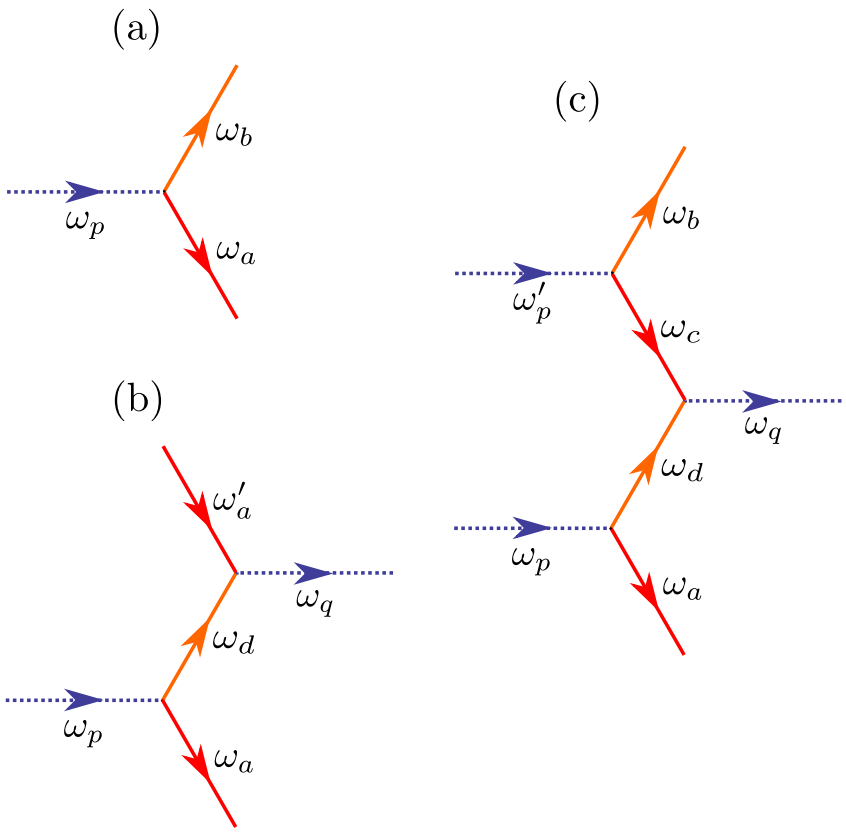

Figure 4.1: Diagrams representing the first, second and third order Magnus terms for PDC. Dashed lines are used to represent pump photons, full lines are used to represent lower energy down converted ones. (a) depicts a photon of frequency ω_p being converted to two photons of frequencies ω_a and ω_b. (b) depicts the second order Magnus term in which one of the photons from a down-conversion event is, with the help of a low energy photon previously present, up converted to a pump photon. Finally, (c) depicts the third order Magnus term in which a pair of photons from two previous down-conversion events is converted to a pump photon.

After some relabeling the second order Magnus term is

$$\hat{\Omega}_2 = -2\pi i\Big(\int d\omega_a d\omega'_a G_2^a(\omega_a,\omega'_a)\hat{a}^\dagger(\omega_a)\,\hat{a}(\omega'_a) + \int d\omega_b d\omega'_b G_2^b(\omega_b,\omega'_b)\hat{b}^\dagger(\omega_b)\,\hat{b}(\omega'_b)\Big), \tag{4.31}$$

with

$$G_2^a(\omega_a,\omega'_a) = \int d\omega_d \oint \frac{d\omega_p}{\omega_p} F(\omega_a,\omega_d,\omega_a+\omega_p+\omega_d)\,F^*(\omega'_a,\omega_d,\omega'_a+\omega_p+\omega_d), \tag{4.32a}$$

$$G_2^b(\omega_b,\omega'_b) = \int d\omega_c \oint \frac{d\omega_p}{\omega_p} F(\omega_c,\omega_b,\omega_b+\omega_c+\omega_p)\,F^*(\omega_c,\omega'_b,\omega'_b+\omega_p+\omega_c). \tag{4.32b}$$

The last expression shows that the second order term corresponds to a frequency conversion process in which a photon of frequency ω'_a (ω'_b) is converted to one of frequency ω_a (ω_b) with probability amplitude $G_2^a(G_2^b)$. These terms once exponentiated correspond to rotation operators $\hat{\mathcal{U}}_{\mathrm{RA}}$ and $\hat{\mathcal{U}}_{\mathrm{RB}}$. If one recognizes that F is associated with down-conversion and F^* with up conversion, then Eqs. (4.32) can be read as follows: first a photon at the pump energy (or two photons for the case of SFWM) is down converted to two photons of energies ω_a (ω_b) and $\omega_d(\omega_c)$. Later the photon of energy $\omega_d(\omega_c)$ interacts with a photon of energy ω'_a (ω'_b) to be up converted to another photon of energy close to the pump energy (or a pair of photons for SFWM), which effectively gives a frequency conversion process from $\omega'_a(\omega'_b)$ to ω_a (ω_b). This is sketched in diagram (b) in Fig. 4.1. For the third order Magnus term we need to calculate the following:

$$\begin{aligned}[\hat{h}(\boldsymbol{\omega}),[\hat{h}(\boldsymbol{\omega'}),\hat{h}^\dagger(\boldsymbol{\omega''})]] = {} & F(\omega_a,\omega_b,\omega_p)\,F\left(\omega'_a,\omega'_b,\omega'_p\right)F^*\left(\omega''_a,\omega''_b,\omega''_p\right)\times \\ & \Big(\delta(\omega''_a-\omega'_a)\,\delta(\omega''_b-\omega_b)\,\hat{b}^\dagger(\omega'_b)\,\hat{a}^\dagger(\omega_a) + \delta(\omega''_a-\omega_a)\,\delta(\omega''_b-\omega'_b)\,\hat{b}^\dagger(\omega_b)\,\hat{a}^\dagger(\omega'_a)\Big).\end{aligned} \tag{4.33}$$

Using Eq. (4.12), after some rearranging of the dummy integration variables we obtain

$$\begin{aligned}\hat{\Omega}_3 = {} & -2\pi i \int d\omega_a d\omega_b \hat{a}^\dagger(\omega_a)\hat{b}^\dagger(\omega_b) \oint d\omega_c d\omega_d d\omega_p d\omega_q \frac{F^*(\omega_d,\omega_c,-\omega_a-\omega_b+\omega_p+\omega_q)}{3} \\ & \times F(\omega_a,\omega_c,\omega_p)\,F(\omega_d,\omega_b,\omega_q)\Big\{\frac{2}{(\omega_a+\omega_c-\omega_p)(\omega_b+\omega_d-\omega_q)} \\ & + \frac{1}{(\omega_a+\omega_c-\omega_p)(\omega_a+\omega_b+\omega_c+\omega_d-\omega_p-\omega_q)} \\ & + \frac{1}{(\omega_b+\omega_d-\omega_q)(\omega_a+\omega_b+\omega_c+\omega_d-\omega_p-\omega_q)}\Big\}.\end{aligned}$$

Switching $\omega_p \to \omega_p + \omega_a + \omega_c$ and $\omega_q \to \omega_q + \omega_b + \omega_d$ the innermost integral becomes

$$\int d\omega_c d\omega_d \fint d\omega_p d\omega_q \frac{F^*\left(\omega_d, \omega_c, \omega_c + \omega_d + \omega_p + \omega_q\right)}{3} F\left(\omega_a, \omega_c, \omega_a + \omega_c + \omega_p\right) \times F\left(\omega_d, \omega_b, \omega_b + \omega_d + \omega_q\right) \left\{ \frac{2}{\omega_p \omega_q} + \frac{1}{\omega_p + \omega_q} \left(\frac{1}{\omega_p} + \frac{1}{\omega_q} \right) \right\}. \tag{4.34}$$

At this point we use the identity (for a proof see Appendix 7 of Ref. [65])

$$\frac{\mathcal{P}}{\omega_p + \omega_q} \left(\frac{\mathcal{P}}{\omega_p} + \frac{\mathcal{P}}{\omega_q} \right) = \frac{\mathcal{P}}{\omega_p} \frac{\mathcal{P}}{\omega_q} + \pi^2 \delta(\omega_p) \delta(\omega_q), \tag{4.35}$$

which is valid under the assumption that the test function over which the principal values are being calculated is well behaved. We can then write

$$\hat{\Omega}_3 = -2\pi i \int d\omega_a d\omega_b \big(J_3(\omega_a, \omega_b) \hat{a}^\dagger(\omega_a) \hat{b}^\dagger(\omega_b) + \text{H.c.} \big), \tag{4.36}$$

with

$$J_3(\omega_a, \omega_b) = \int d\omega_c d\omega_d \Big\{ \frac{\pi^2}{3} F^*\left(\omega_c, \omega_d, \omega_c + \omega_d\right) F\left(\omega_a, \omega_d, \omega_a + \omega_d\right) F\left(\omega_c, \omega_b, \omega_b + \omega_c\right) + \fint \frac{d\omega_p}{\omega_p} \frac{d\omega_q}{\omega_q} F^*\left(\omega_c, \omega_d, \omega_c + \omega_d + \omega_p + \omega_q\right) \times F\left(\omega_a, \omega_d, \omega_a + \omega_d + \omega_p\right) F\left(\omega_c, \omega_b, \omega_b + \omega_c + \omega_q\right) \Big\}. \tag{4.37}$$

As before, a diagram representing the third order processes can be drawn. This corresponds to two down-conversion processes in which one of the converted photons from each process is later used for up-conversion, as is seen in diagram (c) of Fig. 4.1.

Note that the treatment for type I degenerate PDC follows easily from what was done above. One needs only to replace b by a to characterize the fact that both down converted photons are generated with the same polarization and in the same frequency range; the quantity F in Eq. (4.25) will be symmetric in the first two arguments, $F(x, y, z) = F(y, x, z)$, and the expression for ε will differ by a factor of two.

Finally, let us mention that we have developed a numerical library [80] that uses the `cubature` software package [81] to numerically approximate the different Magnus terms for PDC and FWM within the approximations introduced in this chapter.

4.4 Time ordering in Frequency Conversion

Frequency conversion (FC) is another nonlinear process in which three fields interact. In this section we explicitly consider FC employing a χ_2 nonlinearity, but the extension to treat FC by a χ_3 nonlinearity follows in the same way the description of photon generation by SFWM followed from the description of photon generation by SPDC. For a χ_2 nonlinearity, FC occurs when a pump photon with frequency ω_p fuses with a photon with frequency ω_a to create a higher energy photon with frequency $\omega_b = \omega_a + \omega_p$. The Hamiltonian governing this process is derived in a completely analogous manner to the way Eq. (4.19) is derived in Section 3.5. The Hamiltonian governing the process is

$$\hat{H}_I(t) = -\hbar\varepsilon \int d\omega_a d\omega_b d\omega_p e^{i\bar{\Delta}t} \bar{\Phi}(\omega_a, \omega_b, \omega_p)\alpha(\omega_p)\hat{a}(\omega_a)\hat{b}^\dagger(\omega_b) + \text{H.c.}, \tag{4.38}$$

where all the variables have the same meaning as in Eq. (4.19) except that now the phase matching function for uniform non-linearity in the region $-L/2$ to $L/2$ is given by

$$\bar{\Phi}(\omega_a, \omega_b, \omega_p) = \text{sinc}\left(\frac{\overline{\Delta k}L}{2}\right), \quad \overline{\Delta k} = k_b(\omega_b) - k_a(\omega_a) - k_p(\omega_p), \tag{4.39}$$

and

$$\bar{\Delta} = \omega_b - \omega_a - \omega_p. \tag{4.40}$$

The interaction Hamiltonian Eq. (4.38) can be rewritten as

$$\hat{H}_I(t) = \int d\omega_a d\omega_b d\omega_p \left(e^{i\bar{\Delta}t}\hat{h}(\omega_a, \omega_b, \omega_p) + \text{H.c.}\right), \tag{4.41}$$

with

$$\hat{h}(\omega_a, \omega_b, \omega_p) = \hat{a}(\omega_a)\hat{b}^\dagger(\omega_b)\bar{F}\left(\omega_a, \omega_b, \omega_p\right), \tag{4.42}$$

$$\bar{F}(\omega_a, \omega_b, \omega_p) = -\varepsilon\alpha(\omega_p)\bar{\Phi}(\omega_a, \omega_b, \omega_p). \tag{4.43}$$

Note that for the functions associated with FC we used an overbar. The classical pump is described in the same manner for both PDC, FWM and FC and thus we do not use an overbar for it.

For FC the first Magnus term is

$$\hat{\Omega}_1 = -2\pi i \int d\omega_a d\omega_b \big(\bar{J}_1(\omega_a,\omega_b)\hat{a}(\omega_a)\hat{b}^\dagger(\omega_b) + \text{H.c.}\big). \tag{4.44}$$

with

$$\bar{J}_1(\omega_a,\omega_b) = \bar{F}(\omega_a,\omega_b,\omega_b-\omega_a). \tag{4.45}$$

For the higher order terms we find:

$$\hat{\Omega}_2 = -2\pi i\Big(\int d\omega_a d\omega'_a \bar{G}_2^a(\omega_a,\omega'_a)\hat{a}^\dagger(\omega_a)\,\hat{a}\,(\omega'_a) + \int d\omega_b d\omega'_b \bar{G}_2^b(\omega_b,\omega'_b)\hat{b}^\dagger(\omega_b)\,\hat{b}\,(\omega'_b)\Big). \tag{4.46}$$

with

$$\bar{G}_2^a(\omega_a,\omega'_a) = -\int d\omega_q \fint \frac{d\omega_p}{\omega_p}\bar{F}\left(\omega'_a,\omega_q,\omega_q-\omega'_a+\omega_p\right)\bar{F}^*\left(\omega_a,\omega_q,\omega_q-\omega_a+\omega_p\right), \tag{4.47}$$

$$\bar{G}_2^b(\omega_b,\omega'_b) = \int d\omega_q \fint \frac{d\omega_p}{\omega_p}\bar{F}\left(\omega_q,\omega_b,\omega_b-\omega_q+\omega_p\right)\bar{F}^*\left(\omega_q,\omega'_b,\omega'_b+\omega_p-\omega_q\right), \tag{4.48}$$

and

$$\hat{\Omega}_3 = -2\pi i \int d\omega_a d\omega_b \left(\bar{J}_3(\omega_a,\omega_b)\hat{a}(\omega_a)\hat{b}^\dagger(\omega_b) + \text{H.c.}\right), \tag{4.49}$$

with

$$\begin{aligned}\bar{J}_3(\omega_a,\omega_b) = \int d\omega_c d\omega_d \Big\{ &\frac{-\pi^2}{3}\bar{F}^*\left(\omega_c,\omega_d,\omega_d-\omega_c\right)\bar{F}\left(\omega_a,\omega_d,\omega_d-\omega_a\right)\bar{F}\left(\omega_c,\omega_b,\omega_b-\omega_c\right)\\ &+ \fint \frac{d\omega_p}{\omega_p}\frac{d\omega_q}{\omega_q}\bar{F}^*\left(\omega_c,\omega_d,\omega_d-\omega_c+\omega_p-\omega_q\right)\times\\ &\qquad \bar{F}\left(\omega_a,\omega_d,\omega_d-\omega_a-\omega_q\right)\bar{F}\left(\omega_c,\omega_b,\omega_b-\omega_c+\omega_p\right)\Big\}.\end{aligned} \tag{4.50}$$

In the last equation it has been assumed again that the function F is well behaved.

Note the very elegant connection the Magnus series provides between FC and PDC. To obtain the Hamiltonian of FC from that of SPDC it suffices to make the substitutions $\hat{a}(\omega_a) \to \hat{a}^\dagger(\omega_a), \hat{a}^\dagger(\omega_a) \to \hat{a}(\omega_a)$ and $\omega_a \to -\omega_a$. The corresponding Magnus terms of FC are obtained by performing exactly the same substitutions in the SPDC terms, and rearranging the sign of the variables in the principal value integrals over ω_q and ω_p. They can also be represented by diagrams as shown in Figure 4.2. They follow similar

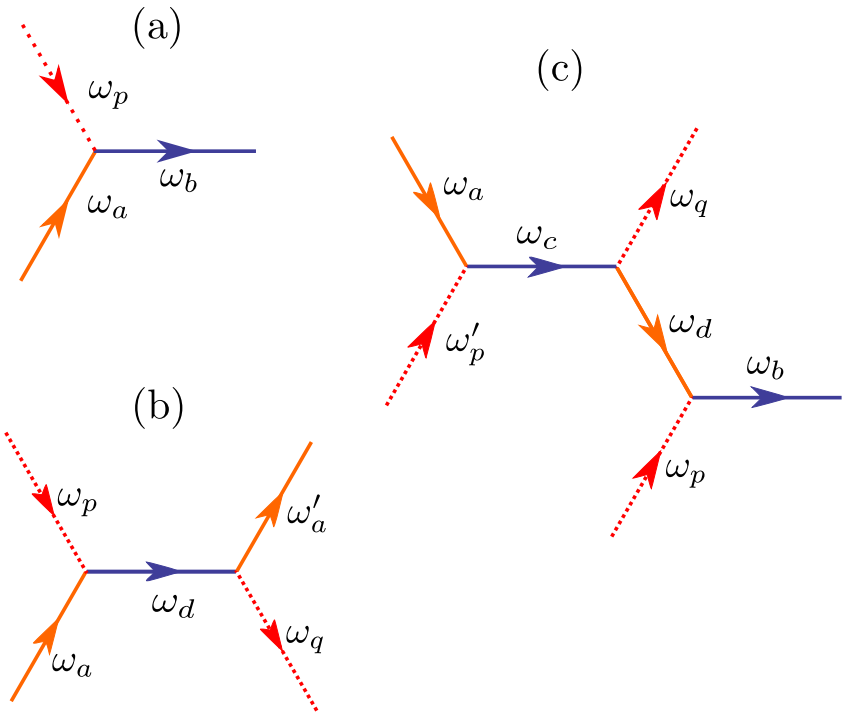

Figure 4.2: Diagrams representing the first, second and third order Magnus terms for FC. Dashed lines are used to represent pump photons, full lines are used to represent photons in fields a and b. (a) depicts a photon from the classical beam ω_p being fused with a photon with frequency ω_a to create a photon of energy ω_b. (b) depicts the second order Magnus term in which one of the up-converted photons decays into to two photons one in field a and one in the classical pump field p. Finally, (c) depicts the third order Magnus term in which two up-conversion processes with a down-conversion process in the middle occur.

rules to the ones derived for the PDC diagrams shown in Figure 4.1. We shall show in Chapter 6 that an even more explicit connection exists for certain simple models of the phasematching function Φ and the pump function α in section 6.4.

4.5 Disentangling the Magnus expansion

The calculations for photon generation used the fact that the commutator of two two-mode squeezing Hamiltonians gives rotation terms terms,

$$\left[\hat{a}^\dagger(\omega_p)\,\hat{b}^\dagger(\omega_q) + \text{H.c.}, \hat{a}^\dagger(\omega_r)\,\hat{b}^\dagger(\omega_s) + \text{H.c.}\right] = \tag{4.51}$$
$$\delta(\omega_q - \omega_s)\hat{a}^\dagger(\omega_r)\,\hat{a}(\omega_p) + \delta(\omega_p - \omega_r)\hat{b}^\dagger(\omega_s)\,\hat{b}(\omega_q) - \text{H.c.},$$

and the fact that the commutator of a rotation term with a two-mode squeezing term is again a two-mode squeezing term,

$$\Big[\hat{a}^\dagger(\omega_s)\,\hat{a}(\omega_r)+\text{H.c.},\hat{a}^\dagger(\omega_p)\,\hat{b}^\dagger(\omega_q)+\text{H.c.}\Big]= \tag{4.52}$$
$$\delta(\omega_s-\omega_p)\hat{b}^\dagger(\omega_q)\,\hat{a}^\dagger(\omega_r)+\delta(\omega_r-\omega_p)\hat{b}^\dagger(\omega_q)\,\hat{a}^\dagger(\omega_s)-\text{H.c.}$$

Likewise for FC they used the fact that the commutator of beam-splitter terms gives rotation terms,

$$\Big[\hat{a}(\omega_p)\,\hat{b}^\dagger(\omega_q)+\text{H.c.}\ ,\hat{a}(\omega_r)\,\hat{b}^\dagger(\omega_s)+\text{H.c.}\Big]= \tag{4.53}$$
$$\delta(\omega_q-\omega_s)\hat{a}^\dagger(\omega_p)\,\hat{a}(\omega_r)+\delta(\omega_p-\omega_r)\hat{b}^\dagger(\omega_q)\,\hat{b}(\omega_s)-\text{H.c.},$$

and that the commutator of a beam-splitter term and a rotation term gives again a beam-splitter term,

$$\Big[\hat{a}^\dagger(\omega_s)\,\hat{a}(\omega_r)+\text{H.c.},\hat{a}^\dagger(\omega_p)\,\hat{b}(\omega_q)+\text{H.c.}\Big]= \tag{4.54}$$
$$\delta(\omega_s-\omega_p)\hat{a}^\dagger(\omega_r)\,\hat{b}(\omega_q)+\delta(\omega_r-\omega_p)\hat{a}^\dagger(\omega_s)\,\hat{b}(\omega_q)-\text{H.c.}$$

These results can be used to inductively show that the unitary that connects states at $t_0\to-\infty$ and $t\to\infty$ has to be of the form:

$$\mathcal{U}_{\text{PDC}}(t,t_0)=\exp\Big(-2\pi i\int d\omega_1 d\omega_2\Big\{\tilde{G}^a(\omega_1,\omega_2)\hat{a}^\dagger(\omega_1)\hat{a}(\omega_2)+\tilde{G}^b(\omega_1,\omega_2)\hat{b}^\dagger(\omega_1)\hat{b}(\omega_2) \tag{4.55}$$
$$+(\tilde{J}(\omega_1,\omega_2)\hat{a}^\dagger(\omega_1)\hat{b}^\dagger(\omega_2)+\text{H.c.})\Big\}\Big),$$

with

$$\tilde{J}=\sum_i J_{2i+1};\quad \tilde{G}^a=\sum_i G^a_{2i};\quad \tilde{G}^b=\sum_i G^b_{2i}, \tag{4.56}$$

for PDC and FWM. For FC one only needs to change

$$\hat{a}^\dagger(\omega_1)\hat{b}^\dagger(\omega_2)\Rightarrow\hat{a}^\dagger(\omega_1)\hat{b}(\omega_2) \tag{4.57}$$

in Eq. (4.55) and put bars over the functions J, G^a, G^b. The result Eq. (4.55) confirms in detail the proof given at the end of section II. Eq. (4.55) shows the great utility of the Magnus expansion. It provides us with the general form of the solution. One only needs to calculate the higher corrections to the coefficients that appear in front of the

squeezing and frequency conversion terms to get an increasingly better approximation to the solution.

Diagrams similar to those presented in Fig. 4.1 can be drawn for the higher order terms. We emphasize that they are used here just as a convenient way of representing the terms in the Magnus expansion; they are *not* Feynman diagrams, of course, and we have not provided any rule to actually do calculations using them. Yet they can help in understanding the physics. In particular, given that the amplitudes they represent will always be multiplied by only pairs of bosonic operators, no matter what the order of the diagram there can be only two free legs at the low down-converted frequencies, which correspond precisely to the frequencies of the bosonic operators that they multiply. The diagrams in Fig. 4.1 are precisely the three simplest diagrams satisfying this selection rule.

While the form Eq. (4.3a) of the unitary operator given by the Magnus expansion identifies the physics of the evolution, particularly as illustrated in the example of Eq. (4.55), it cannot be directly used to calculate the evolution of an initial state, since the terms associated with the functions J_{2i+1} do not commute with the terms associated with the functions G^a_{2i} and G^b_{2i}. In this section we will provide a simple strategy to disentangle the Magnus expansion. We will be able to refactorize the unitary Eq. (4.55) as a product of two unitaries. For the PDC and FWM Hamiltonians Eqs. (4.19,4.23) these unitaries will correspond to pure squeezing term and pure rotation terms

$$\hat{\mathcal{U}}_{\rm PDC} = \hat{\mathcal{U}}_{\rm SQ}\hat{\mathcal{U}}_{\rm RA}\hat{\mathcal{U}}_{\rm RB}, \tag{4.58}$$

$$\hat{\mathcal{U}}_{\rm SQ} = e^{-2\pi i \int d\omega_a d\omega_b J(\omega_a,\omega_b)\hat{a}^\dagger(\omega_a)\hat{b}^\dagger(\omega_b)+\text{H.c.}}, \tag{4.59}$$

$$\hat{\mathcal{U}}_{\rm RA}\hat{\mathcal{U}}_{\rm RB} = e^{-2\pi i \int d\omega_a d\omega'_a G^a(\omega_a,\omega'_a)\hat{a}^\dagger(\omega_a)\hat{a}(\omega'_a)} e^{-2\pi i \int d\omega_b d\omega'_b G^b(\omega_b,\omega'_b)\hat{b}^\dagger(\omega_b)\hat{b}(\omega_b)}.$$

The case of FC is completely analogous and one only need to follow prescription Eq. (4.57) and put an overbar over all the functions. The factorization Eq. (4.58) has two important features. The first one is that if time ordering is irrelevant then $J = J_1$ as given in Eq. (4.28) and $G^a = G^b = 0$. The second is that when acting on the vacuum, the SPDC or SFWM state is simply

$$\begin{aligned} |\psi\rangle &= \hat{\mathcal{U}}_{\rm PDC}|\text{vac}\rangle = \hat{\mathcal{U}}_{\rm SQ}\hat{\mathcal{U}}_{\rm RA}\hat{\mathcal{U}}_{\rm RB}|\text{vac}\rangle = \hat{\mathcal{U}}_{\rm SQ}|\text{vac}\rangle \\ &= e^{-2\pi i \int d\omega_a d\omega_b J(\omega_a,\omega_b)a^\dagger(\omega_a)b^\dagger(\omega_b)+\text{H.c.}}|\text{vac}\rangle, \end{aligned} \tag{4.60}$$

that is J is proportional to the joint spectral amplitude (JSA) of the down converted photons.

To obtain the factorization Eq. (4.58) we will use the Baker-Campbell-Hausdorff lemma Eq. (4.16) and the generalized Baker-Campbell-Hausdorff formula [82],

$$e^{\hat{X}+\hat{Y}} = e^{\hat{X}} e^{\hat{Y}} e^{-\frac{1}{2}[\hat{X},\hat{Y}]} e^{\frac{1}{6}(2[\hat{Y},[\hat{X},\hat{Y}]]+[\hat{X},[\hat{X},\hat{Y}]])\cdots}. \tag{4.61}$$

The lowest order factorization that can be obtained by just going to second order in the Magnus expansion is to write

$$\hat{\mathcal{U}}_{\mathrm{PDC}} = e^{\hat{\Omega}_1+\hat{\Omega}_2} \approx e^{\hat{\Omega}_1} e^{\hat{\Omega}_2} = \hat{\mathcal{U}}_{\mathrm{SQ}} \hat{\mathcal{U}}_{\mathrm{RA}} \hat{\mathcal{U}}_{\mathrm{RB}}. \tag{4.62}$$

When applied to vacuum one simply obtains

$$|\psi_2\rangle = \hat{\mathcal{U}}_{\mathrm{PDC}} |\mathrm{vac}\rangle = e^{\hat{\Omega}_1} |\mathrm{vac}\rangle , \tag{4.63}$$

that is, up to second order the state is not modified by time ordering (since $\hat{\Omega}_2 |\mathrm{vac}\rangle = 0$), reminiscent of what happens when the Dyson series is used for this same problem [60]. Nevertheless, in the Magnus expansion the meaning of the null contribution of the second order in SPDC and SFWM is transparent: this second order term requires at least one down-converted photon to be present and hence it will vanish when applied to the vacuum.

Thus it is clear that to see time-ordering corrections to the expression for the state of the generated photons it is necessary to go to at least to third order. In this case one finds

$$\begin{aligned} e^{\hat{\Omega}_1+\hat{\Omega}_2+\hat{\Omega}_3} &\approx e^{\hat{\Omega}_1+\hat{\Omega}_3} e^{\hat{\Omega}_2} e^{-\frac{1}{2}[\hat{\Omega}_1+\hat{\Omega}_3,\hat{\Omega}_2]} \approx e^{\hat{\Omega}_1+\hat{\Omega}_3} e^{\hat{\Omega}_2} e^{-\frac{1}{2}[\hat{\Omega}_1,\hat{\Omega}_2]} \\ &= e^{\hat{\Omega}_1+\hat{\Omega}_3} e^{\hat{\Omega}_2} e^{-\frac{1}{2}[\hat{\Omega}_1,\hat{\Omega}_2]} e^{-\hat{\Omega}_2} e^{\hat{\Omega}_2} \approx e^{\hat{\Omega}_1+\hat{\Omega}_3} e^{-\frac{1}{2}e^{\hat{\Omega}_2}[\hat{\Omega}_1,\hat{\Omega}_2]e^{-\hat{\Omega}_2}} e^{\hat{\Omega}_2} \\ &\approx e^{\hat{\Omega}_1+\hat{\Omega}_3} e^{-\frac{1}{2}([\hat{\Omega}_1,\hat{\Omega}_2]+[\hat{\Omega}_2,[\hat{\Omega}_1,\hat{\Omega}_2]])} e^{\hat{\Omega}_2} \approx e^{\hat{\Omega}_1+\hat{\Omega}_3} e^{-\frac{1}{2}[\hat{\Omega}_1,\hat{\Omega}_2]} e^{\hat{\Omega}_2} \\ &\approx e^{\hat{\Omega}_1+\hat{\Omega}_3-\frac{1}{2}[\hat{\Omega}_1,\hat{\Omega}_2]} e^{\hat{\Omega}_2}. \end{aligned} \tag{4.64}$$

Here we ignore any fourth order term, resolved the identity as $\hat{\mathbb{I}} = e^{-\hat{\Omega}_2} e^{\hat{\Omega}_2}$, used the Baker-Campbell-Hausdorff lemma and formula and the following relation $e^{\hat{W}} e^{\hat{V}} e^{-\hat{W}} \equiv e^{e^{\hat{W}}\hat{V}e^{-\hat{W}}}$. From the last derivation is seen that to calculate the first non-vanishing correction to the JSA we not only need $\hat{\Omega}_3$ but also $[\hat{\Omega}_1, \hat{\Omega}_2]$. This extra third order correction is easy to understand: The diagram corresponding to $\hat{\Omega}_2$ needs an incoming photon, which can only be provided by a previous down-conversion process event included in $\hat{\Omega}_1$. This process will be of course of third order since it includes two down-conversion events and one up conversion event. If $\hat{\Omega}_1$ is a squeezing term and $\hat{\Omega}_2$ is a rotation term for a and b,

then, their commutator is another two-mode squeezing operator

$$\frac{[\hat{\Omega}_1, \hat{\Omega}_2]}{2} = -2\pi i^2 \int d\omega_a d\omega_b (K_3(\omega_a, \omega_b)\hat{a}^\dagger(\omega_a)\hat{b}^\dagger(\omega_b) - \text{H.c.}), \tag{4.65}$$

with

$$K_3(\omega_a, \omega_b) = \pi \int d\omega \Big(J_1(\omega_a, \omega) G_2^b(\omega_b, \omega) + G_2^a(\omega_a, \omega) J_1(\omega, \omega_b) \Big).$$

Eq. (4.64) provides a compact formula accounting for the effects of time ordering, and leads to an identification of the form of the joint spectral amplitude, which to this level of approximation is proportional to

$$J(\omega_a, \omega_b) = J_1(\omega_a, \omega_b) + (J_3(\omega_a, \omega_b) - iK_3(\omega_a, \omega_b)), \tag{4.66}$$

where the first contribution $J_1(\omega_a, \omega_b)$ neglects effects of time ordering, while the additional terms take corrections into account to all orders lower than the fifth (this last fact we shall prove shortly). This illustrates that as the intensity of the pump field increases and the corrections become larger not only are more squeezed photons generated in the same modes, but their spectral properties change. In particular, if the functions characterizing the pump pulse and the phase-matching functions are real, then as the pump intensity is increased the phase structure of the joint spectral amplitude evolves from trivial to nontrivial.

For FC one will also need the commutator of the first two Magnus terms which is

$$\frac{[\hat{\Omega}_1, \hat{\Omega}_2]}{2} = -(2\pi) i^2 \int d\omega_a d\omega_b (\bar{K}_3(\omega_a, \omega_b)\hat{a}(\omega_a)\hat{b}^\dagger(\omega_b) - \text{H.c.}),$$

where we defined

$$\bar{K}_3(\omega_a, \omega_b) = \pi \int d\omega \left(\bar{J}_1(\omega_a, \omega)\bar{G}_2^b(\omega_b, \omega) - \bar{G}_2^a(\omega, \omega_a)\bar{J}_1(\omega, \omega_b) \right). \tag{4.67}$$

From the general properties of the Magnus expansion, *i.e.* the fact that the n^{th} order Magnus terms is made of $n-1$ commutators, we know that all even Magnus terms will be rotation operators for a and b, whereas all odd terms will be two-mode squeezing operators. This fact can be used to show that the commutator of two Magnus terms $[\hat{\Omega}_i, \hat{\Omega}_j]$ (which is an $i+j$ order term) will be a rotation term if $i+j$ is even and a squeezing term if $i+j$ is odd. With these two facts and after some algebra it can be

shown, that the extension of Eq. (4.64) to fifth order is

$$\hat{\mathcal{U}}_{\rm PDC} = \exp(\hat{\Omega}_1 + \hat{\Omega}_2 + \hat{\Omega}_3 + \hat{\Omega}_4 + \hat{\Omega}_5) = \hat{\mathcal{U}}_{\rm SQ}\hat{\mathcal{U}}_{\rm RA}\hat{\mathcal{U}}_{\rm RB}, \tag{4.68}$$

where the squeezing and rotation unitaries $\hat{\mathcal{U}}_{\rm SQ}$, $\hat{\mathcal{U}}_{\rm RA}\hat{\mathcal{U}}_{\rm RB}$ are

$$\begin{aligned}\hat{\mathcal{U}}_{\rm SQ} =& \exp\left(\hat{\Omega}_1 + \left(\hat{\Omega}_3 - \frac{1}{2}[\hat{\Omega}_1, \hat{\Omega}_2]\right) + \left(\hat{\Omega}_5 - \frac{1}{2}[\hat{\Omega}_1, \hat{\Omega}_4]\right.\right. \\ &\left.\left. - \frac{1}{2}[\hat{\Omega}_3, \hat{\Omega}_2] + \frac{5}{6}[\hat{\Omega}_2, [\hat{\Omega}_2, \hat{\Omega}_1]] + \frac{1}{2}[\hat{\Omega}_1, [\hat{\Omega}_1, \hat{\Omega}_3]]\right)\right),\end{aligned} \tag{4.69}$$

$$\hat{\mathcal{U}}_{\rm RA}\hat{\mathcal{U}}_{\rm RB} = \exp\left(\hat{\Omega}_2 + \left(\hat{\Omega}_4 + \frac{1}{2}[\hat{\Omega}_1, [\hat{\Omega}_1, \hat{\Omega}_2]]\right)\right). \tag{4.70}$$

We now consider difference frequency generation, where besides an injected pump pulse that is treated classically we also seed the modes at ω_a and/or ω_b, with injected pulses described by coherent states. Here the output state can be written as

$$|\psi_3\rangle = e^{\hat{\Omega}_1+\hat{\Omega}_3-\frac{1}{2}[\hat{\Omega}_1,\hat{\Omega}_2]}e^{\hat{\Omega}_2}e^{i\sum_{c=a,b}\left(\int d\omega_c g_c(\omega_c)\hat{c}^\dagger(\omega_c)+\text{H.c.}\right)}|\text{vac}\rangle \tag{4.71}$$

$$= \left(e^{\hat{\Omega}_1+\hat{\Omega}_3-\frac{1}{2}[\hat{\Omega}_1,\hat{\Omega}_2]}\right)\left(e^{\hat{\Omega}_2}e^{i\sum_{c=a,b}\left(\int d\omega_c g_c(\omega_c)\hat{c}^\dagger(\omega_c)+\text{H.c.}\right)}e^{-\hat{\Omega}_2}\right)|\text{vac}\rangle\,. \tag{4.72}$$

Keeping only terms up to third order, we find

$$e^{\hat{\Omega}_2}e^{i\sum_{c=a,b}\left(\int d\omega_c g_c(\omega_c)\hat{c}^\dagger(\omega_c)+\text{H.c.}\right)}e^{-\hat{\Omega}_2} = e^{i\sum_{c=a,b}\left(\int d\omega_c g_c(\omega_c)e^{\hat{\Omega}_2}\hat{c}^\dagger(\omega_c)e^{-\hat{\Omega}_2}+\text{H.c.}\right)} \tag{4.73}$$

$$= e^{i\sum_{c=a,b}\left(\int d\omega_c g_c(\omega_c)\left(\hat{c}^\dagger(\omega_c)+[\hat{\Omega}_2,\hat{c}^\dagger(\omega_c)]\right)+\text{H.c.}\right)}. \tag{4.74}$$

The commutator inside the exponential in Eq. (4.74) can be easily calculated to be

$$[\hat{\Omega}_2, \hat{a}^\dagger(\omega_a')] = -2\pi i \int d\omega_a \hat{a}^\dagger(\omega_a) G_2^a(\omega_a, \omega_a'), \tag{4.75}$$

$$[\hat{\Omega}_2, \hat{b}^\dagger(\omega_b')] = -2\pi i \int d\omega_b \hat{b}^\dagger(\omega_b) G_2^b(\omega_b, \omega_b'). \tag{4.76}$$

This shows that the first effect due to time-ordering corrections in stimulated processes is to modify the shape of the injected seed pulses, since we can incorporate the time-ordering corrections to second order by imagining that the shape of the incoming coherent state (or single photon) is modified according to $g_c(\omega_c) \to g_c(\omega_c) - 2\pi i \int d\omega_c' g_c(\omega_c') G_2^c(\omega_c, \omega_c')$. Although the discussion in this section was phrased in terms of the PDC and FWM Hamiltonian all its conclusions are directly applicable to the case of FC.

4.6 Time-ordering corrections in broadly phase-matched Processes

Here we consider time-ordering corrections in the special limit that the phase matching function is independent of is variables,

$$\Phi(\omega_a, \omega_b, \omega_p) \propto 1, \tag{4.77}$$

in Eqs. (4.22) and (4.39). This implies that the function F in Eqs. (4.25) and (4.43) is a function only of its last argument, $F(x, y, z) = F(z)$. We show below that if this holds the second and third order Magnus terms vanish. Recently Donohue *et al.* [19] showed that all the time-ordering corrections vanish for a flat phase matching function.

To proceed, we look at $G_2^a(\omega_a, \omega_a')$ as a typical term. For PDC, in the limit Eq. (4.77) it becomes

$$G_2^a(\omega_a, \omega_a') = \int d\omega_q \fint \frac{d\omega_p}{\omega_p} F\left(\omega_a + \omega_p + \omega_q\right) F^*\left(\omega_a' + \omega_p + \omega_q\right).$$

In the last equation we are free to move the origin of the integral in ω_q by ω_p to get:

$$G_2^a = \int d\omega_q F\left(\omega_a + \omega_q\right) F^*\left(\omega_a' + \omega_q\right) \fint \frac{d\omega_p}{\omega_p}, \tag{4.78}$$

using the identity $\fint \frac{dx}{x+y} = 0$, the innermost integral is identically zero. The same kind of argument shows that G_2^b vanishes. Finally, to show that the third order term is also zero we proceed along similar lines. Using expression Eq. (4.34), with $F(x, y, z) = F(z)$ we obtain:

$$\int d\omega_c d\omega_d \fint d\omega_p d\omega_q F^*\left(\omega_c + \omega_d + \omega_p + \omega_q\right) F\left(\omega_a + \omega_c + \omega_p\right) F\left(\omega_b + \omega_d + \omega_q\right) \times \frac{1}{3}\left\{\frac{2}{\omega_p \omega_q} + \frac{1}{\omega_p + \omega_q}\left(\frac{1}{\omega_p} + \frac{1}{\omega_q}\right)\right\}. \tag{4.79}$$

As before, we shift the integration axes, in this case, $\omega_c \to \omega_c - \omega_q$, $\omega_d \to \omega_d - \omega_p$ to get:

$$\int d\omega_c d\omega_d F^*\left(\omega_c + \omega_d\right) F\left(\omega_a + \omega_d\right) F\left(\omega_b + \omega_c\right) \fint d\omega_p d\omega_q \left\{\frac{2}{\omega_p \omega_q} + \frac{1}{\omega_p + \omega_q}\left(\frac{1}{\omega_p} + \frac{1}{\omega_q}\right)\right\} = 0. \tag{4.80}$$

4.7 Relation between this work and that of Christ *et al.*

In the previous sections we have argued that the exact propagator of PDC is given by $\hat{\mathcal{U}}_{\text{PDC}} = \hat{\mathcal{U}}_{\text{SQ}}\hat{\mathcal{U}}_{\text{RA}}\hat{\mathcal{U}}_{\text{RB}}$. In the work of Christ *et al.* [52] the authors study the properties of PDC by looking at the action of the propagator on the canonical operators for the different polarizations. In particular they set to solve for functions U_a, V_a, U_b, V_b that satisfy

$$\hat{\mathcal{U}}^{\dagger}_{\text{PDC}}\hat{a}(\omega_a)\hat{\mathcal{U}}_{\text{PDC}} = \int d\omega'_a U_a(\omega_a,\omega'_a)\hat{a}(\omega'_a) + \int d\omega'_b V_a(\omega_a,\omega'_b)\hat{b}^{\dagger}(\omega'_b), \tag{4.81}$$

$$\hat{\mathcal{U}}^{\dagger}_{\text{PDC}}\hat{b}(\omega_b)\hat{\mathcal{U}}_{\text{PDC}} = \int d\omega'_b U_b(\omega_b,\omega'_b)\hat{b}(\omega'_b) + \int d\omega'_a V_b(\omega_b,\omega'_a)\hat{a}^{\dagger}(\omega'_a). \tag{4.82}$$

To link the two approaches one only needs to use the results from this chapter and concatenate the results regarding the transformations of single frequency operators under multimode transformations Table 2.2 and let $F \to J$, $G \to G_a$ and $H \to G_b$ in Eq. (2.79) and Eq. (2.84) to get

$$\begin{aligned}\hat{\mathcal{U}}^{\dagger}_{\text{PDC}}\hat{a}(\omega_a)\hat{\mathcal{U}}_{\text{PDC}} &= \hat{\mathcal{U}}^{\dagger}_{\text{RB}}\hat{\mathcal{U}}^{\dagger}_{\text{RA}}\hat{\mathcal{U}}^{\dagger}_{\text{SQ}}\hat{a}(\omega_a)\hat{\mathcal{U}}_{\text{SQ}}\hat{\mathcal{U}}_{\text{RA}}\hat{\mathcal{U}}_{\text{RB}} \\ &= \int d\omega''_a \underbrace{\left\{\int d\omega'_a \left(\sum_{\lambda} f_{\lambda}(\omega_a) f^{*}_{\lambda}(\omega'_a)\cosh(s_{\lambda})\right)\left(\sum_{\alpha} g_{\alpha}(\omega'_{\alpha}) g^{*}_{\alpha}(\omega''_{\alpha}) e^{iu_{\alpha}}\right)\right\}}_{U_a(\omega_a,\omega''_a)} \hat{a}(\omega''_a) \\ &+ \int d\omega''_b \underbrace{\left\{i\int d\omega'_b \left(\sum_{\lambda} f_{\lambda}(\omega_a) j_{\lambda}(\omega'_b)\sinh(s_{\lambda})\right)\left(\sum_{\beta} h^{*}_{\beta}(\omega'_b) h_{\beta}(\omega''_b) e^{-iv_{\beta}}\right)\right\}}_{V_a(\omega_a,\omega''_b)} \hat{b}^{\dagger}(\omega''_b).\end{aligned} \tag{4.83}$$

In an analogous manner one finds for $b(\omega_b)$

$$\begin{aligned}&\hat{\mathcal{U}}^{\dagger}_{\text{PDC}}\hat{b}(\omega_b)\hat{\mathcal{U}}_{\text{PDC}} = \\ &\int d\omega''_a \underbrace{\left\{i\int d\omega'_a \left(\sum_{\lambda} f_{\lambda}(\omega'_a) j(\omega_b)\sinh(s_{\lambda})\right)\left(\sum_{\alpha} g^{*}_{\alpha}(\omega'_a) g_{\alpha}(\omega''_a) e^{-iu_{\alpha}}\right)\right\}}_{V_b(\omega_b,\omega''_a)} \hat{a}^{\dagger}(\omega''_a) \\ &+ \int d\omega''_b \underbrace{\left\{\int d\omega'_b \left(\sum_{\lambda} \cosh(s_{\lambda}) j_{\lambda}(\omega_b) j^{*}_{\lambda}(\omega'_b)\right)\left(\sum_{\beta} h_{\beta}(\omega'_b) h^{*}_{\beta}(\omega''_b) e^{iv_{\beta}}\right)\right\}}_{U_b(\omega_b,\omega''_b)} \hat{b}(\omega''_b).\end{aligned} \tag{4.84}$$

Similarly to what was done for PDC we showed that the exact propagator for FC can be written as $\hat{\mathcal{U}}_{\mathrm{FC}} = \hat{\mathcal{U}}_{\mathrm{BS}}\hat{\mathcal{U}}_{\mathrm{RA}}\hat{\mathcal{U}}_{\mathrm{RB}}$. Likewise in [52] it is proposed that the canonical operators at the input and output are related via

$$\hat{\mathcal{U}}_{\mathrm{FC}}\hat{a}(\omega_a)\hat{\mathcal{U}}_{\mathrm{FC}}^{\dagger} = \int d\omega_a' \bar{U}_a(\omega_a,\omega_a')\hat{a}(\omega_a') + \int d\omega_b' \bar{V}_a(\omega_a,\omega_b')\hat{b}(\omega_b'), \tag{4.85}$$

$$\hat{\mathcal{U}}_{\mathrm{FC}}\hat{b}(\omega_b)\hat{\mathcal{U}}_{\mathrm{FC}}^{\dagger} = \int d\omega_b' \bar{U}_b(\omega_b,\omega_b')\hat{b}(\omega_b') + \int d\omega_a' \bar{V}_b(\omega_b,\omega_a')\hat{a}(\omega_a'). \tag{4.86}$$

Using again the results in Table 2.2 and letting $K \to \bar{J}$, $G \to \bar{G}_a$ and $H \to \bar{G}_b$ in Eq. (2.79) the two approaches can be related in the following way:

$$\begin{aligned}
&\hat{\mathcal{U}}_{\mathrm{FC}}\hat{a}(\omega_a)\hat{\mathcal{U}}_{\mathrm{FC}}^{\dagger} = \qquad (4.87)\\
&\int d\omega_a'' \underbrace{\left\{ \int d\omega_a' \left(\sum_\theta k_\theta^*(\omega_a) k_\theta(\omega_a') \cos(r_\theta) \right) \left(\sum_\alpha g_\alpha^*(\omega_a') g_\alpha(\omega_a'') e^{iu_\alpha} \right) \right\}}_{\bar{U}_a(\omega_a,\omega_a'')} \hat{a}(\omega_a'')\\
&+ \int d\omega_b'' \underbrace{\left\{ i \int d\omega_b' \left(\sum_\theta k_\theta^*(\omega_a) l_\theta(\omega_b') \sin(r_\theta) \right) \left(\sum_\beta h_\beta^*(\omega_b') h_\beta(\omega_b'') e^{iv_\beta} \right) \right\}}_{\bar{V}_a(\omega_a,\omega_a'')} \hat{b}(\omega_b''),\\
&\hat{\mathcal{U}}_{\mathrm{FC}}\hat{b}(\omega_b)\hat{\mathcal{U}}_{\mathrm{FC}}^{\dagger} = \qquad (4.88)\\
&\int d\omega_a'' \underbrace{\left\{ i \int d\omega_a' \left(\sum_\theta \sin(r_\theta) l_\theta^*(\omega_b) k_\theta(\omega_a') \right) \left(\sum_\alpha g_\alpha^*(\omega_a') g_\alpha(\omega_a'') e^{iu_\alpha} \right) \right\}}_{\bar{V}_b(\omega_b,\omega_a'')} \hat{a}(\omega_a'')\\
&+ \int d\omega_b'' \underbrace{\left\{ \int d\omega_b' \left(\sum_\theta l_\theta(\omega_b) l_\theta^*(\omega_b') \cos(r_\theta) \right) \left(\sum_\beta h_\beta(\omega_b') h_\beta^*(\omega_b'') e^{iv_\beta} \right) \right\}}_{\bar{U}_b(\omega_b,\omega_b'')} \hat{b}(\omega_b'').
\end{aligned}$$

So far we have only shown how to calculate the transformation functions in the Heisenberg picture starting from the unitary evolution operator. In general the inverse mapping is much harder since it is essentially a deconvolution problem. Yet for the special case of SPDC it is possible to invert. In SPDC the state generated by the nonlinear interaction is $\hat{\mathcal{U}}_{\mathrm{PDC}}|\mathrm{vac}\rangle = \hat{\mathcal{U}}_{\mathrm{SQ}}\hat{\mathcal{U}}_{\mathrm{RA}}\hat{\mathcal{U}}_{\mathrm{RB}}|\mathrm{vac}\rangle = \hat{\mathcal{U}}_{\mathrm{SQ}}|\mathrm{vac}\rangle$. Note that $\hat{\mathcal{U}}_{\mathrm{RA}}$ and $\hat{\mathcal{U}}_{\mathrm{RB}}$ disappear from

the problem. With this in mind we can calculate

$$\langle \text{vac}| \hat{\mathcal{U}}^\dagger_{\text{PDC}} \hat{a}(\omega_a)\hat{b}(\omega_b)\hat{\mathcal{U}}_{\text{PDC}} |\text{vac}\rangle = \langle \text{vac}| \hat{\mathcal{U}}^\dagger_{\text{SQ}} \hat{a}(\omega_a)\hat{b}(\omega_b)\hat{\mathcal{U}}_{\text{SQ}} |\text{vac}\rangle \tag{4.89}$$

$$= i \sum_\lambda \frac{\sinh(2s_\lambda)}{2} f_\lambda(\omega_a) j_\lambda(\omega_b) \tag{4.90}$$

$$= i \int d\omega U_a(\omega_a, \omega) V_b(\omega_b, \omega). \tag{4.91}$$

Note that the last quantity can be calculated from the results in [52] and the last equation provides the recipe to obtain the JSA from this last second moment; if we write the Schmidt decomposition

$$i \int d\omega U_a(\omega_a, \omega) V_b(\omega_b, \omega) = i \sum_\lambda \tilde{s}_\lambda \tilde{f}_\lambda(\omega_a) \tilde{j}_\lambda(\omega_b), \tag{4.92}$$

then we can immediately reconstruct the JSA as

$$-2\pi J(\omega_a, \omega_b) = \sum_\lambda s_\lambda f_\lambda(\omega_a) j_\lambda(\omega_b) = \sum_\lambda \frac{\sinh^{-1}(2\tilde{s}_\lambda)}{2} \tilde{f}_\lambda(\omega_a) \tilde{j}_\lambda(\omega_b), \tag{4.93}$$

and identify the Schmidt values s_λ and functions f_λ, j_λ of the JSA. The consistency of the reconstruction Eq. (4.89) can be checked by verifying the following relations

$$\langle \text{vac}| \hat{\mathcal{U}}^\dagger_{\text{PDC}} \hat{a}^\dagger(\omega_a)\hat{a}(\omega'_a)\hat{\mathcal{U}}_{\text{PDC}} |\text{vac}\rangle = \langle \text{vac}| \hat{\mathcal{U}}^\dagger_{\text{SQ}} \hat{a}^\dagger(\omega_a)\hat{a}(\omega'_a)\hat{\mathcal{U}}_{\text{SQ}} |\text{vac}\rangle \tag{4.94}$$

$$= \sum_\lambda \sinh^2 s_\lambda \; f^*_\lambda(\omega_a) f_\lambda(\omega'_a) \tag{4.95}$$

$$= \int d\omega V^*_a(\omega_a, \omega) V_a(\omega'_a, \omega), \tag{4.96}$$

$$\langle \text{vac}| \hat{\mathcal{U}}^\dagger_{\text{PDC}} \hat{b}^\dagger(\omega_b)\hat{b}(\omega'_b)\hat{\mathcal{U}}_{\text{PDC}} |\text{vac}\rangle = \langle \text{vac}| \hat{\mathcal{U}}^\dagger_{\text{SQ}} \hat{b}^\dagger(\omega_b)\hat{b}(\omega'_b)\hat{\mathcal{U}}_{\text{SQ}} |\text{vac}\rangle \tag{4.97}$$

$$= \sum_\lambda \sinh^2 s_\lambda \; j^*_\lambda(\omega_b) j_\lambda(\omega'_b) \tag{4.98}$$

$$= \int d\omega V^*_b(\omega_b, \omega) V_b(\omega'_b, \omega). \tag{4.99}$$

The only reason why one can invert for the JSA of the squeezed state is because we are looking at SPDC, which implies that we take vacuum expectation values that make the contribution from $\hat{\mathcal{U}}_{\text{RA}}$ and $\hat{\mathcal{U}}_{\text{RB}}$ disappear. If they were present one would be dealing with much harder deconvolution problem.

Chapter 5

Generation of bright non-classical light

"Not gaussian" = "An ass outing." A useful anagram?

Stephen "T. Rex" Foster

5.1 Introduction

Particles exhibiting strong, non-classical correlations play a central role in the implementation of quantum-enhanced information processing tasks. As mentioned in the introduction, nonlinear photonic materials provide some of the most versatile sources of these particles. The interactions that give rise to the quantum correlated photons are typically rather weak, but by using a strong classical pump field they can be enhanced by orders of magnitude. Thus the theoretical treatment of photon generation usually involves a time-dependent Hamiltonian in the interaction picture. Because this Hamiltonian generally does not commute with itself at different times, the time evolution operator in these types of problems is not just a simple exponential involving the time integral of the Hamiltonian, and so-called "time-ordering" corrections arise in the description of the quantum state evolution [57, 59, 60].

In this chapter, we introduce an *analytical* model that describes the effects of time ordering in several non-linear quantum optical processes. The model *automatically captures the photon statistics and unitary evolution that characterize the exact solution of the problem.* With this model we provide a simple explanation of when time-ordering effects become important: As long as the generated photons do not significantly copropagate (*i.e.,* reside in the same spatial region at the same time) with the pump photons, time-

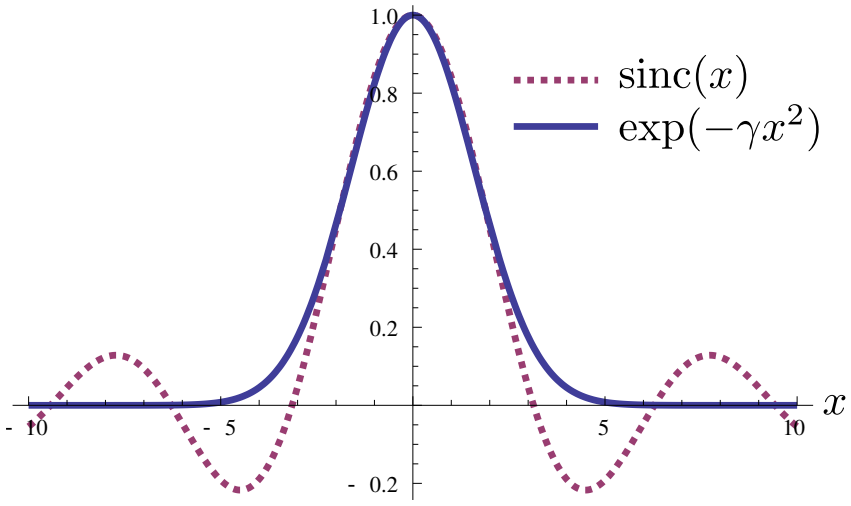

Figure 5.1: Comparison of a sinc function and the gaussian fit $\exp(-\gamma x^2)$.

ordering effects are irrelevant for the description of the generated quantum state. Based on this intuitive idea we propose an experiment using periodically poled lithium niobate where these corrections can be observed. Then we use our simple model to study how the properties of the quantum light produced by the nonlinear material are modified by the time-ordering corrections and we derive useful observables that capture the departure from the first order Magnus correction. Finally, we also study what are the effects of the time-ordering correction in the heralded generation of Fock states using realistic number resolution detectors.

5.2 Model

We consider the following interaction picture Hamiltonian, which can be used to model both spontaneous parametric down-conversion (SPDC) and spontaneous four-wave mixing (SFWM) in a one dimensional geometry, within the undepleted pump and rotating wave approximations:

$$\hat{H}_I(t) = -\hbar\varepsilon \int d\omega_p d\omega_a d\omega_b e^{i\Delta t} \Phi(\omega_a, \omega_b, \omega_p) \alpha(\omega_p) \hat{a}^\dagger(\omega_a) \hat{b}^\dagger(\omega_b) + \text{H.c.} \tag{5.1}$$

Here $a^\dagger(\omega)$ and $b^\dagger(\omega)$ are creation operators for two different fields, and Φ is the phase matching function, which we take to be a Gaussian function,

$$\Phi(\omega_a, \omega_b, \omega_p) = \exp\left(-(s_a \delta\omega_a + s_b \delta\omega_b - s_p \delta\omega_p)^2\right). \tag{5.2}$$

When we take $s_i = \sqrt{\gamma}L/(2v_i) > 0$, where v_i is the group velocity at frequency ω_i, this provides a good approximation to the usual sinc function resulting from a uniform nonlinearity over a region of length L, under the neglect of dispersion effects; the choice of $\gamma = 0.193$ guarantees that the full width at half maximum of the sinc and Gaussian functions agree (See Fig. 5.1). We should mention that by using poling techniques [83] it is possible to engineer approximately the phase matching function in Eq. (5.2). In Eq. (5.2) $\delta\omega_i = \omega_i - \bar{\omega}_i$; in SPDC the central frequencies $\bar{\omega}_i$ are constrained by energy conservation, $\bar{\omega}_a + \bar{\omega}_b = \bar{\omega}_p$, and momentum conservation, $k_a(\bar{\omega}_a) + k_b(\bar{\omega}_b) = k_p(\bar{\omega}_p)$, while for SFWM ω_p is *twice* the frequency of the pump and momentum conservation reads $k_a(\bar{\omega}_a) + k_b(\bar{\omega}_b) = 2k_p(\bar{\omega}_p/2)$ [84]. The parameter ε is a dimensionless constant that characterizes the strength of the interaction (see Eq. (3.28) and Eq. (3.41)); it depends on physical properties such as the effective non-linearity of the medium and the area of the interaction region. We also assume that the classical pump can be described by a Gaussian function,

$$\alpha(\omega_p) = \frac{\tau}{\sqrt{\pi}} \exp\left(-\tau^2 \delta\omega_p^2\right), \tag{5.3}$$

with τ characterizing the temporal duration of the pump pulse. Finally $\Delta = \omega_a + \omega_b - \omega_p$, and in Eq. (5.1) we adopt the convention (used throughout the thesis) that whenever the limits of an integral are not specified they range from $-\infty$ to ∞. We will frame the discussion in terms of photon generation using SPDC but as argued in the previous Chapters the results translate almost immediately to SFWM.

Using the Magnus expansion, we showed in the previous chapter that the unitary evolution operator generated by the Hamiltonian Eq. (5.1) can be factored as $\hat{\mathcal{U}}_{\rm PDC} = \hat{\mathcal{U}}_{\rm SQ}\hat{\mathcal{U}}_{\rm RA}\hat{\mathcal{U}}_{\rm RB}$ with $\hat{\mathcal{U}}_{\rm SQ}$ a pure two-mode squeezing term (generated by terms that are extensions of $\hat{a}^\dagger\hat{b}^\dagger + \text{H.c.}$) and $\hat{\mathcal{U}}_{\rm RA}\hat{\mathcal{U}}_{\rm RB}$ pure "rotation" terms (generated by terms that are extensions of $a^\dagger a + b^\dagger b$),

$$\begin{aligned}\hat{\mathcal{U}}_{\rm PDC} = &\exp\left(-2\pi i \int d\omega_a d\omega_b \sum_n (J_n - iK_n)\hat{a}^\dagger(\omega_a)\hat{b}^\dagger(\omega_b) + \text{H.c.}\right) \\ &\prod_{c=\{a,b\}} \exp\left(-2\pi i \int d\omega_c d\omega_{c'} \sum_m G^c_m(\omega_c, \omega_{c'})\hat{c}^\dagger(\omega_c)\hat{c}(\omega'_c)\right),\end{aligned} \tag{5.4}$$

with n odd and m even. Each of these indices labels the order of the expansion in ε; *e.g.*, $n = 1$ is a term $\propto \varepsilon$ and $m = 2$ is a term $\propto \varepsilon^2$. If a spontaneous process is considered, where the unitary operator $\hat{\mathcal{U}}_{\rm PDC}$ is applied to the vacuum, it is readily seen that the

second exponential in Eq. (5.4) does not modify the initial state; $\hat{\mathcal{U}}_{\rm RA}\hat{\mathcal{U}}_{\rm RB}\left|{\rm vac}\right\rangle = \left|{\rm vac}\right\rangle$, and hence the output state $\left|\psi_{\rm out}\right\rangle = \hat{\mathcal{U}}_{\rm PDC}\left|{\rm vac}\right\rangle = \hat{\mathcal{U}}_{\rm SQ}\left|{\rm vac}\right\rangle$ is generated solely by the squeezing part $\hat{\mathcal{U}}_{\rm SQ}$. With these observations it is easy to identify $J = \sum_n (J_n - iK_n)$ as proportional to the Joint Spectral Amplitude (JSA) of the photons generated in modes a and b in a spontaneous process. The first term of the Magnus expansion for the Hamiltonian Eq. (5.1) is obtained by integrating the Hamiltonian from $-\infty$ to ∞; $K_1 = 0$, and the result for J_1 can be written in the following simple form using the derivations from Sec. 4.3:

$$J_1(\delta\omega_a, \delta\omega_b) = -\frac{\varepsilon\tau}{\sqrt{\pi}} \exp\left(-\mathbf{u}\mathbf{N}\mathbf{u}^T\right), \tag{5.5}$$

$$\mathbf{N} = \begin{pmatrix} \mu_a^2 & \mu^2 \\ \mu^2 & \mu_b^2 \end{pmatrix}, \quad \mathbf{u} = (\delta\omega_a, \delta\omega_b), \tag{5.6}$$

$$\eta_{a,b} = s_p - s_{a,b},\ \mu^2 = \tau^2 + \eta_a\eta_b,\ \mu_{a,b}^2 = \tau^2 + \eta_{a,b}^2.$$

If time-ordering effects were ignored, K_1 would vanish, and J_1 would be the only contribution to J; J_1 would thus completely describe the properties of the state, and would identify the joint spectral amplitude of the generated photons. A measure of entanglement is the Schmidt number introduced in [67] and studied in Chapter 2, which for the state characterized by J_1 is [49, 85]

$$S = \mu_a\mu_b/\sqrt{\mu_a^2\mu_b^2 - \mu^4}. \tag{5.7}$$

In the limit that the matrix $\mathbf{N}$ is diagonal, $\mu \to 0$ and the down converted photons are uncorrelated; here $S = 1$. If in this limit $\mathbf{N}$ were also proportional to the identity matrix, then the photons would not only be uncorrelated but would share the same spectral characteristics; for this to happen we require $\eta_a = -\eta_b = \pm\tau$. In the opposite limit, *i.e.*

$$\tau \ll |\eta_{a,b}|, \tag{5.8}$$

$\mathbf{N}$ becomes rank deficient, the photons generated in the modes a and b are strongly correlated, and $S \to \infty$. A simple way to understand the physics in the limit Eq. (5.8) is to rewrite the inequality as

$$\frac{v_p\tau}{|v_{a,b} - v_p|} \ll \frac{L}{v_{a,b}}. \tag{5.9}$$

That is, in this limit the time the down converted photons spend with the pump photons

is much less than the time they spend in the nonlinear structure. The down converted photons once created thus escape the nonlinear structure without spending appreciable time in the same region as the pump photons, and if the pump intensity is high enough to generate a number of pairs of photons then the stream of pairs is spread over a long time; equivalently, their frequencies are tightly constrained.

5.3 Time-ordering effects in spontaneous photon generation

For the simple Gaussian model considered in this chapter, the real part of the first non-vanishing correction to the JSA due to time ordering is given by

$$J_3(\omega_a,\omega_b) = W(\omega_a,\omega_b) - Z(\omega_a,\omega_b)V(\omega_a,\omega_b), \tag{5.10}$$

$$W(\omega_a,\omega_b) = \frac{2\pi^{3/2}\varepsilon^3\tau^3}{3R^2}\exp\left(-\mathbf{u}\mathbf{Q}\mathbf{u}^T/R^4\right), \tag{5.11}$$

$$Z(\omega_a,\omega_b) = 4\sqrt{\pi}\tau^3\varepsilon^3\exp\left(-\mathbf{u}\mathbf{N}\mathbf{u}^T/3\right), \tag{5.12}$$

$$V(\omega_a,\omega_b) = \int_0^\infty dp\int_0^\infty dq\exp\left(-(p,q)\mathbf{M}(p,q)^T\right)\cos\left(4\tau\eta_{ab}(\delta\omega_a q+\delta\omega_b p)/\sqrt{3}\right), \tag{5.13}$$

with

$$\mathbf{Q} = \begin{pmatrix} M^4\mu_a^2 & \mu^6 \\ \mu^6 & M^4\mu_b^2 \end{pmatrix}, \quad \mathbf{M} = \begin{pmatrix} 2\mu_a^2 & \mu^2 \\ \mu^2 & 2\mu_b^2 \end{pmatrix}, \tag{5.14}$$

$$R^4 = 4\mu_a^2\mu_b^2 - \mu^4 = 4\eta_{ab}^2\tau^2 + 3\mu^4,$$

$$M^4 = 4\mu_a^2\mu_b^2 - 3\mu^4, \quad \eta_{ab} = -\eta_{ba} = \eta_a - \eta_b.$$

The imaginary part of the correction K_3 is given by

$$K_3(\omega_a,\omega_b) = -\varepsilon^3\pi^{3/2}\frac{\tau^3}{R^2}\exp(-\mathbf{u}\mathbf{Q}\mathbf{u}^T/R^4)\left(\mathrm{erfi}(y_{ab})+\mathrm{erfi}(y_{ba})\right),$$

$$y_{ab} = \sqrt{\frac{2}{3}}\frac{\tau\eta_{ba}\left(2\delta\omega_a\mu_a^2-\delta\omega_b\mu^2\right)}{R^2\mu_a} \tag{5.15}$$

and $\mathrm{erfi}(z) = \mathrm{erf}(iz)/i$, with erf being the standard error function. Details of the calculation are given in Appendix D. A useful feature of using Gaussian functions to model both the phase-matching function and the pump pulse is that estimates of the relative sizes of the corrections due to time ordering in SPDC and SFWM can be easily extracted; this

also holds for the time-ordering corrections to frequency conversion. We demonstrate this all below, introducing figures of merit which characterize the size of the time-ordering corrections relative to the uncorrected prediction that would follow from the first order Magnus calculation. Some of the mathematical details are relegated to Appendix D.

To estimate the effects of time ordering on SPDC and SFWM we introduce the following figure of merit,

$$r = \frac{\max_{\omega_a,\omega_b} |J_3(\omega_a,\omega_b)|}{\max_{\omega_a,\omega_b} |J_1(\omega_a,\omega_b)|} = \frac{\sqrt{\pi}}{\varepsilon\tau} \max_{\omega_a,\omega_b} |J_3(\omega_a,\omega_b)|. \tag{5.16}$$

In Appendix D we show that

$$|J_3(\omega_a,\omega_b)| \leq \frac{2\pi^{3/2}\varepsilon^3\tau^3}{R^2}, \tag{5.17}$$

and so we identify the bound

$$r \leq 2\pi^2\varepsilon^2 \left(\frac{\tau^2}{R^2}\right). \tag{5.18}$$

There are two interesting limits of the important ratio τ^2/R^2 that appears in Eq. (5.18). We find

$$\begin{aligned} &\tau \ll |\eta_{a,b}| \;\Rightarrow\; \frac{\tau^2}{R^2} \sim \frac{1}{\sqrt{3}} \frac{\tau}{|\eta_a|} \frac{\tau}{|\eta_b|} \lll 1, \\ &\mu = 0 \Rightarrow\; \frac{\tau^2}{R^2} = \frac{\tau}{2|\eta_{ab}|}. \end{aligned} \tag{5.19}$$

From this we can see that the importance of the time-ordering corrections depends strongly on the entanglement of the photons in modes a and b, and we can also understand this scaling physically. As discussed in the previous section, if the generated photons are highly entangled with a large Schmidt number, the time they overlap the pump field is short. We would then expect on physical grounds that time-ordering corrections should be small, and indeed we see from the first of Eq. (5.19) and Eq. (5.18) that a very large interaction strength ε would be necessary for the time-ordering corrections to come into play. In the reverse limit, the second of Eq. (5.19), the group velocities of the generated photons satisfy $\eta_a\eta_b = -\tau^2$ ($\mu = 0$). To have a significant time-ordering correction, we have from the second of Eq. (5.19) that the group velocities of the downconverted photons must be similar. Note that if the velocities were equal J_3 would vanish identically; see Appendix D. It can also be shown that the maximum of

τ^2/R^2 under the constraint of having $\mu = 0$ is obtained for

$$\eta_a = -\eta_b = \pm\tau \Rightarrow \frac{v_p\tau}{|v_{a,b} - v_p|} = \frac{\sqrt{\gamma}}{2}\frac{L}{v_{a,b}}. \tag{5.20}$$

In such a case τ^2/R^2 equals 1/4. Eq. (5.20) simply tell us that the time the down-converted photons spend with the pump is comparable with the time they spend in the crystal. Note that the entanglement in the downconverted state as predicted by using J_1 for J and the condition Eq. (5.20) is very small, but because of the continued presence of photons being generated with the pump pulse, time-ordering corrections would be physically expected to come into play at a smaller interaction strength ε; this is confirmed by using Eq. (5.20) in Eq. (5.18). Furthermore, besides being simply larger, time-ordering corrections can be expected to be of greater significance here, since they can qualitatively modify the very small entanglement that the approximation of J by J_1 would imply.

When appropriate values of ε are used in Eq. (5.18), we see that our results are consistent with what was found by Christ *et al.* [52], in which simulations showed that extremely high pump intensities are necessary to obtain observable time-ordering effects for very entangled JSAs.

5.4 Time-ordering effects in stimulated photon generation

In this section we turn our attention to stimulated parametric down-conversion/four wave mixing processes, in which the unitary rotation operators $\mathcal{U}_{\mathrm{RA}}\mathcal{U}_{\mathrm{RB}}$ in Eq. (5.4) characterizing single mode frequency conversion become important. The first contribution to the frequency conversion unitary is given by

$$G_2^a(\omega_a, \omega_a') = \varepsilon^2\sqrt{\frac{\pi}{2}}\frac{\tau^2}{\mu_b}e^{-x_-^2 - x_+^2}\mathrm{erfi}(x_+), \quad x_+ = \frac{\tau\eta_{ba}\left(\delta\omega_a' + \delta\omega_a\right)}{\sqrt{2}\mu_b}, \quad x_- = \frac{\left(\omega_a - \omega_a'\right)\mu_a}{\sqrt{2}}. \tag{5.21}$$

To obtain the last equation one needs to use Eq. (4.32a) and the following identity

$$⨍\frac{dx}{x}e^{-ax^2+bx+c} = 2\int_0^\infty \frac{dx}{x}e^{-ax^2+c}\sinh(bx) = e^c\pi\mathrm{erfi}\left(\frac{b}{2\sqrt{a}}\right). \tag{5.22}$$

An analogous formula to Eq. (5.21) can be found for $G_2^b(\omega_b, \omega_b')$ by simply switching $a \leftrightarrow b$ in Eq. (5.21). We consider the scenario of a process seeded by a coherent state in

field a, described by the state

$$|g(\omega_a)\rangle = \exp\left(i\sqrt{N}\int d\omega_a \left(g(\omega_a)a^\dagger(\omega_a) + \text{h.c.}\right)\right)|\text{vac}\rangle\,. \tag{5.23}$$

where $\int d\omega_a |g(\omega_a)|^2 = 1$ and N is the mean number of photons in the state (see Sec. 2.3). Using Eq. (5.4) and the results from the previous chapter we see that the lowest (second) order effect associated with time ordering is

$$\begin{aligned} |\psi_{\text{out}}\rangle &= \hat{\mathcal{U}}_{\text{SQ}}\hat{\mathcal{U}}_{\text{RA}}\hat{\mathcal{U}}_{\text{RA}}\,|g(\omega_a)\rangle = \hat{\mathcal{U}}_{\text{SQ}} \times e^{i\sqrt{N}\int d\omega_a (g(\omega_a)+\delta g(\omega_a))\hat{a}^\dagger(\omega_a)+\text{h.c.}}\,|\text{vac}\rangle\,, \\ \delta g(\omega_a) &= -2\pi i \int d\omega_a' g(\omega_a')G_2(\omega_a,\omega_a'). \end{aligned} \tag{5.24}$$

The last equation can be interpreted as follows: the first effect ($\propto \varepsilon$) of the interaction is that the nonlinear medium acts as a two mode squeezer, generating pairs of photons in fields a and b. The second order effect ($\propto \varepsilon^2$), which appears solely due to time ordering, describes the "dressing" of the seed photons by the pump. That is, the frequency amplitudes of the photons of polarization a are no longer described by $g(\omega_a)$ but rather by $g(\omega_a) + \delta g(\omega_a)$. Finally, note that if instead the seed were prepared in a single photon state $|1_{g(\omega_a)}\rangle = \int d\omega_a g(\omega_a)a^\dagger(\omega_a)\,|\text{vac}\rangle$, the effect of time ordering would be to dress it according to $|1_{g(\omega_a)}\rangle \to |1_{g(\omega_a)+\delta g(\omega_a)}\rangle$.

To quantify the effects of time ordering we estimate the correction given by the second term of Eq. (5.24) relative to the first term. If we take $g(\omega_a) = \nu\exp(-\tau_a^2\delta\omega_a^2)$, in the limit $\tau_a \ll \tau, |\eta_a|$,

$$\int d\omega_a' g(\omega_a')G_2(\omega_a,\omega_a') = \varepsilon^2\nu\frac{\pi^2\tau^2}{\mathcal{N}^2}\exp(-q^2)\text{erfi}(q), \tag{5.25}$$

$$q = \sqrt{2}\omega_a\eta_{ab}\tau\mu_a/\mathcal{N}^2, \quad \mathcal{N}^4 = \mu^4 + 2\tau^2\eta_{ab}^2. \tag{5.26}$$

Note that the maximum value the function $\exp(-q^2)\text{erfi}(q)$ attains is $\xi \approx 0.610503$ and that the function is identically zero if $q = 0$ (which only occurs for the unphysical situation $\eta_a = \eta_b$). As before, we can compare the relative strengths of the amplitudes of the coherent state with and without including time-ordering effects to obtain the following figure of merit:

$$\rho = \frac{\max_{\omega_a}|\delta g(\omega_a)|}{\max_{\omega_a} g(\omega_a)} = 2\pi^3\xi(\varepsilon^2\tau^2/\mathcal{N}^2). \tag{5.27}$$

This quantity measures how much the pump is dressed by the time-ordering effects of the

stimulated process. It has a very simple interpretation: To have important time-ordering effects the seed photons, and the a and b photons created by the nonlinear process, must spend a significant amount of time traveling with the pump pulse. Note in particular that if the photons of type a move significantly faster than those of type b, for example, then $|\eta_{ab}|$ would make the bound Eq. (5.27) go to zero; if on the other hand the a photons travel much faster than those of the pump, then $\eta_a \gg \tau$ and $\eta_b \sim \tau \Rightarrow \mu^2 = \tau^2 + \eta_a\eta_b \gg \tau^2$ and then again $\rho \to 0$. The main conclusion from this section still holds: For stimulated processes time-ordering effects become important only when the photons in the different field photons spend a significant amount of time together.

5.5 Experimental proposal

Although in many applications [86, 87] a simple perturbative treatment of the nonlinear processes described here is appropriate, there are at least two experiments[28, 61] in which this approximation breaks down and a non perturbative treatment is needed. In both experiments a periodically poled Lithium Niobate (PPLN) crystal was used to upconvert a photon from the telecommunication wavelength to the visible with near unit efficiency. The fact that the single photon is converted with nearly unit efficiency implies that the nonlinear medium acts as a frequency beam splitter with reflectivity approaching unity. This immediately implies that $\varepsilon \sim 1$. One could question whether or not in those experiments time ordering effects are important. It turns out that they are not, simply because non-degenerate Type-0 phase matching was used. Since there is only one polarization available and the group velocity curve as a function of frequency is a monotonic function, it is impossible to have pump and down converted photons travelling together for a significant amount of time, and $\tau^2/R^2 \ll 1$. Nevertheless, it is possible to enhance the birefringence of PPLN by adding small amounts of Magnesium Oxide (MgO). In the study of Gayer et al. [88], Sellmeier equations were determined for the ordinary and extraordinary polarizations of PPLN doped with MgO in the wavelength window 0.5 to 4 nm. Although in the experiments mentioned so far a PPLN crystal was used for FC, they could also be used for SPDC. In Table 5.1 we show parameters for which it is possible to have pump and down converted photons travelling together. Using the parameters described in Table 5.1 it would be possible to set up an experiment in which, for the first time, a JSA that is nonlinear in the pump electric field could be observed. Using the parameters from Table 5.1, with $\chi_2 = 10$ pm/V, a crystal length of

Field label	Central frequency	Central wavelength	Index of Refraction	Group velocity	Polarization
p	2.0000 PHz	0.9418 μm	2.15541	$c/2.20054$	e
a	1.2707 PHz	1.4824 μm	2.21112	$c/2.26276$	o
b	0.7293 PHz	2.5827 μm	2.10269	$c/2.17833$	e

Table 5.1: Parameters for Periodically poles Lithium Niobate (PPLN) to observe significant time-ordering effects. To obtain zeroth order phase-matching a periodicity of $\Lambda = 1/|n_e(\lambda_p)/\lambda_p - n_o(\lambda_a)/\lambda_a - n_e(\lambda_b)/\lambda_b| = 58.25\mu$m is required. $n_{o/e}$ are the indices of refraction of the two different polarizations.

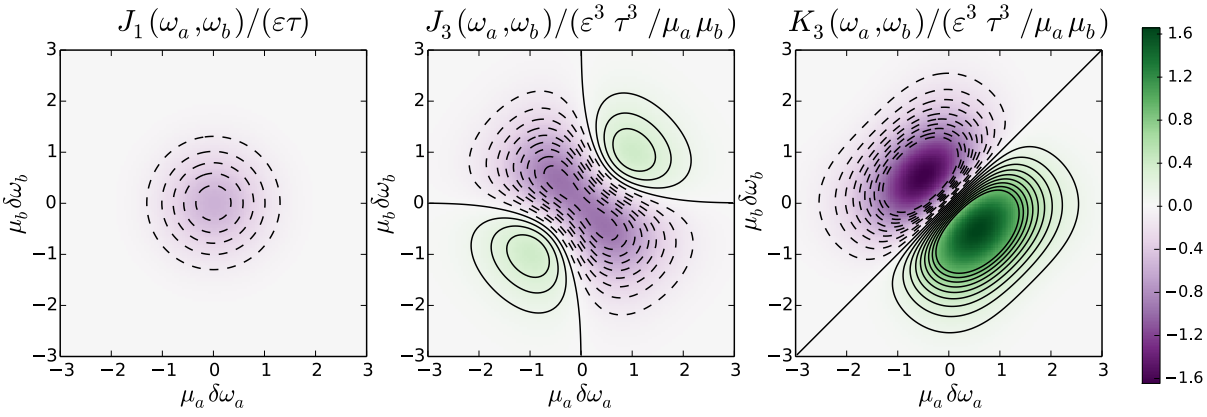

Figure 5.2: First and third order Magnus terms for the parameters from Table 5.1. Note that the function J_1 has been normalized by $\varepsilon\tau$ and J_3, K_3 by $\varepsilon^3\tau^3/\mu_a\mu_b$. For the case when when the lowest order JSA (J_1) is round one has $\mu_a = \mu_b = \sqrt{2}\tau$.

$L = 4$ cm, a pulse duration $\tau = 1$ ps, and a peak electric field of 6 MV/m, we obtain

$$\varepsilon = 0.30 \text{ and } r \leq 2\pi^2\varepsilon^2\frac{\tau^2}{R^2} = 0.46. \tag{5.28}$$

As it is seen in Fig. 5.2 time-ordering effects (encoded in J_3 and K_3) are comparable to the first order Magnus term J_1. These modifications could open an avenue for the generation of squeezed states with very interesting JSAs, and in any case these effects will become important as soon as very squeezed states are generated . As we shall show in the following subsections, time-ordering corrections should also become important whenever bright squeezed states are being used in conjunction with photon number resolving detectors to probabilistically generate heralded Fock states with a high (> 1) photon number.

5.6 Measuring the effects of the time-ordering corrections

Before considering how to measure the effects of time ordering lets us look at what are the consequences of including time-ordering corrections in the state generated in SPDC. If they were ignored then we could write very generally

$$J(\omega_a,\omega_b) = J_1(\omega_a,\omega_b) = \sum_\lambda \frac{(-\varepsilon\tilde{s}_\lambda)}{2\pi} f_\lambda(\omega_a) j_\lambda(\omega_b). \tag{5.29}$$

Because we assumed that the only contribution to J comes from J_1 then ε, the constant characterizing the strength of the interaction, can be factored out and the Schmidt values $s_\lambda(\varepsilon) = \varepsilon\tilde{s}_\lambda$ become linear functions of ε and the Schmidt functions are independent of ε. We can write the squeezed state generated by the interaction as

$$|\psi_{\text{out}}\rangle = e^{i\sum_\lambda(\varepsilon\tilde{s}_\lambda)(\hat{A}_\lambda^\dagger\hat{B}_\lambda^\dagger+\text{H.c.})}|\text{vac}\rangle = \bigotimes_\lambda e^{i(\varepsilon\tilde{s}_\lambda)(\hat{A}_\lambda^\dagger\hat{B}_\lambda^\dagger+\text{H.c.})}|\text{vac}\rangle\,, \tag{5.30}$$

where we used the notation introduced in Eq. (2.87). The last equation tells us that as we increase the energy in the pump pulse (as we increase ε) we simply increase the squeezing parameter $\varepsilon\tilde{s}_\lambda$ linearly and we *do not modify* the spectral shape of the Schmidt modes. We can contrast this with the case where we include time-ordering corrections

$$J(\omega_a,\omega_b) = \underbrace{J_1(\omega_a,\omega_b)}_{\propto\varepsilon} + \underbrace{(J_3(\omega_a,\omega_b) - iK_3(\omega_a,\omega_b))}_{\propto\varepsilon^3} = \sum_\lambda \frac{-s_\lambda(\varepsilon)}{2\pi} f_\lambda(\omega_a;\varepsilon) j_\lambda(\omega_a;\varepsilon). \tag{5.31}$$

In the last equation we cannot simply factor out the ε dependence and thus *because of time-ordering effects the Schmidt coefficients are now nonlinear functions of ε and the Schmidt functions will change as ε is changed.*

We have argued that the ideal parameter region for having significant modifications of the JSA is when one has a nearly uncorrelated JSA for $\varepsilon \ll 1$ ($\mu = 0$ in Eq. 5.5). In this parameter region J_1 can be written as an uncorrelated Gaussian

$$-2\pi J_1(\omega_a,\omega_b) = \frac{2\pi\varepsilon\tau}{\sqrt{\pi}}\exp(-\alpha^2-\beta^2) \tag{5.32}$$

$$= \sqrt{2}\pi\tau\varepsilon f(\alpha)f(\beta), \quad \alpha = \mu_a\delta\omega_a,\ \beta = \mu_b\delta\omega_b, \tag{5.33}$$

where $f(x) = \exp(-x^2)/\sqrt[4]{\pi/2}$ is a normalized Gaussian function. If we ignored time

ordering then

$$|\psi_{\text{out}}\rangle = e^{i\tilde{s}_0\varepsilon \int d\alpha d\beta \left(f(\alpha)f(\beta)a^\dagger(\alpha)b^\dagger(\beta)+\text{H.c.}\right)}|\text{vac}\rangle = e^{i\tilde{s}_0\varepsilon \hat{A}_0^\dagger \hat{B}_0^\dagger+\text{H.c.}}|\text{vac}\rangle \tag{5.34}$$

where the parameter

$$\tilde{s}_0 = \frac{\sqrt{2}\pi\tau}{\sqrt{\mu_a\mu_b}}. \tag{5.35}$$

tells us the rate of change of the squeezing parameter with respect to the dimensionless coupling constant ε. This parameter has another very important physical meaning. Under the separability constraint $0 = \mu^2 = \eta_a\eta_b + \tau^2$ the quantity $\tilde{s}_0$ tells us how much our low energy JSA, J_1 departs from being round. Indeed, for a perfectly round and separable J_1, for which $\mu_a = \mu_b = \sqrt{2}\tau$, the quantity $\tilde{s}_0$ takes its maximum value π. For a more eccentric J_1 the quantity $\tilde{s}_0$ will be less than π and will tend to zero for a J_1 with an aspect ratio tending to zero or infinity.

For the state in Eq. (5.34) the mean number of photons in field a (or b) is

$$\langle\hat{N}_a\rangle = \langle\hat{N}_b\rangle = \sinh^2(\tilde{s}_0\varepsilon), \tag{5.36}$$

$$\hat{N}_a = \int d\omega_a \hat{a}^\dagger(\omega_a)\hat{a}(\omega_a), \quad \hat{N}_b = \int d\omega_b \hat{b}^\dagger(\omega_b)\hat{b}(\omega_b), \tag{5.37}$$

and the Schmidt number $S = 1$ for all values of ε.
Once time ordering is included we need to calculate the corrections J_3 and K_3. As shown in Appendix D for $\mu = 0$ these functions are

$$J_3(\omega_a,\omega_b) = \frac{\pi^{3/2}\tau^3\varepsilon^3 e^{-\alpha^2-\beta^2}\left(3\text{erfi}\left(\sqrt{\frac{2}{3}}\beta\right)\text{erfi}\left(\sqrt{\frac{2}{3}}\alpha\right)-1\right)}{6\mu_a\mu_b}, \tag{5.38}$$

$$K_3(\omega_a,\omega_b) = \pm\frac{\pi^{3/2}\tau^3\varepsilon^3 e^{-\alpha^2-\beta^2}\left(\text{erfi}\left(\sqrt{\frac{2}{3}}\beta\right)-\text{erfi}\left(\sqrt{\frac{2}{3}}\alpha\right)\right)}{2\mu_a\mu_b}, \tag{5.39}$$

and now the Schmidt functions depend on ε and the Schmidt coefficients are no longer

linear functions of ε. The state including time-ordering corrections will be now

$$|\psi_{\text{out}}\rangle = \exp\left(i\int d\alpha d\beta\Big\{(\tilde{s}_0\varepsilon)f(\alpha)f(\beta) + \frac{(\tilde{s}_0\varepsilon)^3}{4}\times \right. \tag{5.40}$$
$$f(\alpha)f(\beta)\Big[\text{erfi}\left(\sqrt{2/3}\beta\right)\text{erfi}\left(\sqrt{2/3}\alpha\right) - 1/3$$
$$\left.\pm i\left(\text{erfi}\left(\sqrt{2/3}\beta\right) - \text{erfi}\left(\sqrt{2/3}\alpha\right)\right)\Big]\Big\}a^\dagger(\alpha)b^\dagger(\beta) + \text{H.c.}\right)|\text{vac}\rangle$$

The expression shows a very interesting feature of the Gaussian model. For the low energy uncorrelated case $\mu = 0$ the corrected JSA is only a function of $\tilde{s}_0\varepsilon$. The last expression shows explicitly that for $\tilde{s}_0\varepsilon \ll 1$ this quantity is precisely the Schmidt number of the mode, but more importantly even when the condition $\tilde{s}_0\varepsilon \ll 1$ is not satisfied this quantity still solely determines the Schmidt numbers and functions. This is not so surprising once one realizes that the correction should be just a function of the aspect ratio of the JSA in the ω_a, ω_b and this information is encoded in $\tilde{s}_0$.

Expressions Eq. (5.32) and Eq. (5.38) can be further specialized to the case discussed in the last section for which J_1 is round by putting $\mu_a = \mu_b = \sqrt{2}\tau$ and $\eta_{ab} = \pm 2\tau$.
In Fig. 5.3 we plot the mean number of photons including and ignoring time-ordering corrections. It is seen that as soon as the mean number of photons generated $N_a \geq 1$ the two theories predict very different results. Thus observing a faster than $\sinh^2(\tilde{s}_0\varepsilon)$ growth in the intensity of the down converted fields could we used as a witness of the nonlinear behaviour of the JSA when time-ordering corrections become important.

Another way of revealing time-ordering effects is by noticing that the time-ordering corrections do not share the following symmetry of J_1 in the limit $\mu = 0$

$$J_1(\delta\omega_a, \delta\omega_b) = J_1(-\delta\omega_a, \delta\omega_b) = J_1(\delta\omega_a, -\delta\omega_b). \tag{5.41}$$

Thus one could also measure correlation functions like

$$\langle\hat{a}^\dagger(\omega_a)\hat{a}(\omega_a)\hat{b}^\dagger(\omega_b)\hat{b}(\omega_b)\rangle = \langle\hat{a}^\dagger(\omega_a)\hat{a}(\omega_a)\rangle\langle\hat{b}^\dagger(\omega_b)\hat{b}(\omega_b)\rangle + \langle\hat{a}^\dagger(\omega_a)\hat{b}^\dagger(\omega_b)\rangle\langle\hat{a}(\omega_a)\hat{b}(\omega_b)\rangle\,. \tag{5.42}$$

to detect the presence of time-ordering corrections. Incidentally, the last equation explicitly shows that for a Gaussian state (like TMSV) the higher order moments of the creation and annihilation operators are functions of the second moments of the same operators.

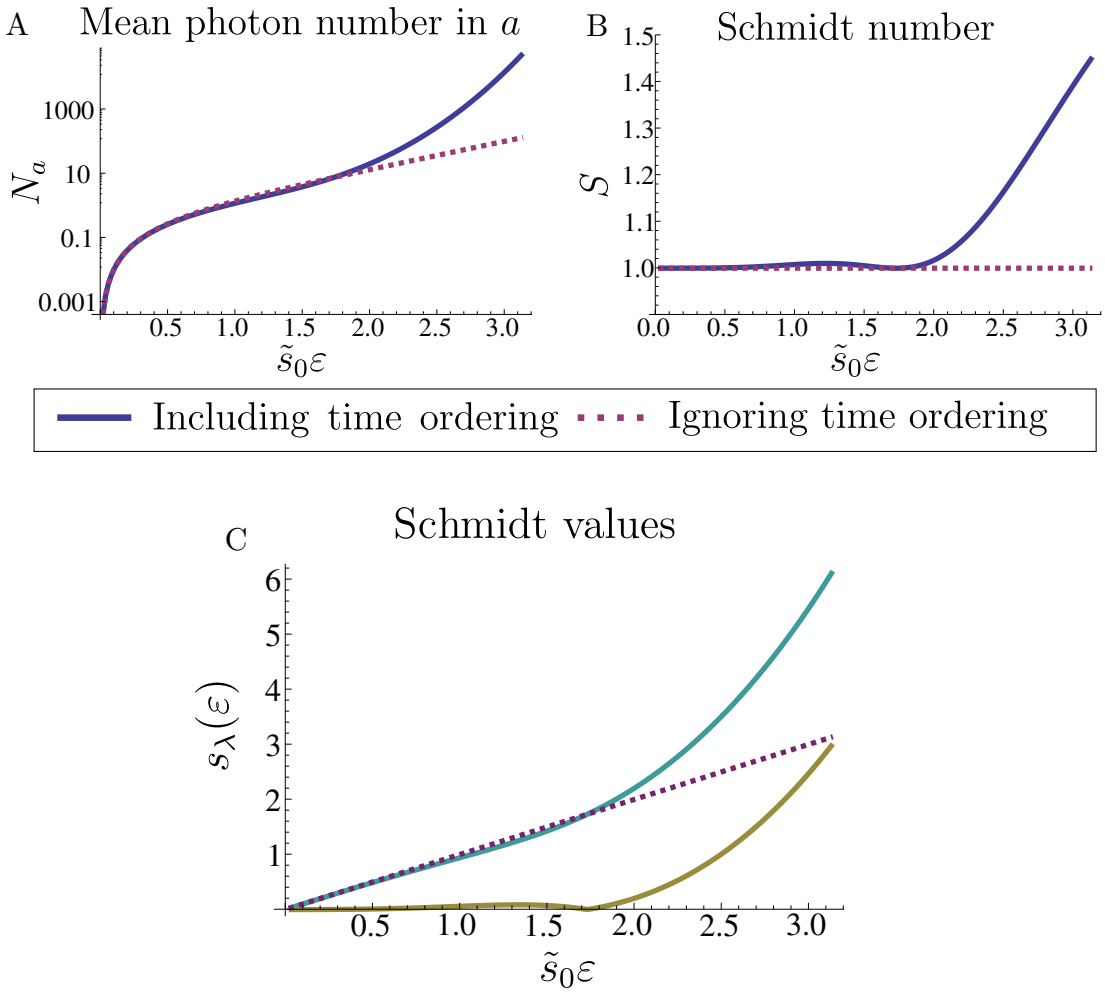

Figure 5.3: Mean number of photons and Schmidt number for the parameters of the JSA in Fig. 5.2 as a function of $\tilde{s}_0\varepsilon$ in A and B. In C we plot the Schmidt number as a function of $\tilde{s}_0\varepsilon$ including (continuous lines) and excluding (dashed lines) time-ordering effects. Note that there are two continuous lines precisely because the time-ordering corrections generate an extra Schmidt mode. In the limit $\varepsilon \ll 1$ this Schmidt mode disappears because its Schmidt number becomes zero.

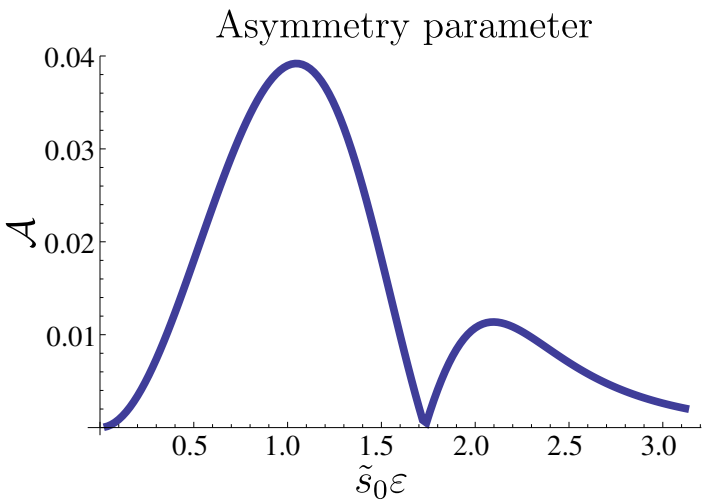

Figure 5.4: Asymmetry parameter $\mathcal{A}$ as a function of ε. If time-ordering effects where ignored this parameter would be zero.

It is more convenient to consider only the correlated part of the the expectation value Eq. (5.42) and thus we subtract the uncorrelated part to get

$$|\langle \hat{a}^\dagger(\omega_a)\hat{b}^\dagger(\omega_b)\rangle|^2 = \langle \hat{a}^\dagger(\omega_a)\hat{a}(\omega_a)\hat{b}^\dagger(\omega_b)\hat{b}(\omega_b)\rangle - \langle \hat{a}^\dagger(\omega_a)\hat{a}(\omega_a)\rangle \langle \hat{b}^\dagger(\omega_b)\hat{b}(\omega_b)\rangle . \tag{5.43}$$

We can evaluate what is the value of this quantity integrated over the four different quadrants

$$\begin{aligned} Q_1 &= \int_{\delta\omega_a>0,\delta\omega_b>0} d\omega_a d\omega_b |\langle \hat{a}^\dagger(\omega_a)\hat{b}^\dagger(\omega_b)\rangle|^2, \quad Q_2 = \int_{\delta\omega_a>0,\delta\omega_b<0} d\omega_a d\omega_b |\langle \hat{a}^\dagger(\omega_a)\hat{b}^\dagger(\omega_b)\rangle|^2, \\ Q_3 &= \int_{\delta\omega_a<0,\delta\omega_b<0} d\omega_a d\omega_b |\langle \hat{a}^\dagger(\omega_a)\hat{b}^\dagger(\omega_b)\rangle|^2, \quad Q_4 = \int_{\delta\omega_a>0,\delta\omega_b<0} d\omega_a d\omega_b |\langle \hat{a}^\dagger(\omega_a)\hat{b}^\dagger(\omega_b)\rangle|^2. \end{aligned} \tag{5.44}$$

The quantities Q_i are the number of correlated photons in each of the quadrants of the (ω_a, ω_b) space centered at $\omega_a = \bar{\omega}_a$ and $\omega_b = \bar{\omega}_b$ ($\delta\omega_a = \delta\omega_b = 0$). Let us introduce the following asymmetry parameter

$$\mathcal{A} = \frac{|Q_1 - Q_2 + Q_3 - Q_4|}{Q_1 + Q_2 + Q_3 + Q_4}. \tag{5.45}$$

This quantity satisfies $0 \leq \mathcal{A} \leq 1$ and should be measurable by inserting frequency filters before intensity detectors. In this idealized situation the filters correspond to sharp Heaviside functions in frequency space.

The quantity $\mathcal{A}$ has two very desirable features. The first one is that for JSAs of the form Eq. (5.32) it vanishes. The second one is that for any JSA that has only one non-zero Schmidt coefficient it is independent of the value of ε. In Fig. 5.4 we plot this parameter as a function of ε. It takes a maximum value of around 4%. Although this value is small, this result illustrates the general idea that any change in the *shape* of the JSA will indicate the appearance of time-ordering contributions.

5.7 Heralded generation of Fock states

With the development of photon number resolving detectors [89, 90] it becomes possible to generate Fock states with more than one photon by doing measurements in one field of a TMSV state. In the very ideal case of a TMSV with just one non-zero Schmidt coefficient

$$|\psi_i\rangle = e^{is_i\left(\hat{A}_i^\dagger \hat{B}_i^\dagger + \text{H.c.}\right)} |\text{vac}\rangle\,, \tag{5.46}$$

and considering ideal detectors modeled by the projection-valued measure (PVM) elements

$$\hat{\Pi}_N^a = \frac{1}{N!}\left(\int \prod_{i=1}^{N} d\omega_j \hat{a}^\dagger(\omega_j)\right) |\text{vac}\rangle\langle\text{vac}| \left(\int \prod_{i=1}^{N} d\omega_j \hat{a}(\omega_j)\right), \tag{5.47}$$

where $\hat{\Pi}_n^a$ is an ideal N-photon projector in field a. One can easily show (see Sec. 2.2.2) that the state of field b when N photons are detected in a is

$$\hat{\rho}_b = \frac{\text{tr}_a\left(\hat{\Pi}_N^a |\psi_i\rangle\langle\psi_i| \hat{\Pi}_N^a\right)}{p_N} = \frac{\text{tr}_a\left(|N_i^a\rangle\langle N_i^a| |\psi_i\rangle\langle\psi_i| |N_i^a\rangle\langle N_i^a|\right)}{p_N} = |N_i^b\rangle\langle N_i^b|\,, \tag{5.48}$$

$$|N_i^b\rangle = \frac{\left(\hat{B}_i^\dagger\right)^N}{\sqrt{N!}} |\text{vac}\rangle\,, \quad |N_i^a\rangle = \frac{\left(\hat{A}_i^\dagger\right)^N}{\sqrt{N!}} |\text{vac}\rangle\,, \quad p_n = \frac{\tanh^{2N} s_i}{\cosh^2 s_i}. \tag{5.49}$$

The state in Eq. (5.48) is a spectrally pure Fock state $|N_i^b\rangle$ having N photons in field b in Schmidt mode i. This outcome of the measurement will occur with probability $p_N = \tanh^{2N}(s_i)/\cosh^2(s_i)$. The probability p_N for fixed N attains its maximum value when the squeezing parameter satisfies $\sinh^2 s_i = N_i^b = \langle \hat{N}_b \rangle$ and is equal to

$$p_N^{(\max)} = \frac{1}{N}\left(1 + \frac{1}{N}\right)^{-N} \underset{N\gg 1}{\to} \frac{1}{eN}. \tag{5.50}$$

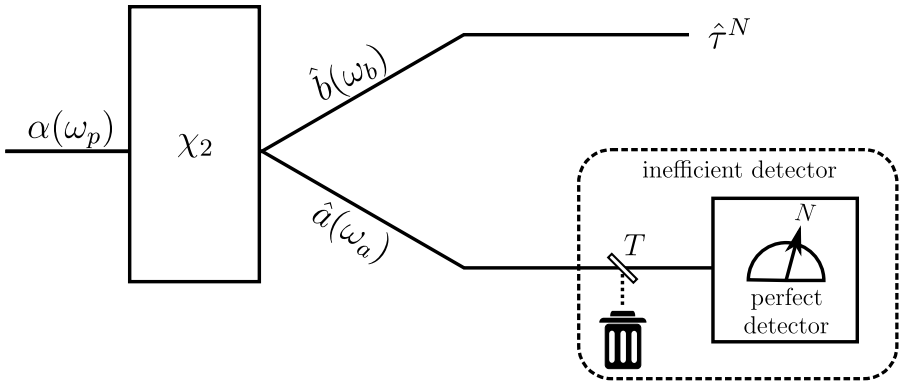

Figure 5.5: Schematic representation of the heralded preparation of a Fock state with N photons using an inefficient detector, modeled as a perfect detector preceded by a loss channel.

The argument presented above is of course an idealization for at least two reasons: realistic detectors are not well represented by the PVM elements in Eq. (5.47), in particular realistic detectors are not 100% efficient. Second, as we showed earlier in this chapter, as soon as one departs from the perturbative regime in SPDC (that is the regime in which mainly pairs are generated) the JSA starts to acquire new Schmidt modes. In the last section we showed that even if the JSA for $\varepsilon \ll 1$ is separable, once one leaves the perturbative regime it becomes entangled. To model real detectors one would use tomographic data of the detectors [91]. Tomography of number resolving detectors is still in active development [92]; so instead of using real tomographic data we will take a more phenomenological approach and model the action of realistic inefficient detectors in the state Eq. (5.46) by considering ideal detectors modeled by the PVM Eq. (5.47) preceded by a loss channel [93]. As mentioned in sec. 2.2.4 one can model losses by coupling via a beam splitter of amplitude transmissivity T the field that will undergo loss to another field prepared in vacuum. The case $T = 1$ corresponds to no loss and $T = 0$ corresponds to complete loss. For the sake of generality we will derive equations for loss in both fields a and b parametrized by amplitude transmissivity coefficients T and T'. Nevertheless, we will only consider the case where the losses occur in the field that is being measured a, this is schematized in Fig. 5.5. Using the results from sec. 2.2.4 we can write the density matrix of TMSV with one nonzero Schmidt mode as

$$\hat{\rho}_i = e^{is_i'(\hat{A}_i^\dagger \hat{B}_i^\dagger + \text{H.c.})} \left(\sum_{n,m=0}^{\infty} \frac{\mathfrak{a}_i^n \mathfrak{b}_i^m}{(1+\bar{n}_i)(1+\bar{m}_i)} \left| n_i, m_i \right\rangle \left\langle n_i, m_i \right| \right) e^{-is_i'(\hat{A}_i^\dagger \hat{B}_i^\dagger + \text{H.c.})}, \qquad (5.51)$$

where

$$|n_i, m_i\rangle = \frac{\left(\hat{A}_i^\dagger\right)^n \left(\hat{B}_i^\dagger\right)^m}{\sqrt{n!m!}} |\text{vac}\rangle\,, \quad \mathfrak{a}_i = \frac{\bar{n}_i}{1+\bar{n}_i}, \quad \mathfrak{b}_i = \frac{\bar{m}_i}{1+\bar{m}_i} \tag{5.52}$$

We can now use this lossy state and the ideal PVM elements in Eq. (5.47) to mimic the statistics of the pure state Eq. (5.46) being measured by realistic inefficient detectors. If the measurement gives us the outcome N then our state will be projected to

$$\hat{\rho}_i \Longrightarrow \hat{\rho}_i^N = \frac{\left(\hat{\Pi}_N^a\right)\hat{\rho}\left(\hat{\Pi}_N^a\right)}{p_N^{(i)}}, \tag{5.53}$$

$$p_N^{(i)} = \text{tr}\left(\hat{\Pi}_N \hat{\rho}_i\right). \tag{5.54}$$

This outcome will occur with probability $p_N^{(i)}$. We want to know now what is the state of the photons in mode b given that we measured N in mode a. We can do this by simply tracing out mode a in the last equation. The normalized state for b conditioned on result N in a is

$$\hat{\tau}_i^N = \frac{1}{p_N^{(i)}} \sum_{M=0}^{\infty} \mathfrak{c}_{i,N,M} \left|M_i^b\right\rangle \left\langle M_i^b\right|.$$

where

$$\mathfrak{c}_{i,N,M} = \sum_{n,m=0}^{\infty} \frac{\mathfrak{a}_i^n \mathfrak{b}_i^m}{(1+\bar{n}_i)(1+\bar{m}_i)} \left|\langle N_i, M_i| e^{is_i'\left(\hat{A}_i^\dagger \hat{B}_i^\dagger + \text{H.c.}\right)} |n_i, m_i\rangle\right|^2 \tag{5.55}$$

and $p_N^{(i)} = \sum_{M=0}^{\infty} \mathfrak{c}_{i,N,M}$. In Fig. 5.6 we plot this probability as a function of the squeezing parameter and the efficiency of the detector. We see that its behaviour is not strongly modified by losses.

We can evaluate the matrix elements of the two-mode squeezing operator in the number basis using the disentangling identity from Eq. (2.55)

$$\langle n_k', m_k'| e^{is_k'\left(\hat{A}_k^\dagger \hat{B}_k^\dagger + \text{H.c.}\right)} |n_k, m_k\rangle = \delta_{m'-m,n'-n} \mathfrak{S}_{n',m';n,m} \tag{5.56}$$

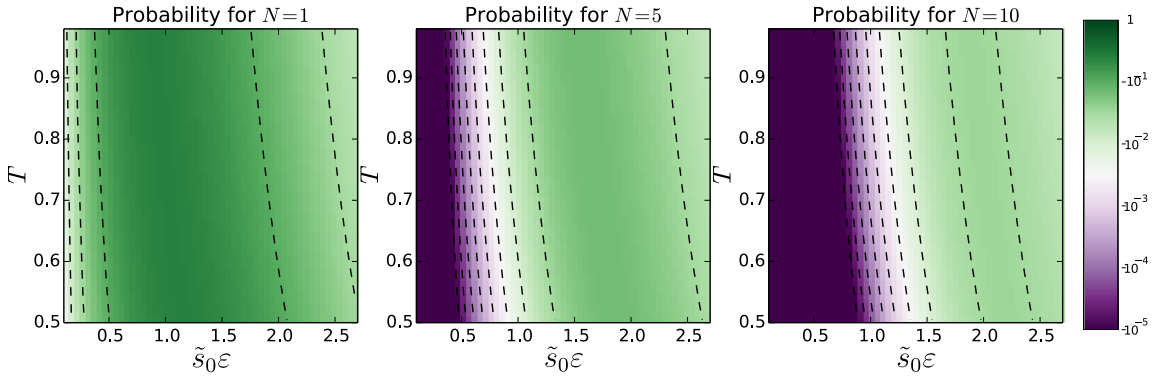

Figure 5.6: Probabilities of obtaining the results $N = 1, 5, 10$ when measuring the photon number in field a for the state Eq. (5.34) ignoring time-ordering corrections. The probability is plotted as a function of the squeezing parameter $\tilde{s}_0\varepsilon$ and the transmissivity T used to parametrize the finite efficiency of the detector. The case $T = 1$ corresponds to ideal detectors.

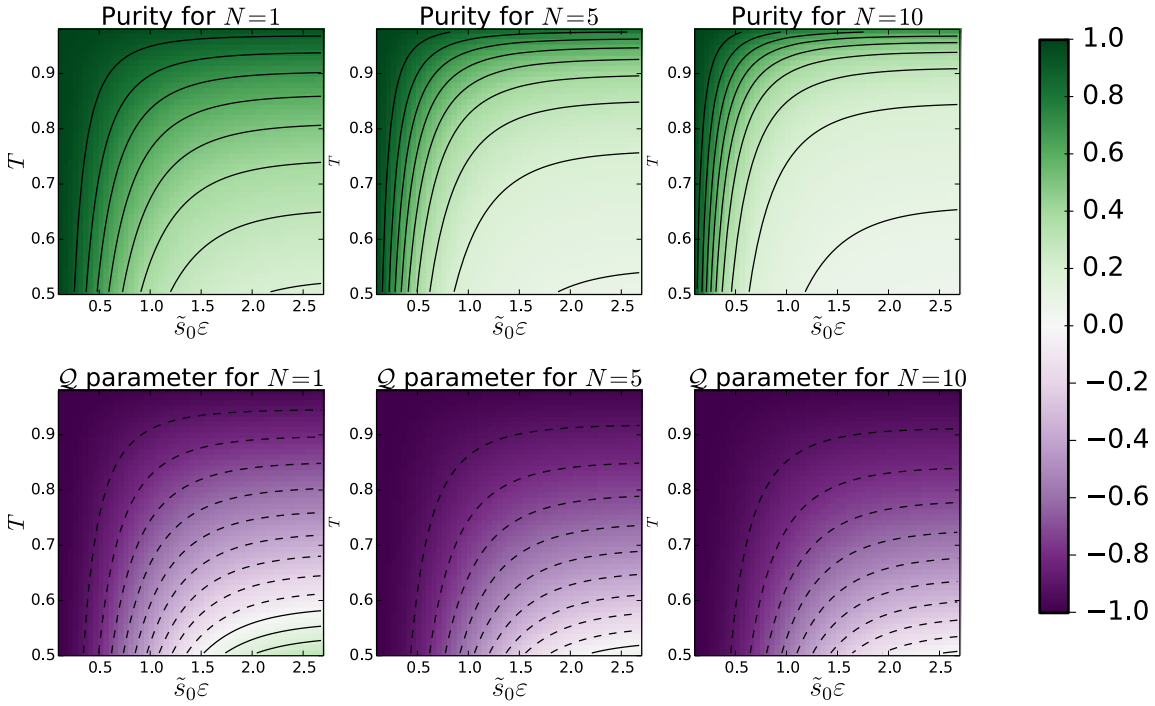

Figure 5.7: Mandel $\mathcal{Q}$ parameter and purity of field b for the heralding outcomes $N = 1, 5, 10$ when measuring the photon number for field a in the state Eq. (5.34) ignoring time-ordering corrections. These parameters are plotted as a function of the squeezing parameter $\tilde{s}_0\varepsilon$ and the transmissivity T used to parametrize the finite efficiency of the detector. The case $T = 1$ corresponds to ideal detectors.

where

$$\mathfrak{s}_{n',m';n,m} = i^d \frac{\tanh^d s_i'}{\cosh^{m+n+1} s_i'} \sqrt{m!n!m'!n'!} \times \sum_{j=\max(0,-d)}^{\min(m,n)} \frac{(-1)^j \sinh^{2j} s_i'}{j!(j+d)!\sqrt{(m-j)!(n-j)!(m'-j-d)!(n'-j-d)!}} \tag{5.57}$$

and $d = m' - m = n' - n$. We can use the selection rule in Eq. (5.56) to rewrite

$$\mathfrak{c}_{i,N,M} = \mathfrak{b}_i^{M-N} \sum_{n=\max(0,N-M)}^{\infty} \frac{(\mathfrak{a}_i \mathfrak{b}_i)^n}{(1+\bar{n}_i)(1+\bar{m}_i)} |\mathfrak{s}_{N,M;n,n-(N-M)}|^2. \tag{5.58}$$

In the case when only field a undergoes losses we know that $\bar{n}_i = 0 = \mathfrak{a}_i$ (see Sec. 2.2.4) and then

$$\mathfrak{c}_{i,N,M} = \begin{cases} \frac{\mathfrak{b}_i^{M-N}}{1+\bar{m}_i} |\mathfrak{s}_{N,M;0,M-N}|^2 & \text{if } M \geq N, \\ 0 & \text{otherwise,} \end{cases} \tag{5.59}$$

and $\mathfrak{s}_{N,M;0,M-N} = i^N \sqrt{\frac{M!}{N!(M-N)!}} \frac{\tanh^N s_i'}{\cosh^{M-N+1} s_i'}$. We can write the density matrix for this case as

$$\hat{\tau}_i^N = \frac{1}{p_N^{(i)}} \sum_{M=N}^{\infty} \left(\frac{\mathfrak{b}_i^{M-N}}{1+\bar{m}_i} \frac{M!}{N!(M-N)!} \frac{\tanh^{2N} s_i'}{\cosh^{2M-2N+2} s_i'} \right) |M_i^b\rangle \langle M_i^b| \tag{5.60}$$

$$= \frac{(1-\mathfrak{r}_i)^{N+1} \mathfrak{r}_i^{-N}}{N!} \sum_{M=N}^{\infty} \frac{M!}{(M-N)!} \mathfrak{r}_i^M |M_i^b\rangle \langle M_i^b|,$$

$$p_N^{(i)} = \frac{1}{1+\bar{m}_i} \frac{\tanh^{2N} s_i'}{\cosh^2 s_i' (1-\mathfrak{r}_i)^{N+1}}, \tag{5.61}$$

where we introduced the parameter

$$\mathfrak{r}_i = \frac{\mathfrak{b}_i}{\cosh^2 s_i'}. \tag{5.62}$$

Using these results, in Fig. 5.7 we plot the purity and Mandel $\mathcal{Q}$ parameter of the state when the measurement outcomes in field a are $N = 1, 5, 10$. The Mandel $\mathcal{Q}$ parameter is defined as [94]

$$\mathcal{Q} = \frac{\langle \hat{N}_b^2 \rangle - \langle \hat{N}_b \rangle^2}{\langle \hat{N}_b \rangle} - 1 \tag{5.63}$$

and characterizes the departure of a field from Poissonian counting statistics. It has the nice feature that for Fock states other than vacuum it takes the value -1. We see that for a transmissivity of $T < 0.9$ one can only find $\mathcal{Q}$ parameters close to -1 in regions where the probability (as plotted in Fig. 5.6) is very small. The purity on the other hand tell us about the mixedness of our state τ_i^N. For an arbitrary, but normalized, quantum state $\hat{\rho}$ it is defined as

$$P(\hat{\rho}) = \mathrm{tr}(\hat{\rho}^2). \tag{5.64}$$

The purity is one for pure states and approaches zero for very mixed states. For the state in Eq. (5.60) we can easily calculate the $\mathcal{Q}$ parameter, and the mean number of photons

$$\mathcal{Q} = \frac{\mathfrak{r}_i}{1-\mathfrak{r}_i} - \frac{N}{N+\mathfrak{r}_i}, \tag{5.65}$$

$$\langle \hat{N}_b \rangle = N + \frac{\mathfrak{r}_i}{1-\mathfrak{r}_i}(N+1). \tag{5.66}$$

With some extra tap dancing of the dummy indices we can also write the purity as

$$P = (1-\mathfrak{r}_i)^{2(N+1)}\, {}_2F_1\left(N+1, N+1; 1; \mathfrak{r}_i^2\right) \tag{5.67}$$

where ${}_2F_1$ is the Gauss Hypergeometric function (see Sec. 15.2 of [95, 96]). From Fig. 5.7 we see that the purity and the Mandel $\mathcal{Q}$ parameter are strongly correlated and give roughly the same information about our state. This is to be expected since the only source of mixedness if there is only one Schmidt mode is the one related to the photon number. One might wonder whether considering one Schmidt mode is a good approximation. In the following paragraphs we will generalize these results but we should also mention that one can fight the time-ordering corrections that cause the appearance of extra Schmidt modes by using cascaded generation devices. This will be explained in detail in Sec. 6.3.

We have so far only considered the case of one Schmidt mode. From the findings of the previous section we know that even if the JSA for low pump energy is separable (has only one Schmidt mode) as soon as one starts to get more than one pair of downconverted photons on average, new Schmidt modes will appear. The case of many Schmidt modes is a straightforward generalization of the previous result. More generally one would have the state

$$|\psi\rangle = \bigotimes_i e^{is_i\left(\hat{A}_i^\dagger \hat{B}_i^\dagger + \mathrm{H.c.}\right)} |\mathrm{vac}\rangle\,. \tag{5.68}$$

To calculate the effect of realistic detectors we need to obtain the multi Schmidt mode lossy density matrix and write the action of the $\hat{\Pi}_n^a$ in such state. The first part of this calculation is trivial since the multimode Schmidt state after loss is simply

$$\hat{\rho} = \bigotimes_i \hat{\rho}_i \tag{5.69}$$

where $\hat{\rho}_i$ is the single mode Schmidt mode lossy state in Eq. (5.51). The last equation simply tell us that losses affect all the Schmidt modes in the same way. The second part of this strategy is to write the action of the projector Eq. (5.47) in state Eq. (5.69). One can write this action for an arbitrary number of Schmidt modes but we will only do it for two (since to first approximation time-ordering corrections only generate one extra Schmidt mode). Assuming there are only two Schmidt modes that we label 0 and 1 we have $\hat{\rho} = \hat{\rho}_0 \otimes \hat{\rho}_1$ and we can write

$$(\hat{\Pi}_N^a)\hat{\rho}(\hat{\Pi}_N^a) = \tag{5.70}$$
$$\left(\sum_{l=0}^{N} |l_0^a\rangle \langle l_0^a| \otimes |(N-l)_1^a\rangle \langle (N-l)_1^a|\right) \hat{\rho} \left(\sum_{l=0}^{N} |l_0^a\rangle \langle l_0^a| \otimes |(N-l)_1^a\rangle \langle (N-l)_1^a|\right)$$

$$|l_0^a\rangle = \frac{\left(\hat{A}_0^\dagger\right)^l}{\sqrt{l!}} |\text{vac}\rangle\,, \quad |(N-l)_1^a\rangle = \frac{\left(\hat{A}_1^\dagger\right)^{N-l}}{\sqrt{(N-l)!}} |\text{vac}\rangle\,. \tag{5.71}$$

We can now trace out mode a and find the density matrix for mode b conditioned on the detection of N photons

$$\hat{\tau}^N = \frac{1}{p_N} \sum_{M,M'=0}^{\infty} \left(\sum_{l=0}^{N} \mathfrak{c}_{0,l,M} \mathfrak{c}_{1,N-l,M'}\right) |M_0^b\rangle \langle M_0^b| \otimes |(M')_1^b\rangle \langle (M')_1^b|\,, \tag{5.72}$$

where now

$$p_N = \sum_{M,M'=0}^{\infty} \left(\sum_{l=0}^{N} \mathfrak{c}_{0,l,M} \mathfrak{c}_{1,N-l,M'}\right). \tag{5.73}$$

In Fig. 5.8 and Fig. 5.9 we plot the probabilities, Mandel $\mathcal{Q}$ parameter and purity for the case when time-ordering corrections are included and allow for the possibility of more than one Schmidt mode. We note that the probabilities and Mandel $\mathcal{Q}$ parameter do not differ significantly from the case without time-ordering corrections. Yet, the overall purity is significantly different from the case without time ordering shown in Figs. 5.6 and 5.7. This result is easy to understand if we realize that time ordering will cause an

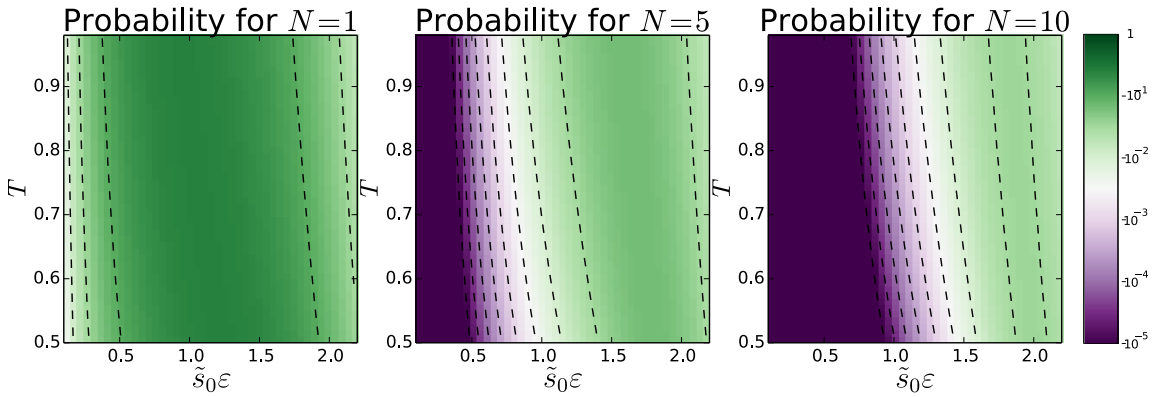

Figure 5.8: Probabilities of obtaining the results $N = 1, 5, 10$ when detecting the photon number in field a for the state Eq. (5.40) including time-ordering corrections. The probability is plotted as a function of the squeezing parameter $\tilde{s}_0\varepsilon$ and the transmissivity T used to parametrize the finite efficiency of the detector. The case $T = 1$ corresponds to ideal detectors.

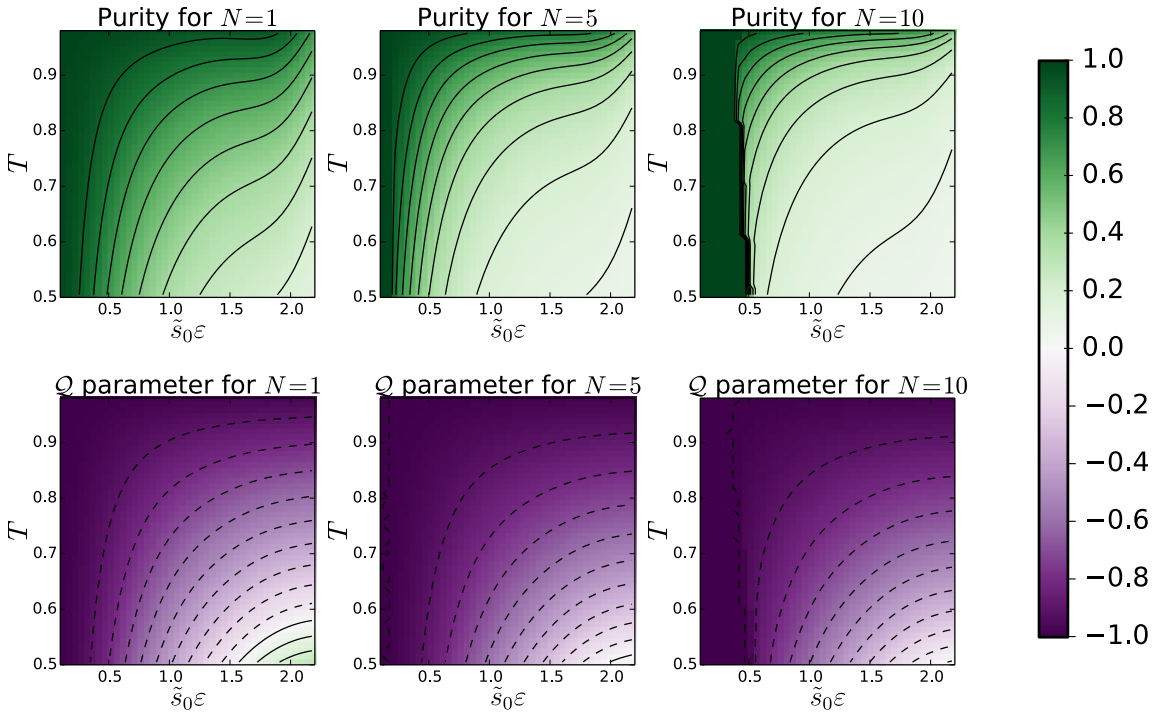

Figure 5.9: Mandel $\mathcal{Q}$ parameter and purity of field b for the heralding outcomes $N = 1, 5, 10$ when measuring the photon number in field a for the state Eq. (5.40) including time-ordering corrections. These parameters are plotted as a function of the squeezing parameter $\tilde{s}_0\varepsilon$ and the transmissivity T used to parametrize the finite efficiency of the detector. The case $T = 1$ corresponds to ideal detectors.

extra Schmidt mode to appear, allowing for the possibility of mixedness in that degree of freedom.

The results of this section show that to prepare highly pure Fock states with more than one photon it is necessary to use very high efficiency photon number resolving detectors or wait for exceedingly long times in order to get at least one detection event in the heralding arm. On the other hand the preparation of single photons does not seem to be constrained by this compromise relation. Using inefficient number resolving detectors one can prepare highly pure single photons with heralding probabilities that are not vanishingly small. This can be contrasted with the case of bucket detectors (binary detectors that distinguish only between having no photons and having any number of photons) where the probability of preparing a single photon with purity $1 - r$ ($r \ll 1$) is roughly $r/2$.

Chapter 6

Highly efficient frequency conversion

You can't always get what you want
But if you try some time, you just might find
You get what you need

The Rolling Stones

6.1 Introduction

Nonlinear photonic materials provide some of the most advanced platforms for manipulating the frequency and spectral profile of photons. This manipulation is typically achieved using a process known as frequency conversion (FC) [24, 25]. In FC, two photons (one of them typically coming from a bright classical field) are fused into another photon with a higher energy. FC has several important applications. First, it can be used to move weak signals from a region of the spectrum where there are no good detectors to another region where there are [28, 61]. A second application is to modify in a controlled manner the properties of weak signals, in particular single photons, for quantum information processing (QIP) tasks. Brecht *et al.* have recently proposed encoding information in large Hilbert spaces using temporal/frequency modes of single photons [20, 21, 22, 23]. One of the components of this and several other [27] QIP protocols using single photons is the ability to completely upconvert a single frequency mode of a given spectral profile while leaving all the other orthogonal frequency profiles untouched. Finally, FC is useful for modifying the spectral profile of single photons, making their sources compatible with existing or proposed quantum memories [18, 19]. For all these applications it is important to have conversion efficiency near unity, and for some of them it is also important to have selectivity in the frequency profiles that are converted.

In this chapter, we examine limitations to highly efficient FC arising from its fundamental quantum mechanical nature. These limitations are due to time-ordering corrections that appear because the interaction picture Hamiltonian that describes the χ_2 interaction between the different fields does not commute with itself at different times. Our study allows us to separate very cleanly the "ideal" operation of an FC device from the "undesirable" effects of time ordering. Thus, we can explicitly write the operation of an FC gate, in a language very close to the one used in quantum information, as a unitary operation $\hat{\mathcal{U}}_{\rm FC} = \exp(\hat{\Omega}_1 + \hat{\Omega}_2 + \hat{\Omega}_3 + \ldots)$ that consists of a desired generator $\hat{\Omega}_1$ and time-ordering corrections $\hat{\Omega}_2, \hat{\Omega}_3, \ldots$ that modify the operation of the gate. This separation is obtained using the Magnus expansion (ME) studied in Chapter 4. Using the ME allows us to understand the scaling of the time-ordering corrections as a function of the energy of the classical pump pulse. Based on this model, we propose a new scheme to achieve highly efficient FC harnessing the until now undesirable time-ordering corrections; this model also allows us to explain, using simple scaling arguments, why the double pass scheme introduced by Reddy *et al.* [23] succeeds in achieving high efficiency FC.

6.2 Ideal frequency conversion

We begin with the Hamiltonian describing a second-order nonlinear optical FC process in the undepleted pump approximation, occurring in a quasi one-dimensional structure of length L and characterized by a nonlinear coefficient χ_2 (Sec. 4.4)

$$\hat{H}_I(t) = -\hbar\varepsilon \int d\omega_p d\omega_a d\omega_b \big(e^{i\bar{\Delta}t}\bar{\Phi}(\omega_a,\omega_b,\omega_p)\alpha(\omega_p)\hat{a}(\omega_a)\hat{b}^\dagger(\omega_b) + \text{H.c.}\big), \tag{6.1}$$

where ω_p refers to a pump frequency, and the shape of the classical pump function $\alpha(\omega_p)$ is taken to be a Gaussian,

$$\alpha(\omega_p) = \tau e^{-\tau^2\delta\omega_p^2}/\sqrt{\pi}, \quad \delta\omega_p = \omega_p - \bar{\omega}_p, \tag{6.2}$$

where $\bar{\omega}_p$ identifies the center pump frequency; τ identifies the duration of the pump pulse, and we specify its energy by U_0. In the FC process frequency components ω_a can be destroyed and frequency components ω_b can be created; associated with this are bosonic destruction and creation operators $\hat{a}(\omega_a)$ and $\hat{b}^\dagger(\omega_b)$ respectively. We assume that the phase-matching function (PMF) $\bar{\Phi}(\omega_a,\omega_b,\omega_p)$, restricts the destroyed and created photons to be in nonoverlapping frequency regions, and/or of different mode profiles

or polarizations; then we can take $[\hat{a}(\omega_a), \hat{b}^\dagger(\omega_b)] = 0$. We reference the frequencies ω_a and ω_b to center frequencies $\bar{\omega}_a$ and $\bar{\omega}_b$ respectively, defined so that energy and momentum conservation are exactly satisfied for the center frequencies, $\bar{\omega}_b - \bar{\omega}_a - \bar{\omega}_p = 0$ and $\overline{\Delta k}(\bar{\omega}_a, \bar{\omega}_b, \bar{\omega}_p) = 0$ (see Eq. (4.39)). Finally, $\bar{\Delta} = \omega_b - \omega_a - \omega_p$, and

$$\varepsilon = 2L\chi_2 \sqrt{\frac{\sqrt{2}U_0 \pi \bar{\omega}_b \bar{\omega}_a}{\sqrt{\pi}(4\pi)^3 \epsilon_0 A c^3 n_a(\bar{\omega}_a) n_b(\bar{\omega}_b) n_c(\bar{\omega}_c)\tau}} \tag{6.3}$$

is a dimensionless constant that characterizes the strength of the interaction; the $n_i(\bar{\omega}_i)$ are the indices of refraction at the central frequencies $\bar{\omega}_i$, and A is the effective overlap area of the spatial fields. We will considered conversion using a χ_2 material. With correspondences presented in the previous chapters, this results can be generalized to the use of χ_3 materials as well.

Ignoring time-ordering corrections, the unitary evolution operator connecting states at $t \to -\infty$ to states at $t \to \infty$ is

$$\hat{\mathcal{U}}_1 = e^{\hat{\Omega}_1} = e^{-\frac{i}{\hbar}\int_{-\infty}^{\infty} dt \hat{H}_I(t)} \tag{6.4a}$$

$$= e^{-2\pi i \int d\omega_a d\omega_b \left(\bar{J}_1(\omega_a,\omega_b)\hat{a}(\omega_a)\hat{b}^\dagger(\omega_b) + \text{H.c.}\right)}, \tag{6.4b}$$

where the quantity $\bar{J}_1$ is, to this level of approximation, the joint conversion amplitude (JCA) and is given by

$$\bar{J}_1(\omega_a, \omega_b) = -\varepsilon \alpha(\omega_b - \omega_a)\bar{\Phi}(\omega_a, \omega_b, \omega_b - \omega_a).$$

To understand how this operator transforms a given input state, let us first introduce the Schmidt decomposition of the function $\bar{J}_1$

$$-\bar{J}_1(\omega_a, \omega_b) = \sum_\theta \frac{r_\theta(\varepsilon)}{2\pi} k_\theta^*(\omega_a) l_\theta(\omega_b), \;\; r_\theta(\varepsilon) = \varepsilon \tilde{r}_\theta, \tag{6.5}$$

where the Schmidt functions $k_\theta(\omega)$ ($l_\theta(\omega)$) are assumed to form a complete and orthonormal set, and the positive quantities $r_\theta(\varepsilon) = \varepsilon\tilde{r}_\theta$ are the Schmidt numbers of the function $\bar{J}_1$. In Eq. (6.5) we have explicitly used the fact that ε is only a *multiplicative constant* in this approximation of the JCA; accordingly, the Schmidt numbers are *linear functions* of this quantity and the Schmidt functions are *independent* of it. Because of the

orthonormality of the functions $k_\theta(\omega)$ and $l_\theta(\omega)$, we can write

$$\hat{\mathcal{U}}_1 = e^{i\sum_\theta r_\theta(\varepsilon)(\hat{\mathcal{A}}_\theta\hat{\mathcal{B}}_\theta^\dagger+\text{H.c.})} = \bigotimes_\theta e^{ir_\theta(\varepsilon)(\hat{\mathcal{A}}_\theta\hat{\mathcal{B}}_\theta^\dagger+\text{H.c.})}, \tag{6.6}$$

$$\hat{\mathcal{A}}_\theta = \int d\omega_a k_\theta^*(\omega_a)\hat{a}(\omega_a),\ \hat{\mathcal{B}}_\theta = \int d\omega_b l_\theta^*(\omega_b)\hat{b}(\omega_b), \tag{6.7}$$

where we introduced broadband Schmidt operators $\hat{\mathcal{A}}_\theta$ and $\hat{\mathcal{B}}_\theta$ for fields a and b. These operators transform in the expected way under $\hat{\mathcal{U}}_1$; for example,

$$\hat{\mathcal{U}}_1\hat{\mathcal{A}}_\theta\hat{\mathcal{U}}_1^\dagger = \cos(r_\theta(\varepsilon))\hat{\mathcal{A}}_\theta - i\sin(r_\theta(\varepsilon))\hat{\mathcal{B}}_\theta. \tag{6.8}$$

Let us consider how the unitary in Eq. (6.4a) transforms a single photon of the form,

$$|1_{g(\omega_a)}\rangle = \int d\omega_a g(\omega_a)\hat{a}^\dagger(\omega_a)\,|\text{vac}\rangle \tag{6.9a}$$

$$= \sum_\theta \left(\int d\omega_a k_\theta^*(\omega_a)g(\omega_a)\right)\hat{\mathcal{A}}_\theta^\dagger\,|\text{vac}\rangle\,. \tag{6.9b}$$

The amplitude g is assumed to be normalized according to $\int d\omega|g(\omega)|^2 = 1$, and in the last equation we used the completeness of the set $\{k_\theta(\omega_a)\}$. We can now use Eq. (6.8) and Eq. (6.9b) to study the effect of the unitary on the single photon state Eq. (6.9a),

$$\hat{\mathcal{U}}_1\,|1_{g(\omega_a)}\rangle = \sum_\theta \left(\int d\omega_a k_\theta^*(\omega_a)g(\omega_a)\right)\left(\cos(r_\theta(\varepsilon))\hat{\mathcal{A}}_\theta^\dagger + i\sin(r_\theta(\varepsilon))\hat{\mathcal{B}}_\theta^\dagger\right)|\text{vac}\rangle\,. \tag{6.10}$$

In particular, if a single photon with frequency profile $k_{\theta'}(\omega_a)$ is initially prepared, it will be upconverted to a photon with profile $l_{\theta'}(\omega_b)$ with probability amplitude $i\sin(\varepsilon r_{\theta'})$. One very interesting case of the last equation is when the JCA is separable $\bar{J}_1(\omega_a,\omega_b) = \varepsilon r_0 k_0(\omega_a)l_0^*(\omega_b)$ and thus has only one nonzero Schmidt number in Eq. (6.5). Then one can selectively upconvert only Schmidt function 0 and leave the rest unchanged; this is precisely the ideal operation of a quantum pulse gate (QPG) as introduced by Eckstein *et al.* [21].

6.3 Time ordering in Frequency Conversion

Let us now investigate the correct unitary evolution operator associated with Eq. (6.1). The $\hat{\mathcal{U}}_1$ in Eq. (6.4a) is not the correct unitary operator since $[\hat{H}_I(t), \hat{H}_I(t')] \neq 0$, and thus Eq. (6.4a) should be premultiplied by the time-ordering operator $\mathcal{T}$. In chapter 4

we have shown that the ME provides a particularly appealing way of approximating the time evolution operator for time-dependent quadratic Hamiltonians [84] like the one in Eq. (6.1). Using the ME, the correct unitary time evolution operator is [84, 97, 98]

$$\hat{\mathcal{U}}_{\mathrm{FC}} = \mathcal{T} e^{-\frac{i}{\hbar}\int_{-\infty}^{\infty} dt \hat{H}_I(t)} = e^{\hat{\Omega}_1 + \hat{\Omega}_2 + \hat{\Omega}_3 + \cdots}. \tag{6.11}$$

In the last equation, the odd order terms are beam-splitter-like operators

$$\hat{\Omega}_{2n+1} = -2\pi i \int d\omega_a d\omega_b \big(\bar{J}_{2n+1}(\omega_a, \omega_b) \hat{a}(\omega_a) \hat{b}^\dagger(\omega_b) + \mathrm{H.c.} \big), \tag{6.12}$$

and the even order terms are rotation-like operators

$$\hat{\Omega}_{2n} = -2\pi i \sum_{c=a,b} \int d\omega_c d\omega_c' \bar{G}^c_{2n}(\omega_c, \omega_c') \hat{c}^\dagger(\omega_c) \hat{c}(\omega_c'). \tag{6.13}$$

As explained in Chapter 4 the functions $\bar{J}_{2n+1}, \bar{G}_{2n}$ can be reduced to quadratures of the pump and PMFs.

One can break the RHS of Eq. (6.11) into a unitary involving only beam-splitter terms and one involving only rotation terms $\hat{\mathcal{U}}_{\mathrm{FC}} = \hat{\mathcal{U}}_{\mathrm{RA}} \hat{\mathcal{U}}_{\mathrm{RB}} \hat{\mathcal{U}}_{\mathrm{BS}}$ where $\hat{\mathcal{U}}_{\mathrm{RA}}$ and $\hat{\mathcal{U}}_{\mathrm{RB}}$ are generated by operators such as Eq. (6.13) and $\hat{\mathcal{U}}_{\mathrm{BS}}$ is generated by operators such as Eq. (6.12). The lowest order example of this factorization is obtained by using the Baker-Campbell-Hausdorff formula

$$\hat{\mathcal{U}}_{\mathrm{FC}} = \left(\hat{\mathcal{U}}_{\mathrm{RA}} \hat{\mathcal{U}}_{\mathrm{RB}} \right) \left(\hat{\mathcal{U}}_{\mathrm{BS}} \right) \approx e^{\hat{\Omega}_2} \, e^{\hat{\Omega}_1 + \hat{\Omega}_3 + \frac{[\hat{\Omega}_1, \hat{\Omega}_2]}{2}}, \tag{6.14}$$

where

$$\frac{[\hat{\Omega}_1, \hat{\Omega}_2]}{2} = (2\pi) \int d\omega_a d\omega_b (\bar{K}_3(\omega_a, \omega_b) \hat{a}(\omega_a) \hat{b}^\dagger(\omega_b) - \mathrm{H.c.}), \tag{6.15}$$

$$\bar{K}_3(\omega_a, \omega_b) = \pi \int d\omega \big(\bar{J}_1(\omega_a, \omega) \bar{G}^b_2(\omega_b, \omega) - \bar{G}^a_2(\omega, \omega_a) \bar{J}_1(\omega, \omega_b) \big). \tag{6.16}$$

The factorization Eq. (6.14) is useful because we can write the unitary for FC as an entangling operation for fields $\hat{a}$ and $\hat{b}$ postmultiplied by local unitaries. These local unitaries cannot alter the entanglement between a and b, and because they involve rotation operators of the form given in Eq. (6.13), they cannot change the total number of photons in fields a and b. Thus the unitary $\hat{\mathcal{U}}_{\mathrm{BS}}$ contains all the information necessary

to calculate the probability of upconversion. The JCA associated with $\hat{\mathcal{U}}_{\rm BS}$ is now

$$\bar{J} = \underbrace{\bar{J}_1}_{\propto\varepsilon} + \underbrace{\bar{J}_3 + i\bar{K}_3}_{\propto\varepsilon^3} + \dots \tag{6.17}$$

We can introduce the Schmidt decomposition of $\bar{J}$ just as was done in Eq. (6.5), except that now the Schmidt numbers are not linear functions of ε, and the Schmidt functions now depend on ε; thus we must replace

$$k_\theta(\omega_a) \to k_\theta(\omega_a;\varepsilon), \quad l_\theta(\omega_b) \to l_\theta(\omega_b;\varepsilon), \tag{6.18a}$$

$$\hat{\mathcal{A}}_\theta \to \hat{\mathcal{A}}_\theta(\varepsilon), \quad \hat{\mathcal{B}}_\theta \to \hat{\mathcal{B}}_\theta(\varepsilon), \tag{6.18b}$$

in Eq. (6.6). Note that Eqs. (6.6,6.9a,6.10) will still hold after the rules Eq. (6.18) are applied. In principle 100% efficiency FC could be achieved were $r_i(\varepsilon) = \pi/2$ for some i and ε and the single photon $\hat{\mathcal{A}}_i^\dagger(\varepsilon)\left|\text{vac}\right\rangle = \int d\omega_a k_\theta(\omega_a;\varepsilon)\hat{a}^\dagger(\omega_a)\left|\text{vac}\right\rangle$ sent to the frequency converter. Of course, this could be hard to attain experimentally, since time-ordering corrections make the JCA a complicated function of ω_a and ω_b, and certainly introduce an imaginary component (see Eq. (6.17)); thus the $k_\theta(\omega_a;\varepsilon)$ can become complicated as well.

Another way of achieving highly efficient FC is by eliminating the time-ordering corrections. To this end note that the $n^{\rm th}$ Magnus term $\hat{\Omega}_n$ scales with ε^n. Now let us imagine that instead of sending our single photon once through an FC device together with a pump pulse of energy U_0, the effect of which is characterized by $\hat{\mathcal{U}}_{\rm FC}(\varepsilon)$, we send it sequentially through N copies of the original FC device, each with the same pump pulse shape but with pump energy U_0/N^2 (equivalently scaling ε by $1/N$). Then the time evolution operator is

$$(\hat{\mathcal{U}}_{\rm FC}(\varepsilon/N))^N = e^{\hat{\Omega}_1 + \hat{\Omega}_2/N + \hat{\Omega}_3/N^2 + \dots}; \tag{6.19}$$

thus by having more than one FC device the time-ordering corrections can be reduced. This observation neatly explains the results of Reddy *et al.* [23], where highly efficient-mode selective FC is achieved using cascaded nonlinear crystals. Note that this scheme does not assume anything about the nature of the time-ordering corrections except their scaling; thus this method should also allow to attenuate time-ordering corrections in SPDC. One complication with this scheme is the fact that it requires multiple FC devices, which typically will imply stabilizing and controlling more complex interferometers.

6.4 Achieving near unit efficiency in Frequency Conversion

Let us now consider the possibility of achieving near unit efficiency FC by harnessing the up to now undesirable time-ordering corrections. That is, can we turn a bug into a feature? We begin by considering for simplicity that the JCA is separable and Gaussian if time-ordering corrections are ignored. This can be achieved by engineering a Gaussian PMF [83]. Gaussian functions can also be used as a simple approximation to the more common sinc function one would encounter for a uniform nonlinearity in over a region of length L. One can match the FWHM of $e^{-\gamma x^2}$ to the FWHM of $\mathrm{sinc}(x)$ by setting $\gamma \approx 0.193$ (see Fig. 5.1). Assuming a Gaussian PMF, we expand the phase mismatch around the central frequencies of the fields involved to get

$$\bar{\Phi}(\omega_a, \omega_b, \omega_p) = e^{-(s_b\delta\omega_b - s_a\delta\omega_a - s_p\delta\omega_p)^2}, \tag{6.20}$$

where $s_i = \sqrt{\gamma}L/(2v_i)$, $\frac{1}{v_i} = \frac{dk_i(\omega_i)}{d\omega_i}|_{\omega_i=\bar{\omega}_i}$ is the inverse group velocity of the i^{th} field, and we have assumed that group velocity dispersion is negligible. Under these approximations, ignoring time-ordering corrections the JCA is

$$\begin{aligned} &\bar{J}_1(\omega_a, \omega_b) = -\varepsilon\tau\ e^{2\mu^2\delta\omega_a\delta\omega_b - \mu_a^2\delta\omega_a^2 - \mu_b^2\delta\omega_b^2}/\sqrt{\pi}, \\ &\mu^2 = \tau^2 + (s_p - s_a)(s_p - s_b),\ \mu_{a,b}^2 = \tau^2 + (s_p - s_{a,b})^2. \end{aligned} \tag{6.21}$$

The necessary and sufficient condition for a separable Gaussian $\bar{J}_1$ is $\mu = 0$. This will give an ideal QPG,

$$\begin{aligned} &\hat{\mathcal{U}}_1 = e^{i\int d\alpha d\beta\left(\tilde{r}_0\varepsilon f(\alpha)f(\beta)\hat{a}(\alpha)\hat{b}^\dagger(\beta) + \text{H.c.}\right)}, \\ &\tilde{r}_0 = \frac{\sqrt{2}\pi\tau}{\sqrt{\mu_a\mu_b}},\ \alpha = \mu_a\delta\omega_a,\ \beta = \mu_b\delta\omega_b,\ f(x) = \frac{e^{-x^2}}{\sqrt[4]{\pi/2}}, \end{aligned} \tag{6.22}$$

for the photon $|1_{f(\alpha)}\rangle = \hat{\mathcal{A}}_0^\dagger|\text{vac}\rangle = \int d\alpha f(\alpha)\hat{a}^\dagger(\alpha)|\text{vac}\rangle$, mapping it to the photon $|1_{f(\beta)}\rangle = \hat{\mathcal{B}}_0^\dagger|\text{vac}\rangle = \int d\beta f(\beta)\hat{b}^\dagger(\beta)|\text{vac}\rangle$. In Eq. (6.22) we have used the fact that the Schmidt functions of Eq. (6.21) with $\mu = 0$ are

$$k_0(\omega_a) = \sqrt{\mu_a}f^*(\alpha) \text{ and } l_0(\omega_b) = \sqrt{\mu_b}f(\beta). \tag{6.23}$$

As soon as one starts to approach a FC efficiency near unity, one needs to include the time-ordering corrections. The unitary connecting inputs and outputs is given by Eq.

(6.14). The efficiency of the conversion is now solely governed by the $\hat{\mathcal{U}}_{\rm BS}$ term in Eq. (6.14), and the associated JCA in Eq. (6.17). The amplitudes in Eq. (6.17) can be related to the terms of the time-ordering corrections for Parametric Down-Conversion (PDC) via (see chapter 4 and [99])

$$\bar{J}_1(\delta\omega_a, \delta\omega_b) = J_1(-\delta\omega_a, \delta\omega_b), \tag{6.24a}$$

$$\bar{G}_2^c(\delta\omega_c, \delta\omega_c') = G_2^c(\delta\omega_c, \delta\omega_c'),\ c = a, b, \tag{6.24b}$$

$$\bar{J}_3(\delta\omega_a, \delta\omega_b) = -J_3(\delta\omega_a, -\delta\omega_b), \tag{6.24c}$$

$$\bar{K}_3(\delta\omega_a, \delta\omega_b) = K_3(-\delta\omega_a, \delta\omega_b), \tag{6.24d}$$

where the unbarred quantities refer to the time-ordering corrections for PDC calculated in Sec. 5.3. These relations hold true under the assumption that the phase matching function is an even function of the phase mismatch and that the pump function satisfies $\alpha(\delta\omega_p) = \alpha(-\delta\omega_p)$. Note that all the bounds obtained for time-ordering corrections derived in Sec. 5.3 will immediately apply to FC.

Note that the time-ordering corrections will typically generate more Schmidt functions; even if $\bar{J}_1$ is separable, $\bar{J}$ in Eq. (6.17) will not be for $\varepsilon \not\leq 1$. For the very simple Gaussian PMF, and assuming $\mu = 0$, it turns out that the Schmidt functions of the time ordered corrected JCA, $\bar{J}$ in Eq. (6.17), are only functions of $\tilde{r}_0\varepsilon$. This happens in complete analogy to how the quantity $\tilde{s}_0\varepsilon$ completely determines the squeezing parameters including time-ordering corrections in Sec. 5.6.

The quantity $\tilde{r}_0\varepsilon$ is the Schmidt number of the Schmidt function of interest in the $\varepsilon \ll 1$ limit (see Eq. (6.5)). Also note that $\tilde{r}_0$ parametrizes the departure of the separable $\bar{J}_1$ from a circle. For a perfectly round JCA it takes the maximum value $\tilde{r}_0 = \pi$.

Now let us consider what would happen if a single photon with fixed Gaussian profile $\hat{\mathcal{A}}_0^\dagger |\text{vac}\rangle$ were sent to the FC device. We look at the probability of upconversion as a function of $\tilde{r}_0\varepsilon$, and plot this probability, including and excluding time-ordering corrections, in Fig. 6.1.A. If time-ordering corrections could be eliminated (for instance following the approach of Reddy *et al.* [23]), we would get $p_b = \sin^2(\tilde{r}_0\varepsilon)$; instead, we get a more complicated curve. The upconversion curve attains a maximum near the ideal $\tilde{r}_0\varepsilon \approx \pi/2$ but only reaches $\sim 80\%$, a value consistent with experiments [100]. The reason for this is easy to understand if we look at Fig. 6.1.B, where we plot the Schmidt numbers and the overlap of the Schmidt functions with the single photon profile $f(\alpha)$. We see that up to $\tilde{r}_0\varepsilon \leq 1.47 \sim \pi/2$, the Schmidt numbers are not significantly modified by the time-ordering corrections. Yet, as can be seen in Fig. 6.1.C, 6.1.D, the Schmidt functions are significantly modified at this point, and thus do not completely overlap with the shape

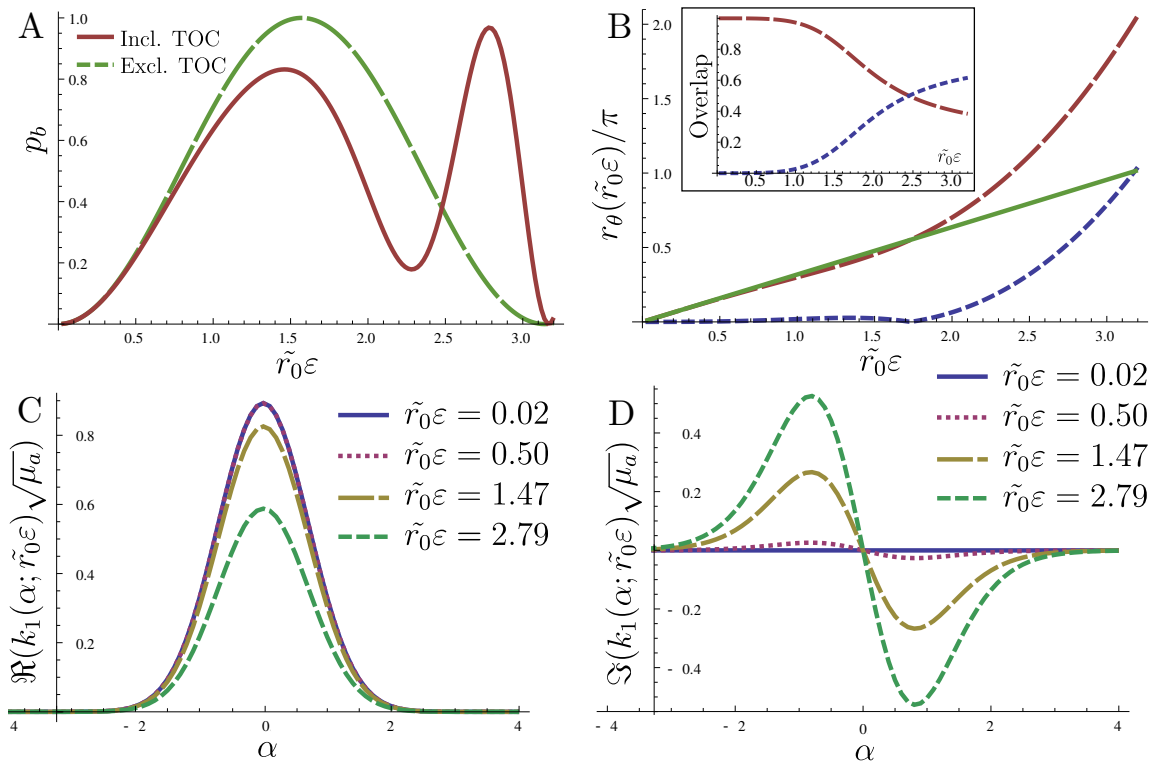

Figure 6.1: In A we plot the probability of upconversion as a function of the interaction strength $\tilde{r}_0\varepsilon$, for a single photon in the Gaussian wave packet $f(\alpha)$ including and excluding time-ordering corrections. In B we plot the Schmidt numbers of $\bar{J}$ including (dashed lines) and excluding (full line) time-ordering corrections. In the inset we plot the overlap between the time ordered corrected Schmidt functions and the Gaussian profile of the incoming single photon. Finally in C and D we plot the real and imaginary parts of the Schmidt functions for different values of $\tilde{r}_0\varepsilon$. For $\tilde{r}_0\varepsilon = 0.02, 0.5 \ll 1$ they are very similar to the Gaussian shape of the input single photon.

of the incoming single photon; see inset of Fig. 6.1.B, where we plot the overlap of the Gaussian wave packet with the two Schmidt functions. As we increase $\tilde{r}_0\varepsilon$ further, the probability of upconversion oscillates faster; this is just a reflection of the fact that past $\tilde{r}_0\varepsilon = \pi/2$ the Schmidt numbers *are* modified by the time-ordering corrections and grow much faster than linearly, as seen in Fig. 6.1.B. This feature could be used as direct experimental evidence of the contribution of the time-ordering corrections to the JCA in FC. The final, most interesting feature of Fig. 6.1.A is that the probability reaches unity for a value near $\tilde{r}_0\varepsilon$ near 2.79. This happens because the two non-zero Schmidt numbers of $\bar{J}$ become odd multiples of $\pi/2$ at the same time. This allows the two Schmidt functions to cooperate and attain 100% efficiency.

The results presented in this chapter give us a very simple picture of the physical mechanisms associated with time-ordering that limit the efficiency of frequency conver-

sion using sum-frequency generation. The use of the Magnus expansion to calculate the unitary evolution operator allowed us to understand what was the effect of these corrections, explain how certain protocols can overcome them, and how they can also be used to our advantage to increase conversion efficiency.

Chapter 7

Conclusions and future directions

> Let's just say we'd like to avoid any Imperial entanglements.
>
> Obi-wan Kenobi

In this thesis we have studied the quantum dynamics of photon generation and conversion. To undertake this study we have looked directly at the properties of the time-evolution operator. This approach is complementary to the approach commonly taken by the nonlinear optics community where one instead looks at the equations of motion for the relevant quantum (or classical) field operators. We believe that the approach in this thesis is very suitable for the study of quantum information applications of nonlinear optics since the description of the transformation of states is written precisely in the language of this discipline. The formalism developed here becomes especially useful when one is interested in understanding, manipulating, minimizing and profiting from the time-ordering corrections (TOCs) associated with time dependent Hamiltonians.
To understand the nature of the TOCs in a very general setting, in Chapter 4 we have used the Magnus expansion to construct solutions to the time-dependent Schrödinger equation describing several nonlinear processes governed by quadratic bosonic Hamiltonians that do not commute at different times: spontaneous parametric down-conversion, spontaneous four wave mixing, and frequency conversion. In the derivation of the Magnus terms for these three processes we found a rather simple form for the second and third order Magnus terms for a broad class of Hamiltonians. The Magnus expansion solution that we found for the time evolution operator was shown to be Gaussian preserving; equivalently, when the unitary operator is used to transform input and output bosonic operators the transformation is Bogoliubov linear. With the expansion we developed, it was easy to explain why the second order effect due to the time ordering in SPDC vanishes: Essentially the second order process needs to be stimulated by a previous photon.

We also showed how to calculate corrections to the Joint Spectral Amplitude (JSA) of the photons in SPDC and SFWM and to the Joint Conversion Amplitude (JCA) in FC, and how even when the phase matching function and pump functions are real the JSA or JCA acquires a non-trivial phase structure due to time ordering; this structure can be investigated via tomographic methods. We also explored how the effect of time ordering acts in stimulated PDC; in particular, we looked at the case when the lower energy photons are prepared in coherent states and showed that the first correction due to time ordering is to modify their spectral structure. The Magnus expansion also allowed us to argue that time ordering is irrelevant if the phase matching function is infinitely broad. With the very general results from the preceding chapter, in Chapter 5 we presented a theory that allows us to understand the effects of time ordering in photon generation processes. We introduced a figure of merit quantifying the effects of time ordering, and it was shown that these effects are only sizable whenever the photons in the down-converted/frequency converted modes copropagate with the pump photons. This agrees with the simple physical intuition that the only way the effect of the Hamiltonian at some posterior time $\hat{H}(t_f)$ can be influenced by the former version of itself $\hat{H}(t_i)$, under the assumption of an undepleted pump, is if the fields associated with the pump photons, any seed photons, and the generated photons spend a significant amount of time in the same regions of space. Under these conditions the time-ordering corrections will also have the most significant qualitative effect, since they will modify the Schmidt number of the quantum correlated photons from the uncorrected value of close to unity. We have used Gaussian functions to approximately describe both the pump pulse and the phase-matching functions that enter the description of the photon generation or conversion. This led to the possibility of constructing analytic expressions for the figures of merit. Nonetheless, the general approach of the Magnus expansion described earlier could be applied to the use of arbitrary functions to model the pump pulse and phase matching. A general result of our investigations here, that strong pump pulses are required for any deviation from the first order Magnus term to be relevant, can be expected to hold more generally. There is thus a wide range of problems where an elementary first order perturbative approach would fail, but a calculation using the first order Magnus term would be sufficient. Yet working at pump intensities high enough that time-ordering corrections appear should lead to new strategies for producing novel quantum states.

In addition to clarifying the physical regimes in which the time-ordering corrections are expected to be relevant we also proposed relevant observables that can be used to witness the contribution of the corrections to the joint spectral amplitude of the generated photons. Finally, in Chapter 5 we also studied how using inefficient detectors one can

probabilistically generate heralded Fock states with many quanta.

In Chapter 6 we have studied the effects of the time-ordering corrections on frequency conversion. We have considered conversion using a χ_2 material and, with correspondences presented in Chapter 3, this can be generalized to the use of χ_3 materials as well. We have shown how the time-ordering corrections modify the ideal operation of a quantum pulse gate and how they can be used to achieve near unity FC using the extra Schmidt functions that are generated by them. Finally, we provided a simple scaling argument that explains the results of Reddy *et al.* [23], in which time-ordering corrections are attenuated by using cascaded FC devices and argued that the same ideas could be used to attenuate time-ordering corrections in photon generation.

The results presented in this thesis allow us to present a simple tool-kit that an experimentalist or a theorist can easily use to assess whether time ordering effects will have any role in their experiment or calculation. First one needs to use the results in Eqs. (3.29) and (3.42) to estimate the value of the dimensionless constants ε or $\tilde{\varepsilon}$ characterizing the strength of the χ_2 or χ_3 process. If this constant is very small, one can ignore time-ordering effects and simply use the first order Magnus term. If they are bigger or close to one, then one can either use the simple analytical bounds summarized in Eq. (5.18) or perform a full numerical calculation of the JSA or JCA using the Magnus library documented in Appendix C. Even though the bounds and the numerical library are presented/documented in terms of photon generation, they can easily be mapped to results for frequency conversion using the equivalences in Eq. (6.24). Finally, the results presented in Figs. 5.6, 5.7, 5.8, 5.9 allow us to evaluate the quality of the Fock states generated by heralding using an imperfect photon-number-resolving detector.

In chapters 4,5 and 6 we showed that there is a very strong parallel between the results of photon generation and photon conversion. This parallel became evident once we used the Magnus expansion to explore the contributions of the time-ordering corrections to the unitary evolution. This parallel would have been extremely hard to unravel using the more commonly used Dyson series. Nonlinear quantum optics is probably not the only area of physics that would benefit from using improved expansions for time-dependent problems. In particular one can show that results related to time averaged dynamics can be understood through the lens of the Magnus expansion and that the effective Hamiltonian discussed in *e.g.* [101] is nothing but the second order Magnus term[102]. Another field where the Magnus expansion could be employed is relativistic quantum information. A typical problem in this field is to study the properties of detectors in different space-time regions that interact with quantum fields[103]. These interactions are typically time-dependent and thus the Magnus expansion should provide a useful method

to evaluate the effects of the fields on the detectors and vice-versa especially in the case when one can model the detectors as harmonic oscillators.

Finally, we should mention that there are of course very interesting questions not addressed with the formalism presented in this thesis, and also questions for which this formalism will probably be insufficient. Chief among the former set, is the inverse problem; that is, given a target time-ordering corrected JSA or JCA what type of pump pulse or phase-matching functions should be engineered to obtain such JSA or JCA. In the latter set is the question of a full quantum mechanical treatment of the nonlinear problem. Even though the dynamics studied here was termed "very" nonlinear (in the sense that the shape of the Schmidt modes in photon generation or conversion is modified significantly by the time-ordering corrections) it is still linear in the quantum operators considered. This linearity is a result of the fact that we are treating the pump field as a classical entity; this approximation is warranted by the experimental conditions in which these questions are investigated. A very interesting question that will soon become relevant for experimentalist and theorists studying microwave photons in superconducting waveguides is how to describe this dynamics when all three (or more) fields involved in the nonlinear interaction must be treated quantum mechanically.

Appendix A

Energy in an Electromagnetic pulse

In this appendix we construct an estimate of the energy of an electromagnetic pulse propagating in vacuum. Since our purpose here is not to give a precise calculation for any particular system, but rather to identify the characteristic size and form of the terms needed in our calculations, we simply approximate the relevant field at each frequency in the linear regime as if it consisted of an area A "cut out" of a linearly polarized plane wave propagating in a direction perpendicular to the plane of the area; this can be taken as a "toy model" of a waveguide mode.

To construct our "toy model" we start with a solution to Maxwell's equations in a medium with index of refraction $n(\omega)$

$$\vec{E}(z,t) = \left(\vec{x}E_0 e^{i(kz-\omega t)}\right) + \text{c.c.}, \tag{A.1}$$

$$\vec{B}(z,t) = \left(\vec{y}B_0 e^{i(kz-\omega t)}\right) + \text{c.c.}, \tag{A.2}$$

with $E_0/B_0 = c/n(\omega)$ and $k = k(\omega)$. To construct pulses we take superpositions,

$$\vec{E}(z,t) = \vec{x}\int_0^\infty d\omega E_0(\omega) e^{i(kz-\omega t)} + \text{c.c.}, \tag{A.3}$$

$$\vec{B}(z,t) = \vec{y}\int_0^\infty d\omega B_0(\omega) e^{i(kz-\omega t)} + \text{c.c.}$$

In what follows we will assume that the amplitude functions $E(\omega)$ and $B(\omega)$ are very narrowly peaked around some central frequency $\bar{\omega}$ and thus over the relevant integration range to good approximation we can write $E(\omega) = E_0 f(\omega)$ and $B(\omega) = B_0 f(\omega)$, where $E_0/B_0 = c/n(\bar{\omega})$, taking $f(\omega)$ to vanish for $\omega < 0$. With this in mind, in a non-magnetic

medium the Poynting vector is

$$\begin{aligned}\vec{S}(z,t) &= \frac{\vec{E}(z,t)\times\vec{B}(z,t)}{\mu_0} && \text{(A.4)}\\ &= \vec{z}\frac{E_0B_0}{\mu_0}\int_0^\infty d\omega d\omega' \times && \text{(A.5)}\\ &\quad \Big(f(\omega)f(\omega')e^{i(k(\omega)+k(\omega'))z-(\omega+\omega')t}+f(\omega)f^*(\omega')e^{i(k(\omega)-k(\omega'))z-(\omega-\omega')t}\Big)+\text{c.c.}\end{aligned}$$

Writing a directed element of area $d\vec{A}$ as $\vec{z}dA$, from Poynting's theorem the energy carried in the pulse over an area A is then given by

$$\begin{aligned}U_0 &= \int_{-\infty}^{\infty}dt\int_A d\vec{A}\cdot\vec{S}(z,t) && \text{(A.6)}\\ &= \frac{2\pi AE_0B_0}{\mu_0}\int_0^\infty d\omega\Big(f(\omega)f(-\omega)e^{i(k(\omega)+k(-\omega))z}|f(\omega)|^2+\text{c.c.}\Big). && \text{(A.7)}\end{aligned}$$

The first term is identically zero since $f(\omega)=0$ if $\omega<0$; if we then, for example, approximate $f(\omega)$ for $\omega>0$ by

$$f(\omega)=\frac{1}{\sqrt{2\pi}\sigma}\zeta(\omega-\bar{\omega}),\quad \zeta(\omega)=\exp(-\omega^2/(2\sigma^2)),$$

and take

$$k(\omega)=k(\bar{\omega})+(\omega-\bar{\omega})/v_g, \tag{A.8}$$

with v_g the group velocity at frequency $\bar{\omega}$, we have

$$\begin{aligned}\vec{E}(z,t) &= 2\vec{x}E_0e^{-\frac{1}{2}\sigma^2(t-z/v_g)^2}\cos(k(\bar{\omega})z-\bar{\omega}t), && \text{(A.9)}\\ \vec{B}(z,t) &= 2\vec{y}B_0e^{-\frac{1}{2}\sigma^2(t-z/v_g)^2}\cos(k(\bar{\omega})z-\bar{\omega}t), && \text{(A.10)}\end{aligned}$$

where we have assumed that $\bar{\omega}\gg\sigma$ and thus one can safely extend the lower integration limit in Eq. (A.3) from 0 to $-\infty$. Averaged over the period $2\pi/\bar{\omega}$, the Poynting vector following from Eq. (A.4) has a standard deviation $\sqrt{2}\sigma$, leading to a full width at half maximum (FWHM) of the intensity of the pulse given by FWHM $=2\sqrt{2\ln 2}(\sqrt{2}\sigma)$, or $\sigma=\text{FWHM}/4\sqrt{\ln 2}\approx 0.3$ FWHM. From (A6,A7), under the same approximations leading to (A10,A11) we have $U_0=2A\epsilon_0n(\bar{\omega})cE_0^2\frac{\sqrt{\pi}}{\sigma}$. This is a useful result that allows to relate the peak amplitude of the electric field E_0 to the net energy in the pulse U_0:

$$E_0=\sqrt{\frac{(U_0/\sqrt{\pi})\sigma}{2\epsilon_0n(\bar{\omega})cA}}. \tag{A.11}$$

Note that even if group dispersion were included in Eq. (A.8):

$$k(\omega) = k(\bar{\omega}) + (\omega - \bar{\omega})/v_g + \frac{1}{2}\kappa_{\bar{\omega}}(\omega - \bar{\omega})^2, \tag{A.12}$$

with $\kappa_{\bar{\omega}} = (d^2k/d\omega^2)_{\omega=\bar{\omega}}$, we would still obtain the same relation between E_0 and U_0.

Appendix B

Numerical calculation of the Schmidt decomposition

Typically the Schmidt decompositions in Eq. (2.79) and Eq. (2.84) cannot be found analytically unless one is dealing with Gaussians [85]. Yet, one can obtain excellent numerical approximations by using the matrix version of the Schmidt decomposition, the singular value decomposition (SVD). To this end let us sample the function $\mathcal{F}(x,y)$ at the $n+1 \times m+1$ points $x_i = x_0 + i\Delta x|_{i=0}^{n}$ and $y_j = y_0 + j\Delta y|_{j=0}^{m}$

$$M_{i,j} = \mathcal{F}(x_i, y_j). \tag{B.1}$$

The question is now, assuming that $\mathcal{F}(x,y) = \sum_k \lambda_k \; u_k(x) \; v_k^*(y)$ how can λ_k, u_k, v_k be approximated from the knowledge of the singular value decomposition of M,

$$M = U\mathrm{diag}(\mu_l)V^\dagger. \tag{B.2}$$

To connect the SVD of M and the Schmidt decomposition of $\mathcal{F}$ let us note first that typically $\mathcal{F}$ has units, for instance for all the functions considered previously $[\mathcal{F}(x,y)] = (xy)^{-1/2}$. From the normalization chosen for the functions u_λ and v_λ we have

$$\int dx \; u_\lambda^*(x) u_{\lambda'}(x) = \int dy \; v_\lambda^*(y) v_{\lambda'}(y) = \delta_{\lambda,\lambda'}, \tag{B.3}$$

from which we deduce that $[u(x)] = x^{-1/2}, [v(y)] = y^{-1/2}$. Simply from the definition of $M_{i,j}$ we have

$$\mathcal{F}(x_i, y_j) = M_{i,j} = \sum_l \mu_l U_{i,l} V_{j,l}^*. \tag{B.4}$$

The identification between the terms of the SVD and the Schmidt decomposition is as follows

$$\lambda_k = \mu_k \sqrt{\Delta x \Delta y}, \quad u_k(x_i) = U_{i,k}/\sqrt{\Delta x}, \quad v_k(y_j) = V_{j,k}/\sqrt{\Delta y}. \tag{B.5}$$

This will automatically yield the correct normalizations

$$\begin{aligned} \int dx(u_k^*(x)\ u_{k'}(x)) &\approx \sum_{i=0}^{N} \Delta x\, (u_k^*(x_i)\ u_{k'}(x_i)) = \sum_{i=0}^{N} \Delta x \left(\frac{U_{i,k}^*}{\sqrt{\Delta x}}\right)\left(\frac{U_{i,k'}}{\sqrt{\Delta x}}\right) \\ &= \sum_{i=0}^{N} U_{i,k}^*\ U_{i,k'} = \delta_{k,k'}. \end{aligned} \tag{B.6}$$

In the last equality we used the fact that the *columns* of U are orthogonal to each other and are normalized. One can find a similar result for v and V (again assuming that the columns of V are orthonormal).

Appendix C

The Magnus library

The Magnus library comprises two different and independent software pieces. Both of them perform numerical integration using the fantastic `Cubature` library developed by Steven G. Johnson at MIT (http://ab-initio.mit.edu/wiki/index.php/Cubature). The Magnus library is freely available at https://github.com/nquesada/magnus.

C.1 Gaussian approximation for the third order Magnus term

The first application, completely contained in the file `gauss_magnus.c`, calculates the third order Magnus correction for Gaussian phase matching and pump functions of the form given in Eq. (5.2) and Eq. (5.3). The third order Magnus term can be written as in Eq. (5.10). The functions in this equation depend on the parameters introduced in Eq. (5.14). They are all functions of the slowness of the modes s_a, s_b, s_p, the time duration of the pump τ and the interaction strength ε. In what follows we fix $\varepsilon = -1$ and use units where the pulse duration is $\tau = 1$. The library computes numerically the integral V defined in Eq. (5.10) using the `hcubature` routine from `cubature`. The user is required to provide values for 4 macros at the beginning of the file. The first three of them

```
#define MAX_EVAL_INT 10000000 //Maximum number of evaluations
#define REQ_ABS_ERROR 1e-10 //Required absolute error
#define REQ_REL_ERROR 1e-8 //Required relative error
```

give the maximum number of times the function being integrated can be evaluated, the second one is the required absolute error in the integration and the third is the required relative error. To calculate numerical integrals extending to infinity one must perform

the following changes of variables:

$$\begin{aligned}\int_{-\infty}^{\infty} dx\ f(x) &= \int_{-1}^{1} dt f\left(\frac{t}{1-t^2}\right)\frac{1+t^2}{(1-t^2)^2}, \\ \int_{0}^{\infty} dx\ f(x) &= \int_{0}^{1} f\left(\frac{t}{1-t}\right)\frac{1}{(1-t)^2}.\end{aligned} \tag{C.1}$$

We can now write V in Eq. (5.10) in following way:

$$V(\omega_a,\omega_b) = \int_0^1 dt_r \int_0^1 dt_q g\left(\omega_a,\omega_b,\frac{t_r}{1-t_r},\frac{t_q}{1-t_q}\right)\frac{1}{(1-t_r)^2}\frac{1}{(1-t_q)^2} \tag{C.2}$$

$$= \int_0^1 dt_r \int_0^1 dt_q \tilde{g}(\omega_a,\omega_b,t_r,t_q), \tag{C.3}$$

$$g(\omega_a,\omega_b,r,q) = \exp\left(-(r,q)\mathbf{M}(r,q)^T\right)\cos\left(4\tau\eta_{ab}(\omega_a q+\omega_b r)/\sqrt{3}\right), \tag{C.4}$$

where $\mathbf{M}$ is defined in Eq. (5.14). With this definitions we now list the different functions in `gauss_magnus.c` where the arguments of the function have the following meaning: `int gaussianarg(unsigned ndim, const double *x, void *fdata, unsigned fdim, double *fval)` calculates precisely $\tilde{g}(\omega_a,\omega_b,t_r,t_q)$:

- `unsigned ndim` should be set to 2, since we are dealing with two dimensional integrals.
- `const double *x` is a two dimensional array containing the values of the variables being integrated, `x[0]`$= t_r$, `x[1]`$= t_q$.
- `void *fdata` is a two dimensional array containing the values of the other variables, `fdata[0]`$= \omega_a$, `fdata[1]`$= \omega_b$.
- `unsigned fdim` should be set to 1 since we are integrating a scalar function.
- `double *fval` is a one dimensional array, `fval[0]`$= \tilde{g}(\omega_a,\omega_b,t_r,t_q)$.

The next function in `gauss_magnus.c`, is `int gaussianval(double fdata[2], double *res)`, it uses `gaussianarg` and `cubature` to calculate the integral Eq. (C.2). Its arguments are:

- `double fdata[2]` is a two dimensional array containing the values of the other variables, `fdata[0]`$= \omega_a$, `fdata[1]`$= \omega_b$.
- `double *res` contains the values of the integral in `res[0]` and the estimated error `res[1]`.

Finally the function `double J3(double wa,double wb)` calculates J_3 as given in Eq. 5.10. It first calculates the analytical bound

$$|J_3(\omega_a,\omega_b)| \;\leq\; \frac{2\pi^{3/2}\varepsilon^3\tau^3}{3R^2}\left(\exp\left(-\mathbf{u}\mathbf{Q}\mathbf{u}^T/R^4\right)+2\exp\left(-\mathbf{u}\mathbf{N}\mathbf{u}^T/3\right)\right). \qquad \text{(C.5)}$$

If this bound is less than the macro `eps` the integral is approximated to 0. If it is bigger than 0 then it is calculated using `gaussianval` and combined with W and Z to give J_3. To test the correctness of the calculation one can check the results for the following set of numerical values

$$s_c=0,\quad s_a=1,\quad s_b=-1,\quad J_3(0,0)=0.19635,\quad J_3(1,1)=-0.0530724. \qquad \text{(C.6)}$$

C.2 General calculation of the Second and Third order Magnus terms

This routines calculate numerically the second and third order Magnus terms for the Hamiltonian in Eq. (4.19) using the function F defined in Eq. (4.25). We use the convention $\int \equiv \int_{-\infty}^{\infty}$. The Magnus correction terms can be written in terms of the functions G_2, H_2, J_3, K_3 introduced in Eqs. (4.32a,4.37,4.66). The first Magnus term is given by $J_1(\omega_a,\omega_b) = F(\omega_a,\omega_b,\omega_a+\omega_b)$. In what follows it is assumed that $F^* = F$. Note that any principal value integral can be written as:

$$⨍\frac{dx}{x}f(x) = \int_0^\infty \frac{dx}{x}(f(x)-f(-x)). \qquad \text{(C.7)}$$

To calculate the Magnus correction three different files are provided. The first one `functionF.c` provides the function $F(\omega_a,\omega_b,\omega_p)$. The evaluation of F should be as efficient as possible since this function will be called many times during the calculation of any Magnus term. In the file `magnus.c` functions that calculate the integrands associated with each magnus term are provided. They nevertheless evaluate the functions in the transformed variables according to Eq. (C.1) and Eq. (C.7).
The functions `int magnus`Nx`(unsigned ndim, const double *x, void *fdata, unsigned fdim, double *fval)` take the same arguments

- `unsigned ndim` the number of dimensions that need to be integrated.
- `const double *x` the values of dummy integration variables.
- `void *fdata` the variables of the actual arguments of the Magnus functions.

- `unsigned fdim` is al always equal to one since the functions being integrated are scalar.
- `double *fval` is where the value of the integrand is returned.

A simple example clarifies the notation. Let us look at

$$G_2(\omega_a,\omega_a') = \int d\omega_d \fint \frac{d\omega_p}{\omega_p} F\left(\omega_a,\omega_d,\omega_a+\omega_p+\omega_d\right) f^*\left(\omega_a',\omega_d,\omega_a'+\omega_p+\omega_d\right) \tag{C.8}$$

$$= \int_{-\infty}^{\infty} d\omega_d \int_0^{\infty} d\omega_p \frac{1}{\omega_p}\Big(F\left(\omega_a,\omega_d,\omega_a+\omega_p+\omega_d\right) F^*\left(\omega_a',\omega_d,\omega_a'+\omega_p+\omega_d\right) - F\left(\omega_a,\omega_d,\omega_a-\omega_p+\omega_d\right) F^*\left(\omega_a',\omega_d,\omega_a'-\omega_p+\omega_d\right)\Big). \tag{C.9}$$

In the last equation identity Eq. (C.7) was used. To perform the integral we need to switch variables again using Eq. (C.1), $\omega_d = t_d/(1-t_d)$, $\omega_p = t_p/(1-t_p^2)$ to obtain:

$$G_2(\omega_a,\omega_a') = \int_0^1 dt_d \int_{-1}^1 dt_p \left\{ \frac{1}{(1-t_d)^2}\frac{1+t_p^2}{(1-t_p^2)^2}\right\} \frac{1}{\frac{t_p}{1-t_p^2}} \times \tag{C.10}$$

$$\left(F\left(\omega_a, \frac{t_d}{1-t_d}, \omega_a+\frac{t_d}{1-t_d}+\frac{t_p}{1-t_p^2}\right) F^*\left(\omega_a', \frac{t_d}{1-t_d}, \omega_a'+\frac{t_d}{1-t_d}+\frac{t_p}{1-t_p^2}\right) - F\left(\omega_a, \frac{t_d}{1-t_d}, \omega_a+\frac{t_d}{1-t_d}-\frac{t_p}{1-t_p^2}\right) F^*\left(\omega_a', \frac{t_d}{1-t_d}, \omega_a'+\frac{t_d}{1-t_d}-\frac{t_p}{1-t_p^2}\right)\right).$$

The term inside the {} is the Jacobian of the transformation. In this example then `x[0]`=t_d, `x[1]`= t_p, `fdata[0]`= ω_a, `fdata[1]`= ω_a'. Having explained the use of the function in `magnus.c` explaining `magnusint.c` is easy. Each function then calls the corresponding function in `magnus.c` and performs the integrals using `cubature`. So for instance `int magnus2aint(double wa, double waa, double *res)` calls `magnus2a` and performs the integral for the values `wa`= ω_a, `waa`= ω_a' returning the value of the integral and its error in `res[0]` and `res[1]`. One final clarification, `magnus2a` calculates G_2, `magnus2b` calculates H_2, `magnus3s` calculates the first term (the one which requires a 2 dimensional integration) that defines J_3 omitting the prefactor of $\pi^2/3$ in Eq. (4.37), `magnus3` calculates the second term in J_3 (which requires a 4 dimensional integration) and finally `magnus3w` calculates K_3 omitting the prefactor of π in Eq. (4.67).

Appendix D

Analytical calculation of the third order Magnus correction

In this Appendix we calculate the third order Magnus term $\hat{\Omega}_3$ and associated JSA contribution J_3 for the Hamiltonian considered in the main Chapter 5. Note that the second order correction $\hat{\Omega}_2$ (and associated functions G_2^a, G_2^b) and the imaginary part of the third order correction K_3 can be calculated directly from the results in Sec. 4.3. For the calculation of J_3 we will not use the results presented in Sec. 4.3. The reason is that integrals of the form $\oint \frac{dx}{x}\frac{dy}{y} f(x,y)$, which are the ones necessary to calculate the third order correction, are hard to bound and cannot be computed analytically for the situation when f is a Gaussian function. To circumvent this difficulty we assume that the Hamiltonian can be written as a function of the frequencies of the down-converted photons and time (ω_a, ω_b, t) but without any explicit dependence of the pump frequency (ω_p) which will be assumed to have been integrated out. This can be done analytically for Gaussian pump profiles and phase-matching functions, as we shall show shortly. Because the time dependence of the Hamiltonian will no longer be harmonic but Gaussian, the time order integrations will not involve any principal value integrals but rather incomplete (*i.e.* not extending over the whole real line) Gaussian integrals.

We will consider the Hamiltonian given by Eq. (5.1) with phase matching function Eq. (5.2) and pump function Eq. (5.3). We remind the reader that the detuning can be written as

$$\Delta = \omega_a + \omega_b - \omega_p = \delta\omega_a + \delta\omega_b - \delta\omega_p.$$

Given the simplicity of the pump and phase matching functions we can perform analyt-

ically the integral over ω_p

$$F(\omega_a,\omega_b,t) = -\varepsilon \int d\omega_p e^{i\Delta t}\alpha(\omega_p)\Phi(\omega_a,\omega_b,\omega_p) = \tag{D.1}$$
$$-\varepsilon\tau\sqrt{\frac{1}{s_p^2+\tau^2}}\exp\left(\frac{\left(-2s_p\left(s_a\delta\omega_a+s_b\delta\omega_b\right)+it\right)^2}{4\left(s_p^2+\tau^2\right)}+it\left(\delta\omega_a+\delta\omega_b\right)-\left(s_a\delta\omega_a+s_b\delta\omega_b\right)^2\right).$$

After the integration the Hamiltonian is now

$$\hat{H}_I(t) = \hbar\int d\omega_a d\omega_b F(\omega_a,\omega_b,t)\hat{a}^\dagger(\omega_a)\hat{b}^\dagger(\omega_b) + \text{H.c.} \tag{D.2}$$

For the third order Magnus term we get

$$\begin{aligned}
\hat{\Omega}_3 &= \frac{(-i)^3}{6\hbar^3}\int dt\int^t dt'\int^{t'} dt''\left\{\left[\hat{H}_I(t),\left[\hat{H}_I(t'),\hat{H}_I(t'')\right]\right]+\left[\left[\hat{H}_I(t),\hat{H}_I(t')\right],\hat{H}_I(t'')\right]\right\}\\
&= \frac{i}{6}\int dt\int^t dt'\int^{t'} dt''\int d\omega_o d\omega_e d\omega_o' d\omega_e' d\omega_o'' d\omega_e'' \qquad \text{(D.3)}\\
&\times\Big(\bar{\delta}\left(\omega_e''-\omega_e\right)\bar{\delta}\left(\omega_o''-\omega_o'\right)F\left(\omega_o,\omega_e,t\right)F\left(\omega_o',\omega_e',t'\right)F^*\left(\omega_o'',\omega_e'',t''\right)\hat{a}^\dagger(\omega_o)\hat{b}^\dagger(\omega_e')\\
&-2\bar{\delta}\left(\omega_e'-\omega_e\right)\bar{\delta}\left(\omega_o'-\omega_o''\right)F\left(\omega_o,\omega_e,t\right)F\left(\omega_o'',\omega_e'',t''\right)F^*\left(\omega_o',\omega_e',t'\right)\hat{a}^\dagger(\omega_o)\hat{b}^\dagger(\omega_e'')\\
&+\bar{\delta}\left(\omega_e''-\omega_e'\right)\bar{\delta}\left(\omega_o''-\omega_o\right)F\left(\omega_o,\omega_e,t\right)F\left(\omega_o',\omega_e',t'\right)F^*\left(\omega_o'',\omega_e'',t''\right)\hat{a}^\dagger(\omega_o')\hat{b}^\dagger(\omega_e)\\
&+\bar{\delta}\left(\omega_e-\omega_e'\right)\bar{\delta}\left(\omega_o-\omega_o''\right)F\left(\omega_o',\omega_e',t'\right)F\left(\omega_o'',\omega_e'',t''\right)F^*\left(\omega_o,\omega_e,t\right)\hat{a}^\dagger(\omega_o')\hat{b}^\dagger(\omega_e'')\\
&-2\bar{\delta}\left(\omega_e'-\omega_e''\right)\bar{\delta}\left(\omega_o'-\omega_o\right)F\left(\omega_o,\omega_e,t\right)F\left(\omega_o'',\omega_e'',t''\right)F^*\left(\omega_o',\omega_e',t'\right)\hat{a}^\dagger(\omega_o'')\hat{b}^\dagger(\omega_e)\\
&+\bar{\delta}\left(\omega_e-\omega_e''\right)\bar{\delta}\left(\omega_o-\omega_o'\right)F\left(\omega_o',\omega_e',t'\right)F\left(\omega_o'',\omega_e'',t''\right)F^*\left(\omega_o,\omega_e,t\right)\hat{a}^\dagger(\omega_o'')\hat{b}^\dagger(\omega_e')\Big)-\text{H.c.}
\end{aligned}$$

In the last equation we use $\bar{\delta}$ for the Dirac distribution. To simplify this expression we perform the following changes of variables in each of the six terms in the last equation

$$\begin{array}{llllll}
\omega_e\to\omega_d & \omega_e''\to\omega_d & \omega_o'\to\omega_c & \omega_o''\to\omega_c & \omega_e'\to\omega_b & \omega_o\to\omega_a\\
\omega_e\to\omega_d & \omega_e'\to\omega_d & \omega_o'\to\omega_c & \omega_o''\to\omega_c & \omega_e''\to\omega_b & \omega_o\to\omega_a\\
\omega_e'\to\omega_d & \omega_e''\to\omega_d & \omega_o\to\omega_c & \omega_o''\to\omega_c & \omega_e\to\omega_b & \omega_o'\to\omega_a\\
\omega_e\to\omega_d & \omega_e'\to\omega_d & \omega_o\to\omega_c & \omega_o''\to\omega_c & \omega_e''\to\omega_b & \omega_o'\to\omega_a\\
\omega_e'\to\omega_d & \omega_e''\to\omega_d & \omega_o\to\omega_c & \omega_o'\to\omega_c & \omega_e\to\omega_b & \omega_o''\to\omega_a\\
\omega_e\to\omega_d & \omega_e''\to\omega_d & \omega_o\to\omega_c & \omega_o'\to\omega_c & \omega_e'\to\omega_b & \omega_o''\to\omega_a,
\end{array} \tag{D.4}$$

to get

$$\hat{\Omega}_3 = \frac{i}{6}\int dt \int^t dt' \int^{t'} dt'' \int d\omega_a d\omega_b d\omega_c d\omega_d \hat{a}^\dagger(\omega_a)\hat{b}^\dagger(\omega_b)\times \tag{D.5}$$
$$\Big(F(\omega_a,\omega_d,t)\,F(\omega_c,\omega_b,t')\,F^*(\omega_c,\omega_d,t'') - 2F(\omega_a,\omega_d,t)\,F(\omega_c,\omega_b,t'')\,F^*(\omega_c,\omega_d,t')$$
$$+ F(\omega_a,\omega_d,t')\,F(\omega_c,\omega_b,t)\,F^*(\omega_c,\omega_d,t'') + F(\omega_a,\omega_d,t')\,F(\omega_c,\omega_b,t'')\,F^*(\omega_c,\omega_d,t)$$
$$- 2F(\omega_a,\omega_d,t'')\,F(\omega_c,\omega_b,t)\,F^*(\omega_c,\omega_d,t') + F(\omega_a,\omega_d,t'')\,F(\omega_c,\omega_b,t')\,F^*(\omega_c,\omega_d,t)\Big)$$
$$- \text{H.c.}.$$

We can now perform the change of variables $t = q+2r+s,\ t' = q-r+s,\ t'' = q-r-2s$ that transforms the integral according to $\int dt \int^t dt' \int^{t'} dt'' = 9\int dq \int_0^\infty dr \int_0^\infty ds$, and also use the fact that $F(\omega_a,\omega_b,-t) = F^*(\omega_a,\omega_b,t)$, where x^* denotes the complex conjugate of x, to obtain

$$\hat{\Omega}_3 = \frac{3i}{2}\int dq \int_0^\infty dr \int_0^\infty ds \int d\omega_a d\omega_b d\omega_c d\omega_d \hat{a}^\dagger(\omega_a)\hat{b}^\dagger(\omega_b)\times \tag{D.6}$$
$$\big(F(\omega_a,\omega_d,q+2r+s)\,F(\omega_c,\omega_b,q-r+s)\,F(\omega_c,\omega_d,-q+r+2s)$$
$$- 2F(\omega_a,\omega_d,q+2r+s)\,F(\omega_c,\omega_b,q-r-2s)\,F(\omega_c,\omega_d,-q+r-s)$$
$$+ F(\omega_a,\omega_d,q-r+s)\,F(\omega_c,\omega_b,q+2r+s)\,F(\omega_c,\omega_d,-q+r+2s)$$
$$+ F(\omega_a,\omega_d,q-r+s)\,F(\omega_c,\omega_b,q-r-2s)\,F(\omega_c,\omega_d,-q-2r-s)$$
$$- 2F(\omega_a,\omega_d,q-r-2s)\,F(\omega_c,\omega_b,q+2r+s)\,F(\omega_c,\omega_d,-q+r-s)$$
$$+ F(\omega_a,\omega_d,q-r-2s)\,F(\omega_c,\omega_b,q-r+s)\,F(\omega_c,\omega_d,-q-2r-s)\big) - \text{H.c.}$$

Note the following: First, r and s can always be swapped since they have the same integration ranges and second, the change $q \to -q$ can always be performed since $\int_{-\infty}^{\infty} dq f(q) = \int_{-\infty}^{\infty} dq f(-q)$. Because of this it is easily seen that in the last equation the sixth term is the complex conjugate of the first, the fifth is the complex conjugate of the second and the fourth is the complex conjugate of the third. So we can more compactly

write

$$\hat{\Omega}_3 = -2\pi i \int d\omega_a d\omega_b \hat{a}^\dagger(\omega_a)\hat{b}^\dagger(\omega_b) J_3(\omega_a,\omega_b) - \text{H.c.} \tag{D.7}$$

$$= -2\pi i \int d\omega_a d\omega_b \hat{a}^\dagger(\omega_a)\hat{b}^\dagger(\omega_b) \left(-\frac{3}{4\pi}\int dq d\omega_c d\omega_d (L_1 - 2L_2 + L_3 + \text{c.c.})\right) - \text{H.c.} \tag{D.8}$$

$$L_1 = \int_0^\infty dr \int_0^\infty ds\ F(\omega_a,\omega_d,q+2r+s)\, F(\omega_c,\omega_b,q-r+s)\, F(\omega_c,\omega_d,-q+r+2s) \tag{D.9}$$

$$L_2 = \int_0^\infty dr \int_0^\infty ds\ F(\omega_a,\omega_d,q+2r+s)\, F(\omega_c,\omega_b,q-r-2s)\, F(\omega_c,\omega_d,-q+r-s) \tag{D.10}$$

$$L_3 = \int_0^\infty dr \int_0^\infty ds\ F(\omega_a,\omega_d,q-r+s)\, F(\omega_c,\omega_b,q+2r+s)\, F(\omega_c,\omega_d,-q+r+2s)\,. \tag{D.11}$$

To get a simpler expression we can perform the following changes of variables: For L_1 in the last equation we put $r \to r' + s', s \to -s'$ to obtain:

$$L_1 = \int_{-\infty}^0 ds' \int_{-s'}^\infty dr' F(\omega_a,\omega_d,q+2r'+s')\, F(\omega_c,\omega_b,q-r'-2s')\, F(\omega_c,\omega_d,-q+r'-s')\,. \tag{D.12}$$

Likewise for L_3 we change $r \to -r' - s'$ and $s \to r'$ to obtain:

$$L_3 = \int_0^\infty dr' \int_{-\infty}^{-r'} ds' F(\omega_a,\omega_d,q+2r'+s')\, F(\omega_c,\omega_b,q-r'-2s')\, F(\omega_c,\omega_d,-q+r'-s')\,. \tag{D.13}$$

Note that now the integrands of L_1, L_2 and L_3 are identical and that $\int_{-\infty}^0 ds' \int_{-s'}^\infty dr' + \int_0^\infty dr' \int_{-\infty}^{-r'} ds' = \int_0^\infty dr' \int_{-\infty}^0 ds'$ so we can write more simply

$$L_1 - 2L_2 + L_3 = \left(\int_0^\infty dr \int_{-\infty}^0 ds - 2\int_0^\infty dr \int_0^\infty ds\right) \times \tag{D.14}$$
$$F(\omega_a,\omega_d,q+2r+s)\, F(\omega_c,\omega_b,q-r-2s)\, F(\omega_c,\omega_d,-q+r-s)\,,$$

we can now write J_3 as

$$J_3(\omega_a,\omega_b) = -\frac{3}{4\pi}\int dq d\omega_c d\omega_d \left(\int_0^\infty dr' \int_{-\infty}^0 ds - 2\int_0^\infty dr' \int_0^\infty ds\right) \times \\ F\left(\omega_a,\omega_d,q+2r+s\right) F\left(\omega_c,\omega_b,q-r-2s\right) F\left(\omega_c,\omega_d,-q+r-s\right). \tag{D.15}$$

Up to this point we have not used the fact that F is Gaussian; now we will use it: The product of three F's is a Gaussian function in $q, r, s, \omega_a, \omega_b, \omega_c, \omega_d$ and hence the integrals over q, ω_c, ω_d are complete (*i.e.* extending over the whole real line) Gaussian integrals and thus can be done analytically, leaving us with a Gaussian function in r, s, ω_a, ω_b. Doing these integrals we obtain

$$\int dq d\omega_c d\omega_d F\left(\omega_a,\omega_d,q+2r+s\right) F\left(\omega_c,\omega_b,q-r-2s\right) F\left(\omega_c,\omega_d,-q+r-s\right) = \\ -\frac{2\pi^{3/2}\tau\varepsilon^3}{3s_a s_b} e^{-\mathbf{u}\mathbf{N}\mathbf{u}^T/3}(f(r,s)+\text{c.c.}), \tag{D.16}$$

with

$$f(r,s) = \exp(\mathbf{x}^T\mathbf{A}\mathbf{x} + i\mathbf{v}^T\mathbf{x}), \quad \mathbf{A} = -\frac{3}{4\tau^2}\begin{pmatrix} \frac{2\mu_b^2}{s_b^2} & \frac{\mu^2}{s_a s_b} \\ \frac{\mu^2}{s_a s_b} & \frac{2\mu_a^2}{s_a^2} \end{pmatrix}, \quad \mathbf{v}^T = 2\eta_{ab}\left(\frac{\delta\omega_a}{s_b}, \frac{\delta\omega_b}{s_a}\right). \tag{D.17}$$

and $\mathbf{N}$ and $\mathbf{u}$ being defined in Eq. (5.14). With this result we can write

$$J_3(\omega_a,\omega_b) = \frac{\sqrt{\pi}\tau\varepsilon^3}{2s_a s_b}\exp\left(-\mathbf{u}\mathbf{N}\mathbf{u}^T/3\right) I \tag{D.18}$$

$$I = \left(\int_0^\infty dr' \int_{-\infty}^0 ds - 2\int_0^\infty dr' \int_0^\infty ds\right) f(r,s) + \text{c.c.} \tag{D.19}$$

Now we will add and subtract the quantity $\int_0^\infty dr \int_0^\infty ds\ f(r,s) + \text{c.c.}$ to I to get

$$I = \left(\int_0^\infty dr \int_{-\infty}^0 ds\ f(r,s) + \int_0^\infty dr \int_0^\infty ds\ f(r,s) + \text{c.c.}\right) \\ - \left(3\int_0^\infty dr \int_0^\infty ds\ f(r,s) + \text{c.c.}\right) = I_1 - I_2. \tag{D.20}$$

Notice that the term in parenthesis, I_1, can be evaluated since:

$$I_1 = \int_0^\infty dr \int_{-\infty}^0 ds\ f(r,s) + \int_0^\infty dr \int_0^\infty ds\ f(r,s) + \text{c.c.} = \int_{-\infty}^\infty dr \int_{-\infty}^\infty ds\ f(r,s) \tag{D.21}$$

$$= \frac{4\pi s_a s_b \tau^2}{3R^2} \exp\left(-\frac{4\tau^2\eta_{ab}^2}{3R^4}\mathbf{u}\mathbf{W}\mathbf{u}^T\right), \quad \mathbf{W} = \begin{pmatrix} 2\mu_a^2 & -\mu^2 \\ -\mu^2 & 2\mu_b^2 \end{pmatrix}. \tag{D.22}$$

As for I_2, we can proceed as follows:

$$I_2 = 3\int_0^\infty dr \int_0^\infty ds\ f(r,s) + \text{c.c.} = 6\int_0^\infty dr \int_0^\infty ds \exp\left(\mathbf{x}^T\mathbf{A}\mathbf{x}\right)\cos\left(\mathbf{v}^T\mathbf{x}\right). \tag{D.23}$$

But now we can let $s \to 2s_a\tau q/\sqrt{3}$ and $r \to 2s_b\tau p/\sqrt{3}$ to get:

$$I_2 = 8s_a s_b \tau^2 \int_0^\infty dq \int_0^\infty dp \exp\left(-(p,q)\mathbf{M}(p,q)^T\right)\cos\left(4\tau\eta_{ab}(\delta\omega_a q + \delta\omega_b p)/\sqrt{3}\right). \tag{D.24}$$

Now we can put all these results together to obtain

$$\begin{aligned} J_3 =& \frac{\sqrt{\pi}\tau\varepsilon^3}{2s_a s_b}\exp\left(-\mathbf{u}\mathbf{N}\mathbf{u}/3\right)\left\{\frac{4\pi s_a s_b\tau^2}{3R^2}\exp\left(-\frac{4\tau^2\eta_{ab}^2}{3R^4}\mathbf{u}\mathbf{W}\mathbf{u}^T\right)\right. \\ &\left. - 8s_a s_b\tau^2\int_0^\infty dq\int_0^\infty dp\exp\left(-(p,q)\mathbf{M}(p,q)^T\right)\cos\left(\frac{4\tau\eta_{ab}(\delta\omega_a q+\delta\omega_b p)}{\sqrt{3}}\right)\right\}. \end{aligned} \tag{D.25}$$

Simplifying and noting that $\mathbf{N}/3 + \mathbf{W} = \mathbf{Q}/R^4$ where $\mathbf{Q}$ and R are defined in Eq. 5.14, we obtain

$$\begin{aligned} J_3 =& \frac{2\pi^{3/2}\tau^3\varepsilon^3}{3R^2}\exp\left(-\mathbf{u}\mathbf{Q}\mathbf{u}^T/R^4\right) - 4\sqrt{\pi}\tau^3\varepsilon^3\exp\left(-\mathbf{u}\mathbf{N}\mathbf{u}^T/3\right)\times \\ &\int_0^\infty dq\int_0^\infty dp\exp\left(-(p,q)\mathbf{M}(p,q)^T\right)\cos\left(4\tau\eta_{ab}(\delta\omega_a q+\delta\omega_b p)/\sqrt{3}\right). \end{aligned} \tag{D.26}$$

This last equation can be rewritten as Eqs. (5.10) using the definitions of Eq. 5.14 in the main text. We now obtain a bound for J_3. First note that $|J_3| \le |W| + |VZ| = W + |V|Z$; the only term that is hard to bound from the last inequality is $|V|$, and to this end we note the following chain of inequalities:

$$\exp\left(-(p,q)\mathbf{M}(p,q)^T\right)\left|\cos\left(4\tau\eta_{ab}(\delta\omega_a q+\delta\omega_b p)/\sqrt{3}\right)\right| \le \exp\left(-(p,q)\mathbf{M}(p,q)^T\right) \tag{D.27}$$

$$\int_0^\infty dp \int_0^\infty dq \exp\left(-(p,q)\mathbf{M}(p,q)^T\right) \left|\cos\left(4\tau\eta_{ab}(\delta\omega_a q + \delta\omega_b p)/\sqrt{3}\right)\right| \leq \int_0^\infty dp \int_0^\infty dq \exp\left(-(p,q)\mathbf{M}(p,q)^T\right). \quad \text{(D.28)}$$

Now note that for any function $g(p,q)$, $|\int_0^\infty dp \int_0^\infty dq\ g(p,q)| \leq \int_0^\infty dp \int_0^\infty dq |g(p,q)|$ and thus we can finally write

$$|V(\omega_a,\omega_b)| = \left|\int_0^\infty dp \int_0^\infty dq \exp\left(-(p,q)\mathbf{M}(p,q)^T\right) \cos\left(4\tau\eta_{ab}(\delta\omega_a q + \delta\omega_b p)/\sqrt{3}\right)\right| \leq \int_0^\infty dp \int_0^\infty dq \exp\left(-(p,q)\mathbf{M}(p,q)^T\right) = V(\bar{\omega}_a,\bar{\omega}_b). \quad \text{(D.29)}$$

The right hand side of the last inequality can be easily evaluated

$$V(\bar{\omega}_a,\bar{\omega}_b) = \begin{cases} \frac{\pi+\tan^{-1}(R^2/\mu^2)}{2R^2}, & \text{if } \mu^2 < 0 \\ \frac{\tan^{-1}(R^2/\mu^2)}{2R^2}, & \text{if } \mu^2 > 0. \end{cases} \quad \text{(D.30)}$$

Note from Eq. (5.10) of the main text that $R^4 \geq 3\mu^4$ this immediately implies that $V(\bar{\omega}_a,\bar{\omega}_b) < \pi/(3R^2)$ and the general bound

$$|J_3(\bar{\omega}_a,\bar{\omega}_b)| < \frac{2\pi^{3/2}\varepsilon^3\tau^3}{3R^2}\left(\exp\left(-\mathbf{u}\mathbf{Q}\mathbf{u}^T/R^4\right) + 2\exp\left(-\mathbf{u}\mathbf{N}\mathbf{u}^T/3\right)\right) \leq \frac{2\pi^{3/2}\varepsilon^3\tau^3}{R^2}, \quad \text{(D.31)}$$

which is Eq. (5.16) The last bound is obtained by taking $\mathbf{u} = \mathbf{0}$. Note that $\max_{\eta_a,\eta_b} \tau^2/R^2 = 1/\sqrt{3}$ is achieved for $\eta_a = \eta_b = 0$. Nevertheless note that for this parameter values ($\eta_{ab} = \eta_a - \eta_b = 0$) J_3 is identically zero. To show this note that if $\eta_{ab} = 0$ then $R^4 = 3\mu^4$, $M^4 = \mu^4$, $\mu^2 > 0$, $\mathbf{Q}/R^4 = \mathbf{N}/3$ and

$$V(\omega_a,\omega_b) = V(\bar{\omega}_a,\bar{\omega}_b) = \frac{\pi}{6R^2}. \quad \text{(D.32)}$$

Finally, let us note that for $\mu = 0$ one can obtain an analytical expression for V,

$$V(\omega_a,\omega_b)|_{\mu=0} = -\frac{\pi e^{-\frac{2}{3}\tau^2\eta_{ab}^2\left(\frac{\delta\omega_a^2}{\mu_b^2}+\frac{\delta\omega_b^2}{\mu_a^2}\right)}\left(\mathrm{erfi}\left(\frac{\sqrt{\frac{2}{3}}\tau\eta_{ab}\delta\omega_b}{\mu_a}\right)\mathrm{erfi}\left(\frac{\sqrt{\frac{2}{3}}\tau\delta\omega_a\eta_{ab}}{\mu_b}\right)-1\right)}{8\mu_a\mu_b}, \quad \text{(D.33)}$$

and with this an analytical expression for J_3

$$J_3(\omega_a,\omega_b) = \frac{\pi^{3/2}\tau^3\varepsilon^3}{6\mu_a\mu_b}e^{-\mu_a^2\delta\omega_a^2-\mu_b^2\delta\omega_b^2}\left(3\mathrm{erfi}\left(\sqrt{\frac{2}{3}}\mu_b\delta\omega_b\right)\mathrm{erfi}\left(\sqrt{\frac{2}{3}}\mu_a\omega_a\right)-1\right) \quad \text{(D.34)}$$

where we used the fact that

$$\mu = 0 \Longrightarrow -\tau^2\eta_{ab}^2 + \mu_a^2\mu_b^2 = 0 \Longrightarrow \left|\frac{\tau\eta_{ab}}{\mu_a\mu_b}\right| = 1. \tag{D.35}$$

Using the last equation we can simplify also the expression for K_3,

$$K_3(\omega_a, \omega_b) = \pm\frac{\pi^{3/2}\tau^3\varepsilon^3}{2\mu_a\mu_b}e^{-\delta\omega_a^2\mu_a^2-\delta\omega_b^2\mu_b^2}\left(\text{erfi}\left(\sqrt{\frac{2}{3}}\mu_b\delta\omega_b\right) - \text{erfi}\left(\sqrt{\frac{2}{3}}\mu_a\delta\omega_a\right)\right) \tag{D.36}$$

where the sign is + if $\eta_{ab} > 0$ and - otherwise.

Bibliography

[1] Y. H. Shih and C. O. Alley. New type of Einstein-Podolsky-Rosen-Bohm experiment using pairs of light quanta produced by optical parametric down conversion. *Phys. Rev. Lett.*, 61:2921–2924, 1988.

[2] Paul G. Kwiat, Klaus Mattle, Harald Weinfurter, Anton Zeilinger, Alexander V. Sergienko, and Yanhua Shih. New high-intensity source of polarization-entangled photon pairs. *Phys. Rev. Lett.*, 75(24):4337, 1995.

[3] Paul G. Kwiat, Edo Waks, Andrew G. White, Ian Appelbaum, and Philippe H. Eberhard. Ultrabright source of polarization-entangled photons. *Phys. Rev. A*, 60(2):R773, 1999.

[4] B. G. Christensen, K. T. McCusker, J. B. Altepeter, B. Calkins, T. Gerrits, A. E. Lita, A. Miller, L. K. Shalm, Y. Zhang, S. W. Nam, N. Brunner, C. C. W. Lim, N. Gisin, and P. G. Kwiat. Detection-loophole-free test of quantum nonlocality, and applications. *Phys. Rev. Lett.*, 111:130406, 2013.

[5] John S. Bell. On the Einstein-Podolsky-Rosen paradox. *Physics*, 1(3):195–200, 1964.

[6] John F. Clauser, Michael A. Horne, Abner Shimony, and Richard A. Holt. Proposed experiment to test local hidden-variable theories. *Phys. Rev. Lett.*, 23(15):880, 1969.

[7] W.P. Grice, A.B. U'Ren, and I.A. Walmsley. Eliminating frequency and space-time correlations in multiphoton states. *Phys. Rev. A*, 64(6):063815, 2001.

[8] Alfred B. U'Ren, Reinhard K. Erdmann, Manuel de La Cruz-Gutierrez, and Ian A. Walmsley. Generation of two-photon states with an arbitrary degree of entanglement via nonlinear crystal superlattices. *Phys. Rev. Lett.*, 97(22):223602, 2006.

[9] Alfred B. U'Ren, Yasser Jeronimo-Moreno, and Hipolito Garcia-Gracia. Generation of fourier-transform-limited heralded single photons. *Phys. Rev. A*, 75(2):023810, 2007.

[10] Peter J. Mosley, Jeff S. Lundeen, Brian J. Smith, Piotr Wasylczyk, Alfred B. U'Ren, Christine Silberhorn, and Ian A. Walmsley. Heralded generation of ultrafast single photons in pure quantum states. *Phys. Rev. Lett.*, 100(13):133601, 2008.

[11] Thomas Gerrits, Martin J. Stevens, Burm Baek, Brice Calkins, Adriana Lita, Scott Glancy, Emanuel Knill, Sae Woo Nam, Richard P Mirin, Robert H. Hadfield, et al. Generation of degenerate, factorizable, pulsed squeezed light at telecom wavelengths. *Opt. Express*, 19(24):24434–24447, 2011.

[12] Andreas Christ, Alessandro Fedrizzi, Hannes Hübel, Thomas Jennewein, and Christine Silberhorn. Chapter 11 - parametric down-conversion. In Jingyun Fan Alan Migdall, Sergey V. Polyakov and Joshua C. Bienfang, editors, *Single-Photon Generation and Detection Physics and Applications*, volume 45 of *Experimental Methods in the Physical Sciences*, pages 351 – 410. Academic Press, 2013.

[13] Charles H. Bennett and Gilles Brassard. Quantum cryptography: Public key distribution and coin tossing. *Theoretical Computer Science*, 2011.

[14] Michael A. Nielsen and Isaac L. Chuang. *Quantum computation and quantum information*. Cambridge university press, 2010.

[15] Emanuel Knill, Raymond Laflamme, and Gerald J. Milburn. A scheme for efficient quantum computation with linear optics. *Nature*, 409(6816):46–52, 2001.

[16] Robert Raussendorf, Daniel E. Browne, and Hans J. Briegel. Measurement-based quantum computation on cluster states. *Phys. Rev. A*, 68(2):022312, 2003.

[17] Dietrich Dehlinger and M. W. Mitchell. Entangled photons, nonlocality, and Bell inequalities in the undergraduate laboratory. *Am. J. Phys.*, 70(9):903–910, 2002.

[18] Jonathan Lavoie, John M. Donohue, Logan G. Wright, Alessandro Fedrizzi, and Kevin J. Resch. Spectral compression of single photons. *Nat. Photonics*, 7(5):363–366, 2013.

[19] John M. Donohue, Michael D. Mazurek, and Kevin J. Resch. Theory of high-efficiency sum-frequency generation for single-photon waveform conversion. *Phys. Rev. A*, 91:033809, 2015.

[20] B. Brecht, Dileep V. Reddy, C. Silberhorn, and M.G. Raymer. Photon temporal modes: a complete framework for quantum information science. *arXiv preprint arXiv:1504.06251*, 2015.

[21] Andreas Eckstein, Benjamin Brecht, and Christine Silberhorn. A quantum pulse gate based on spectrally engineered sum frequency generation. *Opt. Express*, 19(15):13770–13778, 2011.

[22] Michael G. Raymer and Kartik Srinivasan. Manipulating the color and shape of single photons. *Phys. Today*, 65(11):32–37, 2012.

[23] Dileep V. Reddy, Michael G. Raymer, and Colin J. McKinstrie. Efficient sorting of quantum-optical wave packets by temporal-mode interferometry. *Opt. Lett.*, 39(10):2924–2927, 2014.

[24] Prem Kumar. Quantum frequency conversion. *Opt. Lett.*, 15(24):1476–1478, 1990.

[25] Jianming Huang and Prem Kumar. Observation of quantum frequency conversion. *Phys. Rev. Lett.*, 68(14):2153, 1992.

[26] Aaron P. VanDevender and Paul G. Kwiat. Quantum transduction via frequency upconversion. *J. Opt. Soc. Am. B: Opt. Phys.*, 24(2):295–299, 2007.

[27] T. C. Ralph, I. Söllner, S. Mahmoodian, A. G. White, and P. Lodahl. Photon sorting, efficient Bell measurements, and a deterministic controlled-z gate using a passive two-level nonlinearity. *Phys. Rev. Lett.*, 114:173603, 2015.

[28] Carsten Langrock, Eleni Diamanti, Rostislav V. Roussev, Yoshihisa Yamamoto, Martin M. Fejer, and Hiroki Takesue. Highly efficient single-photon detection at communication wavelengths by use of upconversion in reverse-proton-exchanged periodically poled linbo3 waveguides. *Opt. Lett.*, 30(13):1725–1727, 2005.

[29] Offir Cohen, Jeff S. Lundeen, Brian J. Smith, Graciana Puentes, Peter J. Mosley, and Ian A. Walmsley. Tailored photon-pair generation in optical fibers. *Phys. Rev. Lett.*, 102:123603, 2009.

[30] M. Halder, J. Fulconis, B. Cemlyn, A. Clark, C. Xiong, W. J. Wadsworth, and J. G. Rarity. Nonclassical 2-photon interference with separate intrinsically narrowband fibre sources. *Opt. Express*, 17(6):4670–4676, 2009.

[31] P.A. Franken, A.E. Hill, C.W. Peters, and G. Weinreich. Generation of optical harmonics. *Phys. Rev. Lett.*, 7(4):118–119, 1961.

[32] Zhenshan Yang, Marco Liscidini, and J. E. Sipe. Spontaneous parametric down-conversion in waveguides: A backward Heisenberg picture approach. *Phys. Rev. A*, 77:033808, 2008.

[33] B. Ya Zel'Dovich and D.N. Klyshko. Field statistics in parametric luminescence. *ZhETF Pisma Redaktsiiu*, 9:69, 1969.

[34] David C. Burnham and Donald L. Weinberg. Observation of simultaneity in parametric production of optical photon pairs. *Phys. Rev. Lett.*, 25:84–87, 1970.

[35] Stuart J. Freedman and John F. Clauser. Experimental test of local hidden-variable theories. *Phys. Rev. Lett.*, 28(14):938, 1972.

[36] Alain Aspect, Jean Dalibard, and Gérard Roger. Experimental test of Bell's inequalities using time-varying analyzers. *Phys. Rev. Lett.*, 49(25):1804, 1982.

[37] Antonio Acín, Nicolas Gisin, and Lluis Masanes. From Bell's theorem to secure quantum key distribution. *Phys. Rev. Lett.*, 97:120405, 2006.

[38] Christian Kurtsiefer, Sonja Mayer, Patrick Zarda, and Harald Weinfurter. Stable solid-state source of single photons. *Phys. Rev. Lett.*, 85:290–293, 2000.

[39] Charles Santori, David Fattal, Jelena Vučković, Glenn S. Solomon, and Yoshihisa Yamamoto. Indistinguishable photons from a single-photon device. *Nature*, 419(6907):594–597, 2002.

[40] K.D. Jons, P. Atkinson, M. Muller, M. Heldmaier, S.M. Ulrich, O.G. Schmidt, and P. Michler. Triggered indistinguishable single photons with narrow line widths from site-controlled quantum dots. *Nano Lett.*, 13(1):126–130, 2012.

[41] Carlton M. Caves. Quantum-mechanical noise in an interferometer. *Phys. Rev. D*, 23:1693–1708, 1981.

[42] Jaspreet Sahota and Nicolás Quesada. Quantum correlations in optical metrology: Heisenberg-limited phase estimation without mode entanglement. *Phys. Rev. A*, 91:013808, 2015.

[43] Nicolás Quesada, Jaspreet Sahota, and Daniel F.V. James. Physical resources for quantum-enhanced phase estimation. *in preparation*, 2015.

[44] Seth Lloyd and Samuel L. Braunstein. Quantum computation over continuous variables. *Phys. Rev. Lett.*, 82:1784–1787, 1999.

[45] Christian Weedbrook, Stefano Pirandola, Raúl García-Patrón, Nicolas J. Cerf, Timothy C. Ralph, Jeffrey H. Shapiro, and Seth Lloyd. Gaussian quantum information. *Rev. Mod. Phys.*, 84:621–669, 2012.

[46] H. J. McGuinness, M. G. Raymer, C. J. McKinstrie, and S. Radic. Quantum frequency translation of single-photon states in a photonic crystal fiber. *Phys. Rev. Lett.*, 105:093604, 2010.

[47] H.J. McGuinness, M.G. Raymer, and C.J. McKinstrie. Theory of quantum frequency translation of light in optical fiber: application to interference of two photons of different color. *Opt. Express*, 19(19):17876–17907, 2011.

[48] Wojciech Wasilewski, A. I. Lvovsky, Konrad Banaszek, and Czesław Radzewicz. Pulsed squeezed light: Simultaneous squeezing of multiple modes. *Phys. Rev. A*, 73:063819, 2006.

[49] A. I. Lvovsky, Wojciech Wasilewski, and Konrad Banaszek. Decomposing a pulsed optical parametric amplifier into independent squeezers. *J. Mod. Opt.*, 54(5):721–733, 2007.

[50] A. Gatti, R. Zambrini, M. San Miguel, and L. A. Lugiato. Multiphoton multimode polarization entanglement in parametric down-conversion. *Phys. Rev. A*, 68:053807, 2003.

[51] L. Caspani, E. Brambilla, and A. Gatti. Tailoring the spatiotemporal structure of biphoton entanglement in type-I parametric down-conversion. *Phys. Rev. A*, 81:033808, 2010.

[52] Andreas Christ, Benjamin Brecht, Wolfgang Mauerer, and Christine Silberhorn. Theory of quantum frequency conversion and type-II parametric down-conversion in the high-gain regime. *New. J. Phys.*, 15(5):053038, 2013.

[53] Danna Rosenberg, Adriana E. Lita, Aaron J. Miller, and Sae Woo Nam. Noise-free high-efficiency photon-number-resolving detectors. *Phys. Rev. A*, 71:061803, 2005.

[54] Nicolás Quesada, J.E. Sipe, and Agata M. Brańczyk. Optimized generation of bright squeezed and heralded-Fock states using parametric down-conversion. *in preparation*, 2015.

[55] M.J. Holland and K. Burnett. Interferometric detection of optical phase shifts at the Heisenberg limit. *Phys. Rev. Lett.*, 71(9):1355, 1993.

[56] Ulrik L. Andersen and Timothy C. Ralph. High-fidelity teleportation of continuous-variable quantum states using delocalized single photons. *Phys. Rev. Lett.*, 111:050504, 2013.

[57] W. P. Grice and I. A. Walmsley. Spectral information and distinguishability in type-II down-conversion with a broadband pump. *Phys. Rev. A*, 56(2):1627, 1997.

[58] Mayukh Lahiri, Radek Lapkiewicz, Gabriela Barreto Lemos, and Anton Zeilinger. Theory of quantum imaging with undetected photons. *arXiv preprint arXiv:1504.00402*, 2015.

[59] Agata M. Brańczyk. *Non-classical States of Light*. PhD thesis, The University of Queensland, 2010.

[60] Agata M. Brańczyk, Thomas M. Stace, and T.C. Ralph. Time ordering in spontaneous parametric down-conversion. In *AIP Conference Proceedings*, volume 1363, page 335, 2011.

[61] Aaron P. Vandevender and Paul G. Kwiat. High efficiency single photon detection via frequency up-conversion. *J. Mod. Opt.*, 51(9-10):1433–1445, 2004.

[62] Jun John Sakurai. *Modern quantum mechanics*. Addison-Wesley, 2011.

[63] Christopher Gerry and Peter Knight. *Introductory quantum optics*. Cambridge university press, 2005.

[64] Herbert Goldstein. *Classical mechanics*. Pearson Education, 1957.

[65] Stephen Barnett and Paul M Radmore. *Methods in theoretical quantum optics*, volume 15. Oxford University Press, 2002.

[66] J. Eisert and M. M. Wolf. Gaussian quantum channels. *eprint arXiv:quant-ph/0505151*, 2005.

[67] C. K. Law and J. H. Eberly. Analysis and interpretation of high transverse entanglement in optical parametric down conversion. *Phys. Rev. Lett.*, 92:127903, 2004.

[68] J. E. Sipe, Navin A. R. Bhat, Philip Chak, and Suresh Pereira. Effective field theory for the nonlinear optical properties of photonic crystals. *Phys. Rev. E*, 69:016604, 2004.

[69] Navin A. R. Bhat and J. E. Sipe. Hamiltonian treatment of the electromagnetic field in dispersive and absorptive structured media. *Phys. Rev. A*, 73:063808, 2006.

[70] John D. Joannopoulos, Steven G. Johnson, Joshua N. Winn, and Robert D. Meade. *Photonic crystals: molding the flow of light*. Princeton university press, 2011.

[71] M.M. Fejer, G.A. Magel, Dieter H. Jundt, and R.L. Byer. Quasi-phase-matched second harmonic generation: tuning and tolerances. *IEEE J. Quantum Electron.*, 28(11):2631–2654, 1992.

[72] G. Imeshev, M. M. Fejer, A. Galvanauskas, and D. Harter. Pulse shaping by difference-frequency mixing with quasi-phase-matching gratings. *J. Opt. Soc. Am. B: Opt. Phys.*, 18(4):534–539, 2001.

[73] Lukas G. Helt, Marco Liscidini, and John E. Sipe. How does it scale? comparing quantum and classical nonlinear optical processes in integrated devices. *J. Opt. Soc. Am. B*, 29(8):2199–2212, 2012.

[74] John E. Sipe. SFWM in birefrigent fibers. *Unpublished*, 2014.

[75] Nicolás Quesada and John E. Sipe. *In preparation*, 2015.

[76] Samuel L. Braunstein. Squeezing as an irreducible resource. *Phys. Rev. A*, 71:055801, 2005.

[77] Wilhelm Magnus. On the exponential solution of differential equations for a linear operator. *Commun. Pure Appl. Math.*, 7(4):649–673, 1954.

[78] Sergio Blanes, F. Casas, J. A. Oteo, and José Ros. The Magnus expansion and some of its applications. *Phys. Rep.*, 470(5):151–238, 2009.

[79] Jamy Moreno. Spontaneous four-wave mixing in standard birefringent fiber. Master's thesis, University of Delaware, 2012.

[80] Nicolás Quesada. SPDC Magnus library. `https://github.com/nquesada/magnus`.

[81] Steven G. Johnson. Cubature (multi-dimensional integration). `http://ab-initio.mit.edu/wiki/index.php/Cubature`.

[82] Fernando Casas, Ander Murua, and Mladen Nadinic. Efficient computation of the Zassenhaus formula. *Comput. Phys. Commun.*, 183(11):2386 – 2391, 2012.

[83] Annamaria Dosseva, Lukasz Cincio, and Agata M. Brańczyk. Shaping the spectrum of downconverted photons through optimized custom poling. *arXiv preprint arXiv:1410.7714*, 2014.

[84] Nicolás Quesada and J. E. Sipe. Effects of time ordering in quantum nonlinear optics. *Phys. Rev. A*, 90:063840, 2014.

[85] Wolfgang Mauerer, Malte Avenhaus, Wolfram Helwig, and Christine Silberhorn. How colors influence numbers: Photon statistics of parametric down-conversion. *Phys. Rev. A*, 80:053815, 2009.

[86] Hannes Hübel, Deny R. Hamel, Alessandro Fedrizzi, Sven Ramelow, Kevin J. Resch, and Thomas Jennewein. Direct generation of photon triplets using cascaded photon-pair sources. *Nature*, 466(7306):601–603, 2010.

[87] Christoph Söller, Offir Cohen, Brian J. Smith, Ian A. Walmsley, and Christine Silberhorn. High-performance single-photon generation with commercial-grade optical fiber. *Phys. Rev. A*, 83:031806, 2011.

[88] O. Gayer, Z. Sacks, E. Galun, and A. Arie. Temperature and wavelength dependent refractive index equations for mgo-doped congruent and stoichiometric linbo3. *Appl. Phys. B*, 91(2):343–348, 2008.

[89] Aaron J. Miller, Sae Woo Nam, John M. Martinis, and Alexander V. Sergienko. Demonstration of a low-noise near-infrared photon counter with multiphoton discrimination. *Appl. Phys. Lett.*, 83(4):791–793, 2003.

[90] Adriana E. Lita, Aaron J. Miller, and Sae Woo Nam. Counting near-infrared single-photons with 95% efficiency. *Opt. Express*, 16(5):3032–3040, 2008.

[91] J.S. Lundeen, A. Feito, H. Coldenstrodt-Ronge, K.L. Pregnell, C. Silberhorn, T.C. Ralph, J. Eisert, M.B. Plenio, and I.A. Walmsley. Tomography of quantum detectors. *Nat. Phys.*, 5(1):27–30, 2009.

[92] Peter C. Humphreys, Benjamin J. Metcalf, Thomas Gerrits, Thomas Hiemstra, Adriana E. Lita, Joshua Nunn, Sae Woo Nam, Animesh Datta, W. Steven Kolthammer, and Ian A. Walmsley. Tomography of photon-number resolving continuous-output detectors. *arXiv preprint arXiv:1502.07649*, 2015.

[93] Pieter Kok, W. J. Munro, Kae Nemoto, T. C. Ralph, Jonathan P. Dowling, and G. J. Milburn. Linear optical quantum computing with photonic qubits. *Rev. Mod. Phys.*, 79:135–174, 2007.

[94] Leonard Mandel. Sub-poissonian photon statistics in resonance fluorescence. *Optics Lett.*, 4(7):205–207, 1979.

[95] NIST Digital Library of Mathematical Functions. http://dlmf.nist.gov/, Release 1.0.9 of 2014-08-29. Online companion to [96].

[96] F. W. J. Olver, D. W. Lozier, R. F. Boisvert, and C. W. Clark, editors. *NIST Handbook of Mathematical Functions*. Cambridge University Press, New York, NY, 2010. Print companion to [95].

[97] N. Quesada and J. E. Sipe. Limits in high efficiency quantum frequency conversion. *arXiv preprint arXiv:1508.03361*, 2015.

[98] Nicolas Quesada and John E. Sipe. Observing the effects of time ordering in single photon frequency conversion. In *CLEO: 2015*, page JTu5A.3. Optical Society of America, 2015.

[99] Nicolás Quesada and J. E. Sipe. Time-ordering effects in the generation of entangled photons using nonlinear optical processes. *Phys. Rev. Lett.*, 114:093903, 2015.

[100] Benjamin Brecht, Andreas Eckstein, Raimund Ricken, Viktor Quiring, Hubertus Suche, Linda Sansoni, and Christine Silberhorn. Demonstration of coherent time-frequency Schmidt mode selection using dispersion-engineered frequency conversion. *Phys. Rev. A*, 90:030302, 2014.

[101] Omar Gamel and Daniel F. V. James. Time-averaged quantum dynamics and the validity of the effective Hamiltonian model. *Phys. Rev. A*, 82:052106, 2010.

[102] Nicolás Quesada. On the relation between the effective Hamiltonian and the Magnus expansion. *in preparation*, 2015.

[103] Alejandro Pozas-Kerstjens and Eduardo Martin-Martinez. Harvesting correlations from the quantum vacuum. *arXiv preprint arXiv:1506.03081*, 2015.